science.sciencemag.org/cgi/content/full/science.aba0909/DC1

Supplementary Materials for

Ancient DNA indicates human population shifts and admixture in northern and southern China

Melinda A. Yang, Xuechun Fan, Bo Sun, Chungyu Chen, Jianfeng Lang, Ying-Chin Ko, Cheng-hwa Tsang, Hunglin Chiu, Tianyi Wang, Qingchuan Bao, Xiaohong Wu, Mateja Hajdinjak, Albert Min-Shan Ko, Manyu Ding, Peng Cao, Ruowei Yang, Feng Liu, Birgit Nickel, Qingyan Dai, Xiaotian Feng, Lizhao Zhang, Chengkai Sun, Chao Ning, Wen Zeng, Yongsheng Zhao, Ming Zhang, Xing Gao, Yinqiu Cui, David Reich, Mark Stoneking, Qiaomei Fu*

*Corresponding author. Email: fuqiaomei@ivpp.ac.cn

Published 14 May 2020 on *Science* First Release
DOI: 10.1126/science.aba0909

This PDF file includes:

Materials and Methods
Supplementary Text
Figs. S1 to S18
Tables S1 to S9
References

Other Supplementary Material for this manuscript includes the following:
(available at science.sciencemag.org/cgi/content/full/science.aba0909/DC1)

MDAR Reproducibility Checklist (.pdf)

Materials and Methods

Ancient DNA extraction, sequencing, and data processing

DNA was extracted from less than 100 mg of bone or tooth powder from samples deriving from 26 ancient human remains (Table 1) (*33*). For petrous bone samples, we used two methods. When the petrous bone was isolated, we drilled a small hole on the inner side to obtain petrous bone powder from the cochlea (*34*). When the petrous bone could not be isolated from the complete skull (i.e. Xiaogao) (*35*), we drilled through the bottom of the skull to obtain powder from the cochlea to avoid destroying typical identifying characters on the specimen. Photos of all specimens were taken both before and after drilling. For all but six specimens, a single-stranded protocol ("SS") (*36, 37*) was used to prepare the libraries. The single-stranded libraries for Boshan, Liangdao1 and Liangdao2 were treated with uracil-DNA-glycosylase (UDG) from *E. coli* and endonuclease (Endo VIII) ("SS UDG") (*17*). Libraries for Yumin, Xiaojingshan and Xiaogao were prepared using a double-stranded protocol ("DS") (*36*), while libraries for Bianbian were prepared using both single-stranded and double-stranded protocols (Table 1). Libraries were amplified using the AccuPrimepfx DNA enzyme. The amplification process underwent 35 cycles to make sure enough ancient DNA was available for capture. To specific libraries, the P5 and P7 primers were added, and a NanoDrop2000 spectrometer was used to determine the amount of DNA extracted per sample.

In solution capture of mitochondrial DNA and nuclear DNA

DNA capture enriches for DNA sequences of preference, allowing us to efficiently sequence ancient DNA from samples with high levels of contaminating environmental DNA (*15*). Thus, we focused on DNA capture techniques to increase the number of individuals that could be sampled and compared to other humans. We used oligonucleotide probes synthesized from the complete human mitochondrial genome (mtDNA) to capture human mtDNA (*19*). For the nuclear genome, we used probes that enrich for 1.2 million SNPs, see Panels 1 and 2 in (*16*). These oligonucleotide probes were synthesized by Agilent Technologies (California, USA).

Sequencing and reads alignment

Illumina Miseq or Hiseq4000 sequencing machines were used to generate 2×76bp paired-end reads from the enriched mitochondrial DNA libraries, while Illumina Hiseq4000 sequencing machines were used to generate 2×100bp and 2×150bp paired-end reads from the enriched nuclear DNA libraries. Adaptors were trimmed and paired-end reads were merged into one sequence (a minimum overlap of 11 base pairs was needed to merge paired-end reads) using *leeHom* (https://github.com/grenaud/leeHom), a software that uses a Bayesian framework to account for challenges in sequencing libraries with short DNA fragments like those typical of ancient DNA (*38*).

Using only merged reads with a length of at least 30 bp, we then aligned the reads from the enriched mitochondrial DNA libraries to the revised Cambridge Reference Sequence (rCRS) (*39*) and the reads from the enriched nuclear DNA libraries to the human reference

genome *hg19*. BWA (*40*) (version 0.6.1) using the *samse* command and the arguments -n 0.01 and -l 16500 to map the reads. Duplicates were removed, where a read was considered a duplicate if it had the same orientation, start, and end positions as another read. For duplicated reads, we kept the highest quality sequence for analysis. Fragments with a mapping quality score below thirty were removed.

Test for contamination and genotyping

The libraries from all but one sample have ≥10% of terminal nucleotides of the read fragments that are cytosines in the reference genome but thymines in the read fragment, which is expected for authentic ancient DNA (*41*) (Table 1).

We estimated the contamination rate using two methods. For all individuals, we determined the mtDNA contamination rate by comparing mtDNA fragments for each individual to the consensus mitochondrial genome for that individual and for 311 present-day world-wide sequences using ContamMix (*19*). We ignore the first five and last five positions of the fragments to avoid the damage pattern counting as contamination. If >3% of the fragments matched one of the worldwide sequences better than the consensus, we treated that library as contaminated. We found that Qihe2, SuogangB1, SuogangB3, L5692, L5706, L7417, L5696, L5698, L5701, L5703, and L5704 showed signs of contamination. For males, we additionally used a test of contamination for the X-chromosome (*18*). As only one copy of the X-chromosome is found in males, we do not expect to observe polymorphisms in X-chromosome DNA sequences. A contamination rate was estimated based on this assumption, and for those with a contamination rate greater than 3%, we treated the library as contaminated (Table 1).

To retain as many as possible of the individuals for analysis, for libraries with substantial contamination, we restricted analyses to use the fragments with characteristics typical of ancient DNA, i.e. showing a damage pattern not found in present-day DNA (*17*). We used pmdtools0.60 with the --customterminus parameter (*42*) to filter out fragments with at least one C→T substitution in the first three positions at the 5'-end and the last three positions at the 3'-end . We refer to these libraries as damage-restricted libraries. Samples where damage-restricted libraries were used are shown in Table 1.

For each SNP covered at least once in an individual, we randomly sampled one sequence to determine an allele for that individual (*16*). Thus, we have effectively haploid data. In total, 24 out of 26 individuals sampled were used in our analyses.

Principal components analysis

We took 34 populations from the Human Origin (HO) SNP Panel (*43*), 17 Tibetan and Han populations from (*44*) to perform a principal components analysis (PCA) with the smartpca program of the EIGENSOFT package (*45*) using default options except lsqproject: YES, numoutlieriter: 0 and shrinkmode: YES. Results are shown in Fig. S1. All the newly sequenced ancient individuals as well as the previously published ancient Asians found in Table S1 were then projected onto the principal components for present-day East Asians (Fig. 1C).

F_3- and f_4-analyses

We use a number of f-statistics to determine genetic relationships in East Asia. Here, we briefly describe the methods referenced, in order of appearance. For all f-statistics, we used frequency data if the number of individuals in a group was greater than one (Table S1), and we used a 0/1 count otherwise. The software used, Admixtools can accommodate both count and frequency data, and the f-statistic is shown to act similarly for both data types (*46*). We describe the combinations tested for each f-statistic in more detail in the next section.

(1) Outgroup f_3-analysis – This method, first developed by Raghavan et al (*22*), uses an f-statistic of the form $f_3(Mbuti; X, Y)$, where the present-day Central African Mbuti are used to represent an outgroup to populations X and Y. We used the software qp3Pop in the AdmixTools (*43*) software package (version 412), and we created the heatmap in Fig. 1D using heatmap.2 in R. Those that share high f_3 values can be interpreted to have high genetic similarity with each other, allowing us to determine clusters of shared ancestry in a pairwise comparison.

(2) f_4-analysis - We used f_4-statistics and the software qpDstat (version 712) in AdmixTools (*43*) to assess the relative connections these ancient individuals share with each other and other ancient and present-day populations. The general form of the f_4-statistic we use is $f_4(Mbuti, P2; P3, P4)$, where the Mbuti are again used as an outgroup to the individuals or populations represented by P1, P2, and P3. $f_4>0$ ($Z>3$) indicates that P2 shares more alleles with P4 than P3, $f_4<0$ ($Z<-3$) indicates that P2 shares more alleles with P3 than P4, and $f_4\sim0$ ($|Z|<3$) indicates that P2 shares a similar number of alleles with both P3 and P4. More description of the f_4-tests highlighted in this study can be found in the Supplementary Text (sections 3-4).

Testing for archaic admixture using an f_4-ratio test

We also tested for archaic admixture in the North and South groups. We performed an f_4-ratio test (*47*) to estimate the amount of Denisovan ancestry in a target population. The f_4-ratio is given by:

$$\frac{f_4(Denisovan, Mbuti; X, Eurasian)}{f_4(Denisovan, Mbuti; Papuan, Eurasian)}$$

where X is the target population and the Eurasian is either the Han or French (Table S3).

Estimating a maximum likelihood phylogeny with migration events

We used Treemix v1.13 (*23*) to determine the phylogenetic relationships of various East Eurasians that were previously explored using f-statistics. The populations included are as listed in the Supplementary Text (section 5). We used the options "-root Mbuti –k 500" to root the tree by the Central African Mbuti and to make blocks of 500 SNPs. We ran 1,000 replicates for each tree, adding the options "-bootstrap -q". We then assessed the 1,000

bootstrap trees in *phylip* using the *consense* command to count the number of times certain individuals grouped with each other relative to all others in the analysis. Results are shown in Fig. S5 for m=0 to m=3, with visualization of the residuals in Fig. S6. The maximum likelihood phylogeny with three migration events is also included as Fig. 2A.

Developing a model by comparison of all f_2, f_3, and f_4-statistics of sets included in tree

We also assessed whether we could develop a tree model satisfying the conditions that all f_2-, f_3-, and f_4-values between populations and individuals fit the proposed relationships within the tree (|maxZ|<3) using qpGraph (*43*) with the parameter "allsnps: NO". We add each population in turn, starting with a base graph as described in the Supplementary Text (section 7), where we allow each new tip to be derived entirely from a single ancestry or a mixture of ancestry from populations related to two different branches of the tree. We exclude those graphs with 100% admixture branches and branch lengths of zero, as they indicate a simpler graph is available. We show plausible models after addition of each set (Fig. S16-S17), with the final set of possible tree models shown in Fig. S18 and Fig. 2B. Using the tree model in Fig. 2B, we add each remaining present-day and ancient population in turn, recording the mixture proportions and source ancestry describing each population from the best fitting tree (as described in section 7 of the Supplementary Text). This is visualized in Fig. 2C-2D.

Test of genetic differentiation (F_{st})

We used the smartpca program of the EIGENSOFT package (*45*) using inbreed: YES and fstonly: YES to estimate F_{st} for select ancient and present-day East Asian groups. To represent ancient northern East Asians, we used the merged coastal nEastAsia_EN into a single group. To represent the ancient southern East Asians, we merged two groups. The Early Neolithic southern East Asians (Liangdao) were considered as a single group, and the Late Neolithic southern East Asians were merged into a single group (Table S1). We used three groups to represent present-day northern East Asians: Hezhen, Korean, and Han. We used three groups to represent present-day southern East Asians: Dai, Lahu, and She. The distribution of F_{st} values comparing within and between these four categories (ancient northern and southern, present-day northern and southern East Asians) are shown in Fig. S11.

ADMIXTURE

Using the dataset from the PCA and omitting deeply diverged samples (i.e. Tianyuan and G1), we pruned the dataset to account for linkage disequilibrium using PLINK (*48*) (v1.90b3.40) with parameters "--indep-pairwise 200 25 0.4". We then used ADMIXTURE (*49*) implementing a model-based maximum likelihood (ML) clustering algorithm to estimate individual ancestries and determine population structure with cross-validation. We did not require that data overlapped for all samples, to allow inclusion of low-coverage individuals. For each *K*, we re-ran the software 100 times using different seeds, to estimate the cross validation, which helps to define the 'best' *K*, associated with the lowest CV error. For this analysis, the lowest CV is when K=3 (Fig. S10A), although the CV is almost as

low for K=2 and K=4. We therefore present the *ADMIXTURE* results with *K* from 2 to 4 in Fig. S10B.

Inferring admixture with an explicitly modeled phylogeny

To further study the relationships between the ancient East Asians sampled in this study, we used qpWave (*36*) and qpAdm (*15*) with the parameter "allsnps: NO" to model ancient and present-day East Eurasians as mixtures of ancestry related to one, two, or three different sources. This method compares the relationship between each set of target and sources with a set of populations (denoted **Right**) that differ in their genetic relationships with the targets and sources. This method is particularly useful because detailed knowledge of the phylogenetic relationships among the populations in **Right** is not needed, so long as they do not show recent admixture with any of the target and source populations. In the Supplementary Text (section 6), we list the populations included in **Right**. A detailed description of how we estimated mixture proportions is also found in section 6 of the Supplementary Text. Results are shown in Table S6 and are visualized in Fig. 3D-3F and Fig. S13.

Supplementary Text

1. Site and specimen description

The individuals sampled in this study are from archaeological sites in mainland East Asia, as well as from two islands off the coast of southeastern East Asia (Fig. 1A, main text). All new samples used for ancient DNA are under the custodianship of archaeologist co-authors of the study and were obtained with full permission from the related archaeological institutes or universities. The review board of the Institute of Vertebrate Paleontology and Paleoanthropology approved for study the ancient genomes sampled in this project (review no. 201910250003), following a protocol used in other ancient human genetic studies (*20, 50*) that specifies that our use of the samples is specifically to study population history.

The new samples span a time period of 9,500-3,00 years ago, which covers the early to mid-Holocene and much of the early and middle Neolithic, with one recent individual from Fujian. The Qinling-Huaihe line (Fig. 1A) acts as a consensus reference line to distinguish Northern and Southern China. Geographically, China can be divided into North and South by the Qinling-Huaihe line, corresponding to the humid zone and semi-humid zone, and the warm temperate zone and subtropical zone (*51*). Cultural divisions based on crops, farming system, cuisine, and lifestyle loosely corresponds to this line (*52*). We sampled Early Neolithic individuals from both the northern and southern regions. In the north, we sampled individuals from Shandong and Inner Mongolia that date to ~9,500-8,000 years ago. In the south, we sampled individuals from Fujian and the nearby Liang Island from ~8,400-7,500 years ago. We also obtained data from individuals dating to 4,600-4,200 years ago from Taiwan and Fujian, and one individual dating to ~300 years ago from Fujian.

Five samples are dated and published elsewhere (*28, 53-55*) (Table 1). Others were ^{14}C dated by the accelerator mass spectrometry (AMS) (Table 1), and were calibrated using OxCal v4.2.4 (*56*) and the INTCAL13 calibration curve (*57*) . All ages are reported as cal BP, relative to AD 1950.

Coastal and inland northern East Asians

Here, we focus particularly on individuals from the Shandong region, in the lower Yellow River Valley basin (coastal nEastAsia). We also include one individual from Inner Mongolia (inland nEastAsia, Table S1). These individuals date to the Early Neolithic. The oldest site has features more similar to Late Paleolithic sites, but the bulk of the Shandong sites are related to the Houli culture, which show some plant cultivation, though it is unlikely they were full agriculturalists (*11*).

Bianbian - The oldest archaeological site in this study is Bianbian, a cave site from Yiyuan in central Shandong of China (*12*). Materials found have included animal bones, ash pits, pottery shards, and grinding stones. Pottery shards show similarities to later local vessels from the Houli culture (8,500-7,500 BP) found in the Shandong region, making this the earliest known pottery in Shandong thus far (*58*). Useware and starch grain analysis indicates that grinding stones found in this cave were likely used for processing nuts (*59*). Microlithic tools have been found in the earliest layers, which suggests that the earliest

people at this site were more like Late Paleolithic rather than Early Neolithic populations, but it remains unclear if these tools were associated with the sampled specimen (*58*). Assessment of the faunal assemblage suggests that in the earliest layers, hunting-gathering was the major subsistence strategy (*60*). We sequenced one specimen from Bianbian Cave, a male skull, which was directly radiocarbon dated to 9,545-9,480 cal BP.

Xiaojingshan –This site is near Diaozhen Qiezhuang village in Zhangqiu, Shandong, China. Tombs, houses, and pottery and stone artifacts have been found that are associated through pottery shards with the Houli Culture. Xiaojingshan is notable for possessing a moat in the western portion of the settlement, with numerous Houli period houses and at least three cemeteries (*61*). These characteristics have been used to argue that the residents were fairly sedentary, though the ceramic and dietary habits suggest farming was not the dominant economy (*11*). While millet seems to have been part of the diet of Xiaojingshan people, it was not the main contributor (*59*). Many grinding stones can be observed, likely suggesting higher nut consumption (*11*). We sampled 13 individuals from the Xiaojingshan site and successfully sequenced three individuals: M7, M16 and M4. They were directly radiocarbon dated to 7,872-7,721 cal BP (M7) and 7,935 - 7,786 cal BP (M16), and 7,877 – 7,735 cal BP (M4).

Xiaogao – The Xiaogao archaeological site is located in Zhangdian District, Zibo City, Shandong, China. The archaeological material at this site is mostly identified as related to the Houli culture. We sequenced a single individual from this site, identified to be female, directly radiocarbon dated to 8,777-8,591 cal BP.

Boshan – The specimen is Boshan 11, a fossil that was collected in Boshan Mountain in Shandong, China. We sequenced a single individual from this site, identified to be male. His mitochondrial DNA was sequenced and assigned to haplogroup B4c1a, and the specimen was radiocarbon dated to 8,320-8,040 cal BP (*53*).

Yumin – The Yumin archaeological site is located in Huade County, Ulanqab city, Inner Mongolia Autonomous Region of China. Yumin culture is the earliest Neolithic culture found in Inner Mongolia thus far. Radiocarbon analysis of charcoal samples associated with the remains of a house were dated to ~8,400 cal BP (*62*). We sequenced a single individual (M1) from this site, identified to be female, and she was directly radiocarbon dated to 8,415-8,335 cal BP.

Coastal southern East Asians

The coastal southern East Asians were excavated in Fujian province, China, as well as islands in the Taiwan Strait. This area is notable for possessing very different features from other parts of East Asia. Its location has suggested a close connection to Southeast Asia and the Pacific, particularly regarding their relationship to Austronesians, who are widespread across Pacific Islands, including Taiwan (*25*). Most of the inland terrain of Fujian is marked by a mountainous landscape, where basins, river valleys, and coastal plains are suitable for human settlement. The coastline differs from the mountainous terrain further inland, with many offshore islands, especially off the Fujian coast. The early

Holocene shows Paleolithic-related materials fairly late, with increasing Neolithic-related materials gradually entering the region (*25*).

Qihe – The Qihe cave site (Qihedong) is located in the Wuyi-Nanling zone, near Zhangping, Fujian, China. Houses and ash pits have been found possibly indicating sedentism, and pottery shards have also been found. The pottery style seems similar to that observed in Taiwan, but these date to a much earlier time (*26, 63*). Three cultural phases (I-III) have been found in this cave, which have been radiocarbon dated to ~17,000-13,000 BP, 12,000-10,000 BP, and 10,000-7,000 BP. Its continuous dating through the Late Paleolithic into the Early Neolithic suggests that it is informative on the transition from the Paleolithic to the Neolithic. Three human skulls were found in Phase III, the youngest layer. The individual sequenced in this study (Qihe2) was directly radiocarbon dated to 8,428-8,359 cal BP.

Tanshishan – The Tanshishan site is found on the lower reaches of the Min River in Minhou County, Fujian, China. Both rice grains and domesticated pigs can be found at this site, but no evidence for agricultural activity has been found (*11*) and the high frequency of marine shellfish and fish suggest that the dominant subsistence strategy was marine foraging rather than food production (*25*). The source material for several adzes found at Tanshishan culture sites are nonlocal volcanic rocks. Some have suggested that these materials came from the Penghu archipelago in Taiwan Strait (*11*). We sampled five individuals from the Tanshishan site and successfully sequenced four individuals: M20, M6, M26-1 and M12. We performed direct radiocarbon dating and found that M6 dates to 4,419 – 4,246 cal BP, M20 dates to 4,526-4,417 cal BP, and M26-1 dates to 4,410-4,225 cal BP.

Xitoucun – The Xitoucun archaeological site was also found in Minhou County, Fujian, China, about 15 kilometers away from the Tanshishan site. Material remains excavated from the Xitoucun site belong to the Tanshishan culture (5,000-4,3000 BP) (*64*). We sampled eight individuals from the site, and obtained sufficient data for analysis from seven of them (M49, M32, M26, M15, M13, M44 and M18-2). These individuals were directly radiocarbon dated to 4,419-4,246 cal BP (M49), 4,530-4,417 cal BP (M32), 4,530-4,417 cal BP (M26), 4,527-4,406 cal BP (M15), 4,580-4,423 cal BP (M13), 4,644-4,500 cal BP (M44), and 4,418-4,240 cal BP (M18-2), respectively.

Chuanyun – The Chuanyun cave site (Chuanyundong) is located in Zhangping City, Fujian, China. The archaeological deposits continue from the Late Paleolithic to the Bronze Age. A burial was found in the Bronze Age layer, and the associated burial artifacts suggest that the human specimen was from the Shang and Zhou dynasties (*65*). However, through direct radiocarbon dating of the Chuanyun specimen, we found that this male individual was a recent intrusion, with an age of 334 - 281 cal BP.

Liangdao – Liangdao, or Liang Island, is in the Matsu archipelago just 24 km offshore from Fujian in the Taiwan Strait. A male skeleton (Liangdao1) was found below a shell mound that contains pottery shards, stone tools, bone tools and faunal remains. Ancient mitochondrial DNA was sequenced from Liangdao1, showing that he has haplogroup E, closest to present-day Formosans, the indigenous present-day populations from the highlands of Taiwan (*28*). A second female skeleton was found on the island

(Liangdao2). She was buried erect supine extended among shell middens, within four meters of and above Liangdao1. We obtained genome-wide data from both individuals. Liangdao1 was radiocarbon dated to 8,320-8,060 cal BP (*28*) and Liangdao2 was radiocarbon dated to 7,590-7,560 cal BP (*54*).

<u>*Suogang*</u> – The Suogang site is located in Magong city, Penghu County, on the southeastern coast of the Penghu archipelago in the Taiwan Strait. This site is the type for representing the 'Suogang period' (or Suo-kang period) in Penghu, and associated cultural materials are closely related to the contemporary 'Fine Cord Marked Culture' on the west coast of Taiwan (*55*). Archaeological features associated with the Suogang period are also observed in coastal mainland China like Guangdong and Fujian, especially the Fujian Damaoshan site (*66*). Composition analysis indicates that Suogang pottery was not from Penghu and is similar to that associated with the Niuchouzi Culture (3,800-3,300 BP) in southwest Taiwan. Meanwhile, all basaltic stone tools from the Niuchouzi culture sites were from Penghu (*67*), indicating close interaction between Penghu and southwestern Taiwan. We sequenced two individuals from this site, B1 and B3.Associated shells were radiocarbon dated to 4,633 -4,287 cal BP and 4,793 - 4,407 cal BP (*55*).

2. <u>Description of nomenclature used in study</u>

To compare our ancient individuals to each other and previously published individuals, we collected genetic data for individuals found in East and Southeast Asia possessing Asian-related ancestry. We grouped data for samples that derived from the same archaeological site and time period to increase the number of SNPs at a given site where genetic information is available for at least one individual, increasing our statistical power for inferring genetic relationships. We confirmed that there were no outliers in our principal component analysis (Fig. 1C). This increases statistical power for inferring genetic relationships.

We also developed nomenclature to refer to sets from a similar geography but different archaeological sites, summarized in Table S1. For instance, our newly sampled ancient individuals were divided into several regional groupings. Bianbian, Boshan, Xiaogao, and Xiaojingshan all derive from the lower reaches of the Yellow River in northern China during the early Neolithic, so we refer to them as coastal northern East Asians (coastal nEastAsia). This contrasts with Yumin from Inner Mongolia who also dates to the Early Neolithic, whom we refer to as an inland northern East Asian (inland nEastAsia). We also sampled individuals from Fujian province in mainland China and islanders from the Taiwan Strait dating to the Early Neolithic (Qihe, Liangdao1, Liangdao2), Late Neolithic (Xitoucun, Tanshishan, Suogang), and Historic (Chuanyun) periods, whom we denote as coastal southern East Asians (coastal sEastAsia).

Previously published ancient individuals closely related to East Asians were grouped into one of four categories – steppe or coastal Siberians dating to the Early Neolithic (steppe or coastal Siberia), Tibetans dating for 3,150-1,250 years ago (Tibetan), Southeast Asian and Pacific islanders closely related to present-day Austronesian speakers (Austronesian), and coastal or inland Southeast Asians (coastal or inland SoutheastAsia).

The newly sampled northern and southern East Asians were also assigned to one of three time periods – 9,500-7,500 years ago, 5,000-3,000 years ago, and <2,000 years ago – based on radiocarbon dating described in section 1 of the Supplementary Text. We refer to these time periods as the Early Neolithic (EN), Late Neolithic (LN), and Historic (H), which we add to the regional labels from all ancient individuals closely related to present-day East Asians. For populations dating to between 3,000 and 2,000 years ago, we denote them as 'B', as most derive from the Bronze Age. We emphasize that these groupings do not reflect the complexity of the changes in archaeology across this time period. While imperfect, they aid in clarifying the major patterns we observe over time. We highlight the temporal and geographic nomenclature we used throughout this study in Table S1.

3. Genetic relationships between newly sampled individuals and various Neolithic and present-day Asian populations

(1) **Relationship of newly sampled individuals to individuals with 'early Asian' ancestry:** We define 'early Asian' as those ancient individuals with ancestry that is distantly related to East Asians (e.g. outgroup to present-day East Asians and Native Americans), though they may not be closely related to each other. These include Tianyuan, G1, and Ikawazu (Table S1). Based on previously published studies and verified here (Fig. 1C), Neolithic Siberians and Tibetans all share a closer relationship to present-day East Asians than any 'early Asians'. We refer to them as 'peripheral East Asians'. We used the outgroup f_3*(Mbuti; X, Y)* test, with the Central African Mbuti as the outgroup, X as a newly sampled ancient individual, and Y as one of the 'early Asians', Siberians, Tibetans, or newly sampled ancient individuals (Fig. S2). We used f_4*(Mbuti, X; present-day East Asian, 'early Asian')* to assess whether each newly sampled ancient individual shares more alleles with present-day East Asians (*68*) or an 'early Asian' individual (Table S2), and we also assessed the complementary f_4-statistic of *f4(Mbuti, 'early Asian'; present-day East Asian, X)*.

(2) **Genetic relationships within Neolithic East Eurasia highlight a northern and southern East Asian ancestry:** We next explored genetic structure in East Asia. To do this, we primarily compared our newly sampled individuals to the previously published Neolithic and Bronze Age individuals carrying East Asian ancestry from Tibet and Siberia, as well as the Southwest Pacific island of Vanuatu (Table S1). We consider Southeast Asians separately due to their shared ancestry with Hòabìnhians (*7*). We first used outgroup f_3*(Mbuti; X, Y)* to do a pairwise comparison of all the above individuals to determine whether certain groups share high levels of genetic similarity (Fig. 1D). Then, to test whether our observed clusters are significantly meaningful, we conducted all f_4-tests placing each ancient East Asian (newly sampled and previously published) as one of P2, P3, or P4, with Central African Mbuti as outgroup. In Fig. S4 and S7-S9, we highlight important trends characterizing the genetic structure in Neolithic East Asia.

(3) Increase in northern East Asian ancestry in southern China to the present-day: To test changes in affinity to northern and southern East Asian ancestry over time, we conducted a symmetry test using f_4*(Mbuti, X; Qihe, Bianbian)*, where Qihe is the oldest individual from southern East Asia (8,400 BP) and Bianbian is the oldest individual from

northern East Asia (9,500 BP). We tested every Neolithic and present-day East Eurasian, asking whether they were more closely related to an Early Neolithic southern East Asian or northern East Asian (Fig. 3A-3C, Table S5A). We then substituted Qihe with another coastal sEastAsia_EN (Liangdao1) or substituted Bianbian with the inland nEastAsia_EN (Yumin) to check the robusticity of our result (Fig. S12, Table S5B-C). Lastly, because the inland and coastal nEastAsia_EN show some differing relationships with respect to other East Eurasians, we tested f_4*(Mbuti, X; Bianbian, Yumin)* to determine the type of northern East Asian ancestry observed in other sampled Neolithic and present-day East Eurasians (Fig. S15, Table S5D).

4. Tests of admixture with populations not of East Asian ancestry using f_4-analyses

We examined a series of f_4-statistics addressing the relationship of several more distantly related populations to East Asians, Tibetans, and Siberians to determine asymmetric relationships that suggest admixture.

(1) **Native Americans:** It has previously been observed that some South Americans (*69*) (e.g. Surui) share excess ancestry with present-day Papuan and Onge (*70*), as well as a 40,000-year-old Tianyuan individual, unlike other Native Americans (e.g. Mixe). We used f_4*(Mbuti, North/South; Surui, Mixe)* to test for this connection in the North and South groups (Fig. S3A, S3D).

(2) **Ancient West Eurasians:** A 35,000-year-old individual from Belgium (*69*) was shown to share connections to the 40,000-year-old Tianyuan individual (*20*), and some 8,000-year-old West European hunter-gatherers (Loschbour) showed connections to present-day East Asians (*20, 69*). We tested for these West Eurasian connections in the North and South groups, using f_4*(Mbuti, North/South; Vestonice16, GoyetQ116-1/Loschbour)* (Fig. S3B-3C, S3E-3F), where Vestonice16 is a 35,000-year-old European (*69*).

(3) **Paleosiberian:** A 9,800-year-old individual with a close relationship to Native Americans (Kolyma) was also sequenced from Siberia (*9*). We performed a symmetry test, using f_4*(Mbuti, Kolyma; X, Y),* where X and Y are all Neolithic East Asians, Siberians, and Tibetans of East Asian ancestry (Table S4).

(4) **Southeast Asia:** 'Early Asian' ancestry found in Hòabìnhians (G1) that exist in partial amounts in ancient Southeast Asians (*7*) make it difficult to use f-statistics to explore the relationship of Southeast Asians to East Asians. Different types of East Asian ancestry have had an influence on ancient Southeast Asians (*6, 7*), so we developed a symmetry test to determine the types of East Asian ancestry that played a role in migration to Southeast Asia (Table S7).

(5) **Jōmon:** A connection between the Jōmon (Ikawazu) and Hòabìnhians (G1) has been previously proposed. Here, we test the connection to Hòabìnhians, as well as East Asians. We performed the outgroup f_3-test, f_3*(Mbuti; Hòabìnhian, X)*, where X are ancient and present-day East Eurasians, and the f_4-test, f_4*(Mbuti, G1; Ikawazu, North/South)*, to determine if the Jōmon share higher genetic similarity with G1 than East Asians (Table

S8a). We also used a symmetry test for Ikawazu, of the form *f_4(Mbuti, Ikawazu; North/South, North/South)*, with results in Table S9.

5. Inferring a maximum likelihood phylogeny with migration events

In the Treemix analysis, we included the following populations.

1. Mbuti: present-day population from Central Africa that we designated as outgroup (*68*)
2. UstIshim: 45,000-year-old individual from a population basal to both Europeans and Asians (*71*)
3. Yana: two 37,000-year-old individuals from Siberia with early European affiliations (*9*)
4. Tianyuan: 40,000-year-old 'early Asian' from China from a population that separated early from East Asians (*20*)
5. Ikawazu: 2,700-year-old 'early Asian' from the Japanese archipelago belonging to the Jōmon culture (*7*)
6. Shamanka_EN: 7,900-year-old individuals from the Lake Baikal region with a close relationship to East Asians belonging to the steppe Siberia_EN group (*72*)
7. DevilsCave_EN: 7,700-year-old individuals from the Primorye region with a close relationship to East Asians (*72*), in the coastal Siberia_EN group
8. Chokhopani: 3,150-year-old individual from the Himalayan region of the Tibetan Plateau with a close relationship to East Asians (*68*), in the Tibet_LN group
9. Vanuatu: 2,900-year-old individuals from Vanuatu island in the southwest Pacific related to the Lapita culture with a close relationship to Austronesians (*73*), in the Austronesian_LN/B group
10. Yumin: 8,500-year-old newly sampled individual from Inner Mongolia belonging to the inland nEastAsia_EN group
11. Coastal nEastAsia_EN: 9,500-7,500-year-old newly sampled individuals from the lower reaches of the Yellow River
12. sEastAsia_EN: 9,000-7,500-year-old newly sampled individuals from southern mainland China and Liang Island in the Taiwan strait
13. sEastAsia_LN: 5,000-4,000-year-old newly sampled individuals from southern mainland China and Penghu Island in the Taiwan strait

The coastal nEastAsia_EN and sEastAsia_EN/LN groups merged individuals from Table S1 belonging to that group. For instance, Xitoucun, Suogang, and Tanshishan individuals were all included in coastal sEastAsia_LN.

6. Inferring admixture without an explicitly modeled phylogeny

To use qpWave and qpAdm to infer mixture proportions, the first step is to develop an outgroup set, or the 'Right' set, that must differ in their relationship to the samples under assessment (*15*). That is, they must not all share the same relationship to all assessed individuals (e.g. in a study on East Asia, a 'Right' set of only present-day Africans would have little to no power to inform on different relationships within East Asians. Our right population include one ancient Ethiopian, a diverse set of ancient individuals from West Eurasia, Central Asia, and South Asia, and North America, as well as two present-day

populations from the Andamanese Islands and Papua New Guinea. We also added an Upper Paleolithic individual from East Asia and other populations on the Asian lineage such as Hòabìnhians (G1), Paleosiberians (Kolyma), and Jōmon (Ikawazu). Finally, we included the two oldest individuals from our newly sampled East Asians – the northern East Asian Bianbian and the southern East Asian Qihe.

Right: Mota (*74*), UstIshim (*71*), Kostenki14 (*69, 75*), Iran_N (*76*), Yana1 (*9*), Karelia (*15*), Okunevo_EMBA (*9*), IndusPeriphery (merged Gonur2_BA and Shahr_I_Sokhta_BA2 from (*77*)), Papuan (*68*), Onge (*68*), USR1 (*78*), Tianyuan, G1 (*7*), Kolyma (*9*), Ikawazu (*7*), Qihe, and Bianbian.

We tested for admixture using the following logic. We first needed to choose samples to represent source populations. Ideally, we want the representative samples to be unadmixed and in particular, not be admixed with each other. As Boshan and Liangdao2 are the most closely related to Qihe and Bianbian in our right set, representing northern and southern East Asians, respectively, we tested whether they would be appropriate representative sources. To make sure that their ancestries were distinct from each other (thus representing two distinct sources), we used qpWave to check if they can be described as a single wave of ancestry ($p>0.05$). If they cannot be described as a single wave of ancestry ($p<0.05$), then they come from two distinct source populations. We found that they cannot be described by a single wave of ancestry in a qpWave analysis (reject rank 0: $p=4.6e-9$), allowing us to treat Boshan and Liangdao2 as representative of two distinct sources – a northern and southern East Asian source, respectively.

We then investigated whether ancient and present-day populations in Asia could be described as a mixture of three ancestries. Two of these ancestries were represented by Boshan and Liangdao2 (for northern and southern East Asian, respectively), and the third was one representing another Asian ancestry (either Ikawazu, G1, or Kolyma – individuals with Jōmon, Hòabìnhian, or Paleosiberian ancestry).

The three-source model was retained if all conditions were satisfied – particularly that a three-source model was significantly better than a two-source model ($pnest<0.05$). Other conditions included that a three-source mixture model was not rejected ($rank0>0.05$), the estimated admixture proportions were between 0 and 1, and $\min(f_1, f_2, f_3)>0$. In these cases, we can reject a model with fewer sources.

When we could not reject a model with fewer sources, we then considered every two-source model. Here, we followed a similar procedure, where we retained the two-source model if it was significantly better than a single source model ($pnest<0.05$). Other conditions included that a two-source model was not rejected ($rank0>0.05$), the estimated admixture proportions were between 0 and 1, and $\min(f_1, f_2)>0$. In these cases, we can reject a model with a single source. When a single source model could not be rejected, we then considered a single source model, asking which source was the best fit to the target population (highest rank0). These results are included in Table S6 and visualized in Fig. 3D-3F and S13.

7. Building an Admixture Graph using newly sampled individuals and select ancient Asians

To build an Admixture Graph, we started with a base graph including the central African Mbuti as an outgroup, and the early European Kostenki14 and early Asian Tianyuan. To these we added the ancient North Siberian Yana, who fit best as a mixture of these two ancestries, consistent with Yana possessing both early European and Tianyuan-related ancestry (*9*).

To this graph, we added the following: Yumin, Liangdao2, Boshan, Kolyma, Shamanka_EN, Xiaogao, Qihe. We tested altering the order of addition of several sets, particularly whether Liangdao2 could be added after Boshan is already in the model. In this and other orderings, we either found that a full model (including all sets described above) is not feasible (|maxZ|>3) or the pattern was very similar to what is described below.

We first added Yumin, an 8,400-year-old individual from Inner Mongolia. While a few trees satisfy the above conditions, two do not require admixture, where Yumin is either added to the Tianyuan branch before (|maxZ|=1.028) or after (|maxZ|=0.899) the Yana admixture event. As they are more parsimonious than trees with an admixed Yumin, and other results do not indicate strong mixture patterns for Yumin, we build further from these two trees. Adding the 7,600-year-old Liangdao2, we again observe several graphs that are feasible. As we did not observe patterns suggesting Liangdao2 is admixed previously, we focus on two graphs – one where Liangdao2 is a mixture of the shared Asian branch (88%) and the Yumin branch (|Z|<1.229), and the other where Liangdao2 is most closely related to Yumin (|Z|<1.893). Totaling to four graphs, accounting for each of the possibilities for Yumin and Liangdao2, we next add the 8,300-year-old Boshan individual (Fig. S16).

To these graphs, we next added Kolyma, an ancient Paleosiberian, and Shamanka_EN, an Eastern Steppe individual with a close relationship to Yumin (Fig. S17). We next added Xiaogao and Qihe. When the graph has an admixed coastal Neolithic northern East Asian population, we find that Xiaogao can be included as unadmixed, closest to the Boshan branch. While there are other feasible graphs, we focus on this pattern as it is most parsimonious. When Boshan is unadmixed, we observe that the only feasible graph is where Xiaogao is included as a mixture of the Boshan branch and the Liangdao2 branch. To these three graphs, we added Qihe. The graphs in Fig. 2B and S17 are not the only ones that fit the data with |maxZ|<3, but they capture many patterns discussed previously.

Adding other East Asians to Fig. 2B

We next considered adding other ancient or present-day East Asians to the graph in Fig. 2B, to explore which ancestries may have contributed to which East Asian populations. Using this base graph, we ask with which one or two ancestries is each East Asian most associated. While this base graph is one of many feasible trees, we expect that overall, the general relationships will remain consistent, even if proportions vary slightly. One limitation to keep in mind is that each target can be described as a single ancestry or a mixture of two ancestries, but not more. Thus, East Asians who are a mixture of more than

two ancestries may not be well described. We add each East Asian in turn to the graph in Fig. 2B, choosing the graph with the lowest |maxZ|, no 100% admixtures, and where the zero branch lengths are not ones leading to the newly added East Asian. We emphasize that these conditions do not indicate the best-fitting tree – the lowest |maxZ| may be above three, which would suggest the base graph is not a good fit, and there may be multiple trees with a |maxZ|<3. We still highlight the single tree to point to general patterns observed by testing the inclusion of other East Asians to the base graph. These results are shown in Fig. 2C-2D.

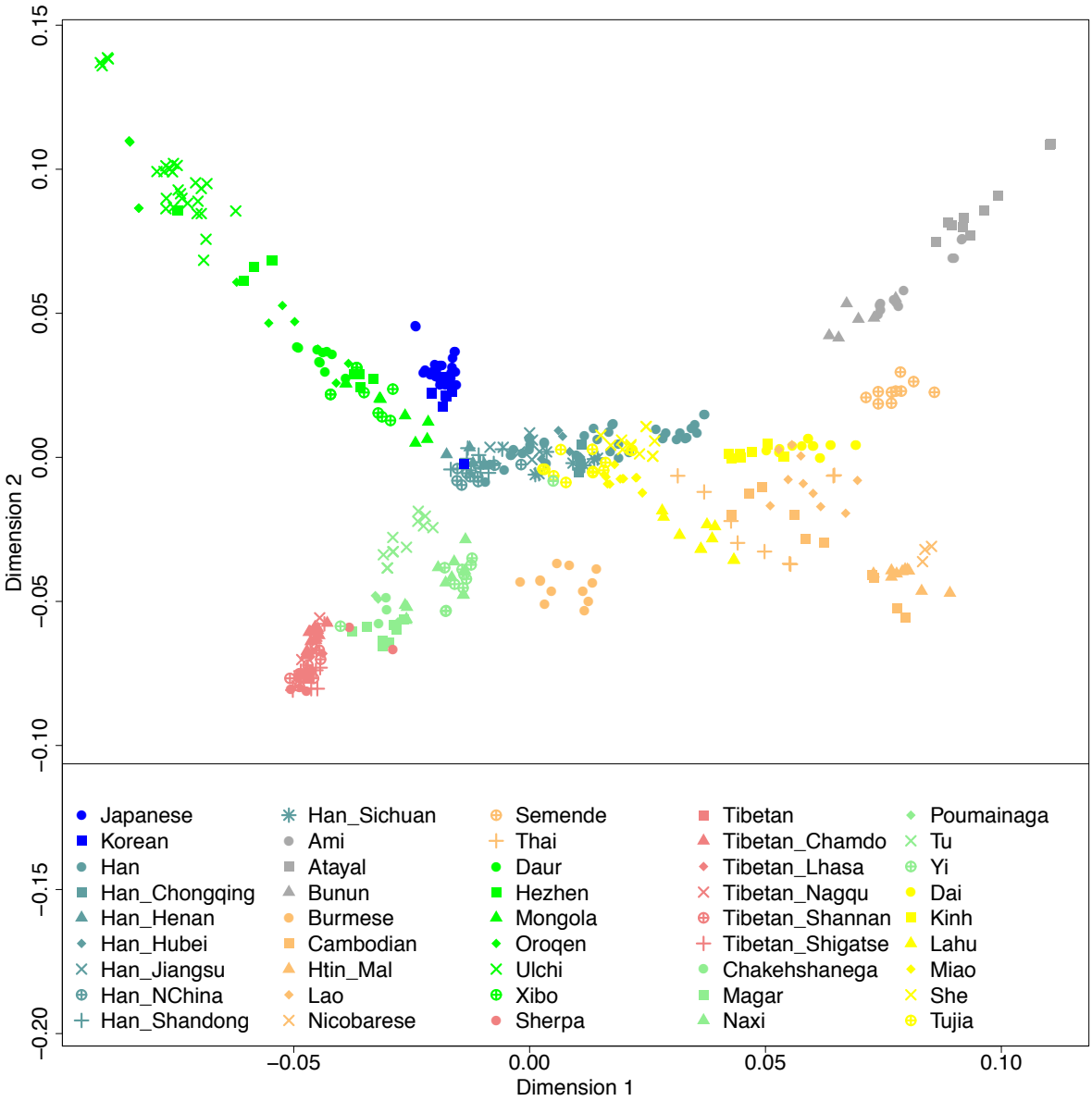

Figure S1. Principal components analysis (PCA) for present-day East Asians for PC1 and PC2. The PCA includes 34 present-day populations from the Human Origin (HO) SNP Panel (*43*), as well as 17 previously published present-day Tibetan and Han populations from ref. (*44*). Ancient individuals from Table S1 were then projected onto these data in Fig. 1C. Present-day East and Southeast Asians from northern (bright green, blue), Tibetan (pastel green and red), and southern regions (gray, orange, yellow) form three distinct clines moving away from the origin, where more centrally located populations (dark green) such as the Han are located. Populations from southern East Asia and Southeast Asia separate Austronesian speakers (e.g. Ami, gray) from the Dai-Kradai (e.g. Dai) and Austroasiatic (e.g. Kinh) speakers.

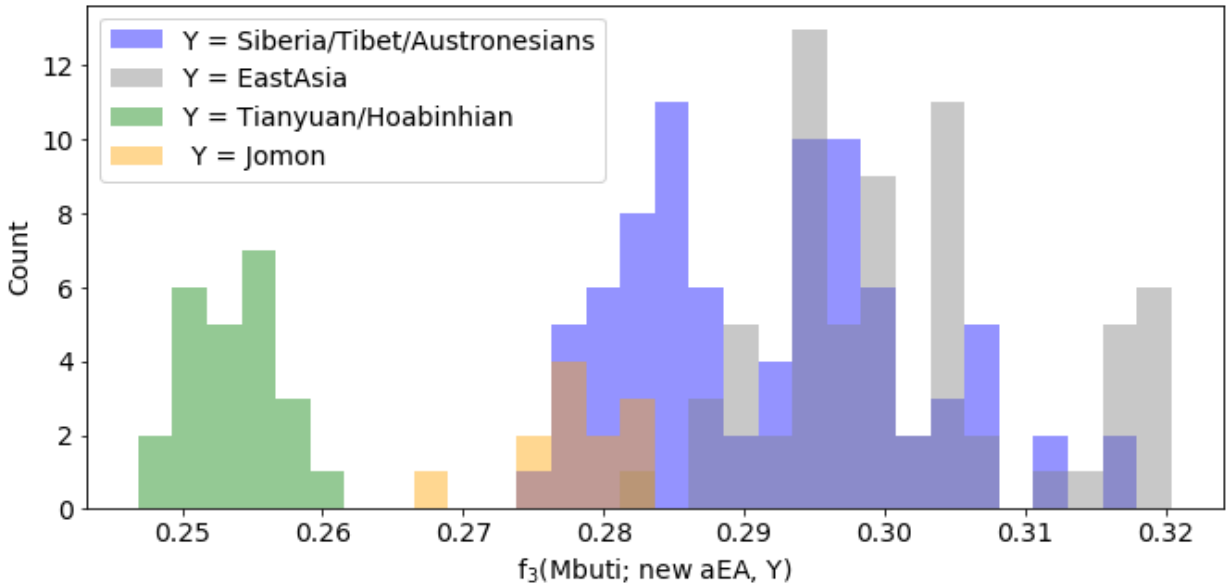

Fig. S2 Genetic similarity between newly sampled ancient East Asians (EastAsia) and previously published ancient individuals (Y) using outgroup *f_3(Mbuti; EastAsia, Y)*. The present-day Central African Mbuti are used as an outgroup to different pairs of East Asians. A higher f_3 value indicates greater genetic similarity between the newly sampled ancient East Asian and the population represented by Y. We find that any pair consisting of a newly sampled individual and an 'early Asian' (Tianyuan, Hòabìnhian, Jōmon) tends to show lower genetic similarity between pairs (0.243-0.279, green and orange) than those consisting of a newly sampled individual and an ancient individual previously observed to share a close genetic relationship to present-day East Asians (0.274-0.316, blue). Comparisons to the Jōmon individual from the Japanese archipelago (Ikawazu) are higher than those to the Tianyuan or Hòabìnhian (G1) individuals, consistent with Jōmon populations sharing a much closer relationship to East Asians than the other two 'early Asians' (*7, 79*). Overlap with Jōmon comparisons are primarily those including the coastal sEastAsia_EN (Qihe, Liangdao) and ancient Tibetans (Tibet_LN/H) or steppe Siberia_EN. Overall, we observe a close genetic affinity between our newly sampled East Asians and ancient individuals previously found to possess high East Asian ancestry.

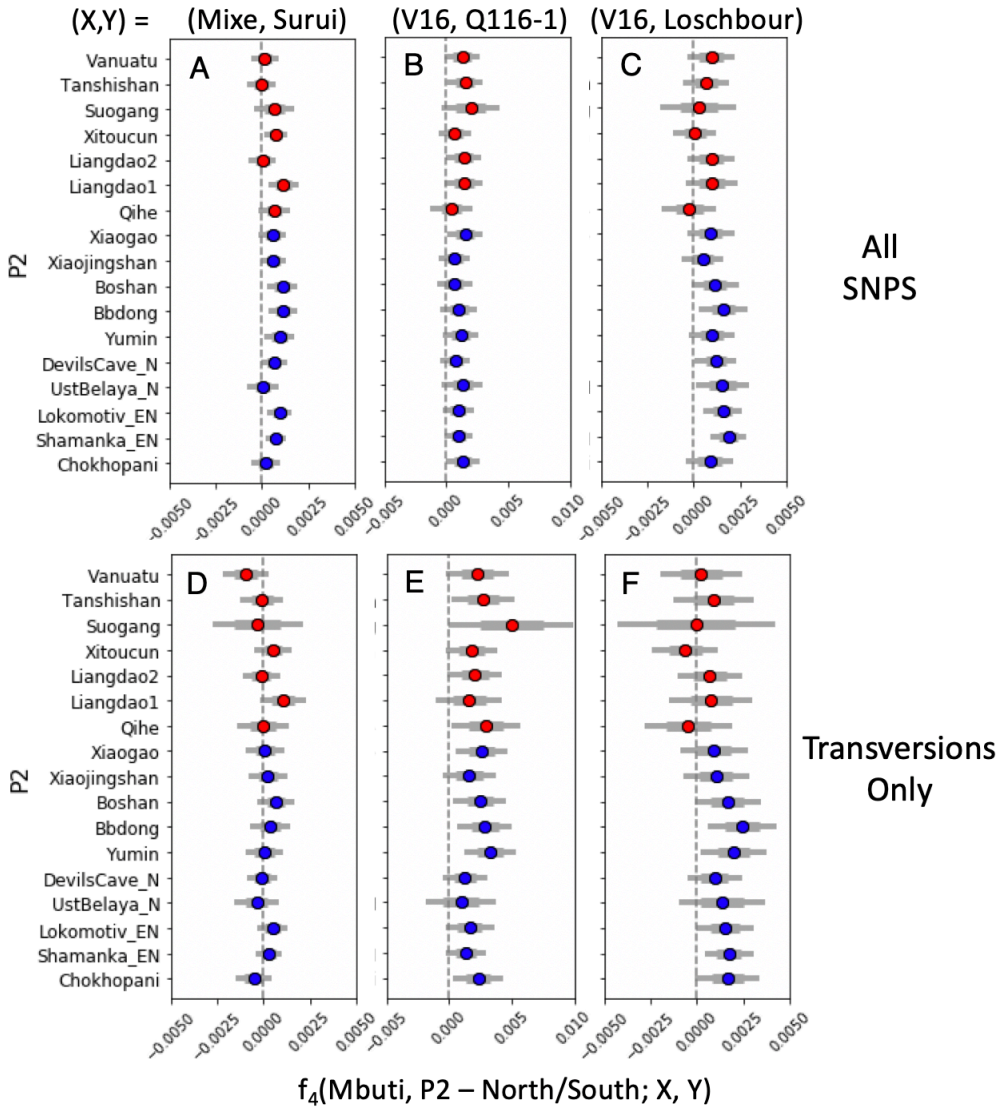

Fig. S3. Results for *f_4(Mbuti, P2 – North/South; X, Y)*, where X and Y are populations without East Asian ancestry. North/South refer to ancient groups of East Asian ancestry (Table S1). Significant positive values indicate that the ancient East Asian shares ancestry with Y while significant negative values indicate that the ancient East Asian shares ancestry with X. A-C are for all SNPs and D-F are for transversions only. A and D shows *f_4(Mbuti, P2 – North/South; Mixe, Surui)*; B and E shows *f_4(Mbuti, P2 – North/South; Vestonice16, GoyetQ116-1)*; and C and F shows *f_4(Mbuti, P2 – North/South; Vestonice16, Loschbour)*. V16 stands for Vestonice16, and Q116-1 refers to GoyetQ116-1. The red points indicate comparisons to South samples, while the blue points indicate comparisons to the North samples. The dashed line indicates where *f_4=0*. The thick gray bar indicates one standard error, while the thin gray bar indicates two standard errors. We observe some affinity to the South American Surui using all sites, but we no longer observe this pattern using transversions only. For transversions only, some populations carrying northern East Asian ancestry share a slight connection to the 35,000-year-old individual from Belgium (GoyetQ116-1) (*69*), while populations carrying northern East Asian ancestry share a slight connection to the West European 8,000-year-old hunter-gatherer (Loschbour).

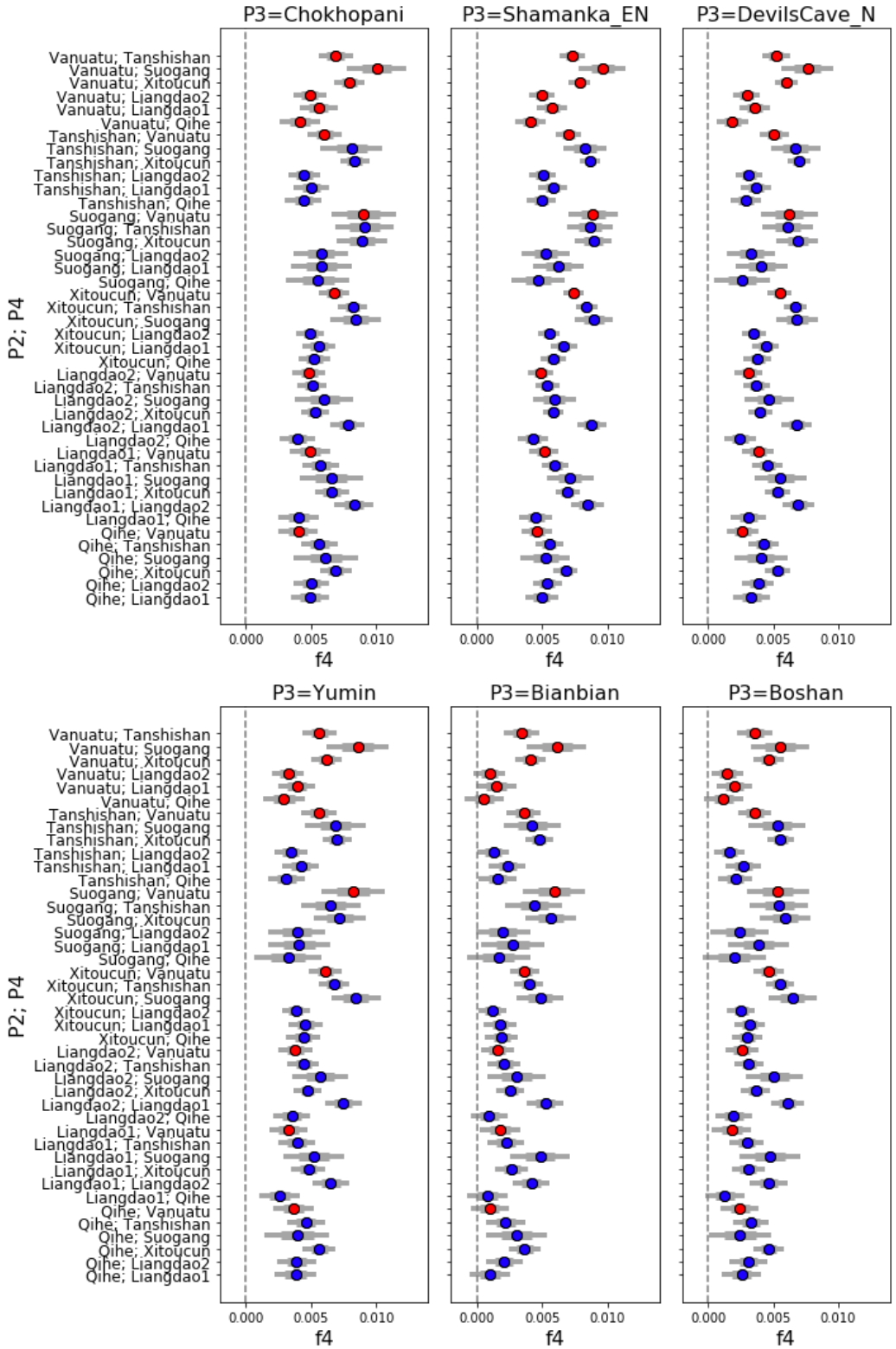

Fig. S4A. F_4-statistics assessing the genetic relationship of Neolithic southern East Asians and the Southwest Pacific Vanuatu (South) relative to Neolithic northern East Asians, Tibetans, and Siberians (North). Results for *f_4(Mbuti, South; North, South)*. See legend after Fig. S4B.

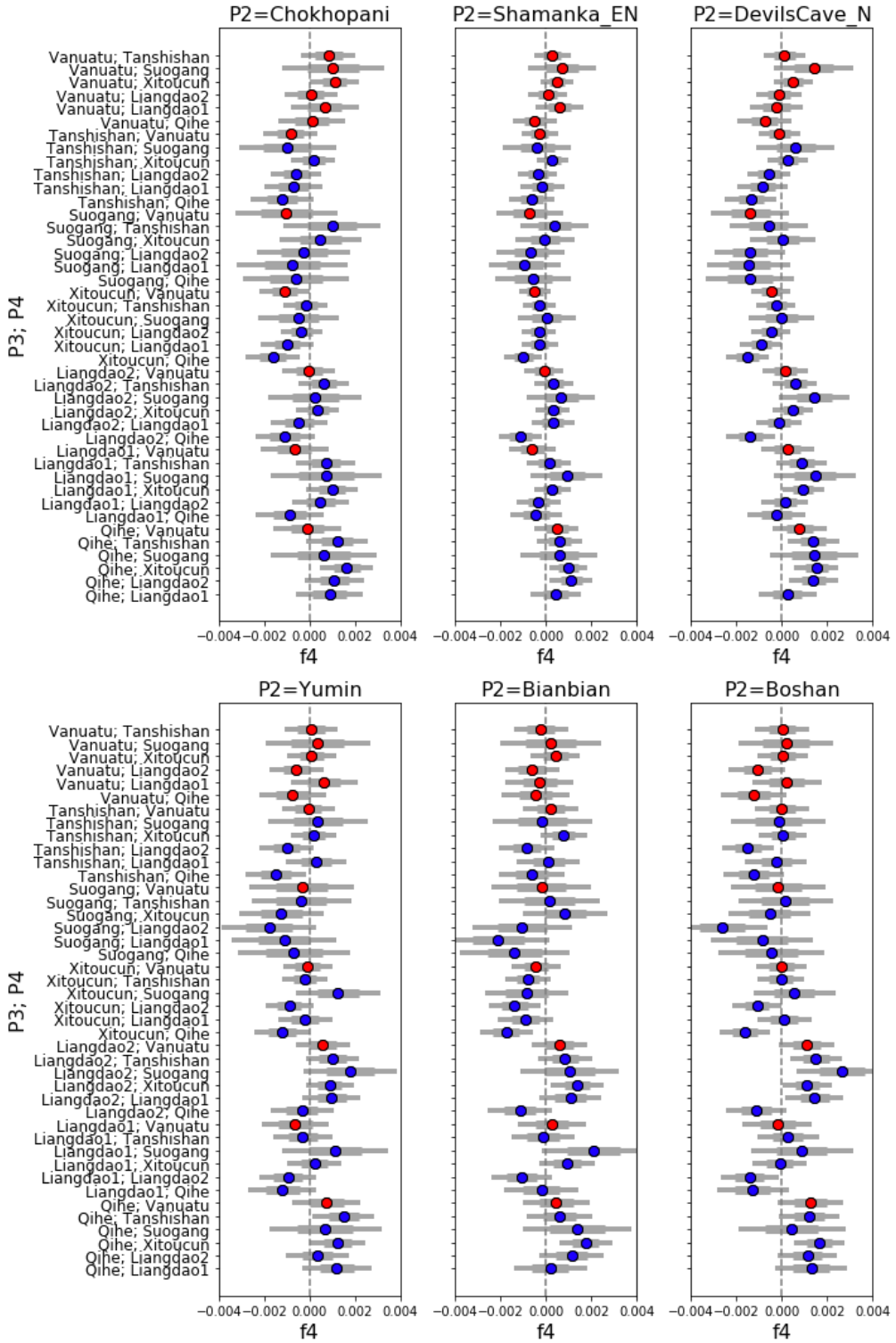

Fig. S4B. F_4-statistics assessing the genetic relationship of Neolithic southern East Asians and the Southwest Pacific Vanuatu (South) relative to Neolithic northern East Asians, Tibetans, and Siberians (North). Results for *f_4(Mbuti, North; South, South)*. See legend on next page.

Fig. S4. F_4-statistics assessing the genetic relationship of Neolithic southern East Asians and the Southwest Pacific Vanuatu (South) relative to Neolithic northern East Asians, Tibetans, and Siberians (North). We carried out analyses of the form f_4*(Mbuti, P2; P3, P4)* where the Y-axis for each panel gives the samples in the P2 and P4 positions and the label at the top of the panel gives the sample in the P3 position. Significant positive values of this statistic indicate shared ancestry between the samples in the P2 and P4 positions. Significant negative values indicate shared ancestry between the samples in the P2 and P3 positions. For more details on samples included, see Table S1. Red points indicate comparisons including Austronesian_LN/BA (Vanuatu). The dashed line indicates where $f_4=0$. The thick gray bar indicates one standard error, while the thin gray bar indicates two standard errors. In (A), which compares f_4*(Mbuti, South; North, South)*, significant positive values indicate shared ancestry between two samples from the South, while significant negative values indicate shared ancestry between a South sample and a North sample. Almost all samples in the South group tend to share a closer relationship with each other than to any sample in the North group, including the Southwest Pacific islander who shares a close relationship to present-day Austronesian speakers (Vanuatu, red). In (B), which compares f_4*(Mbuti, North; South, South)*, significant positive or negative values indicate excess connection of a South sample with the North sample, while non-significant values indicate the South samples are similarly related to the North sample. Almost all samples in the South group are similarly related to the North sample to which they were compared. The main exceptions are those cases where a Late Neolithic southern East Asian (most robust for Xitoucun) shares excess genetic similarity to a North sample relative to an Early Neolithic southern East Asian (most robust for Qihe).

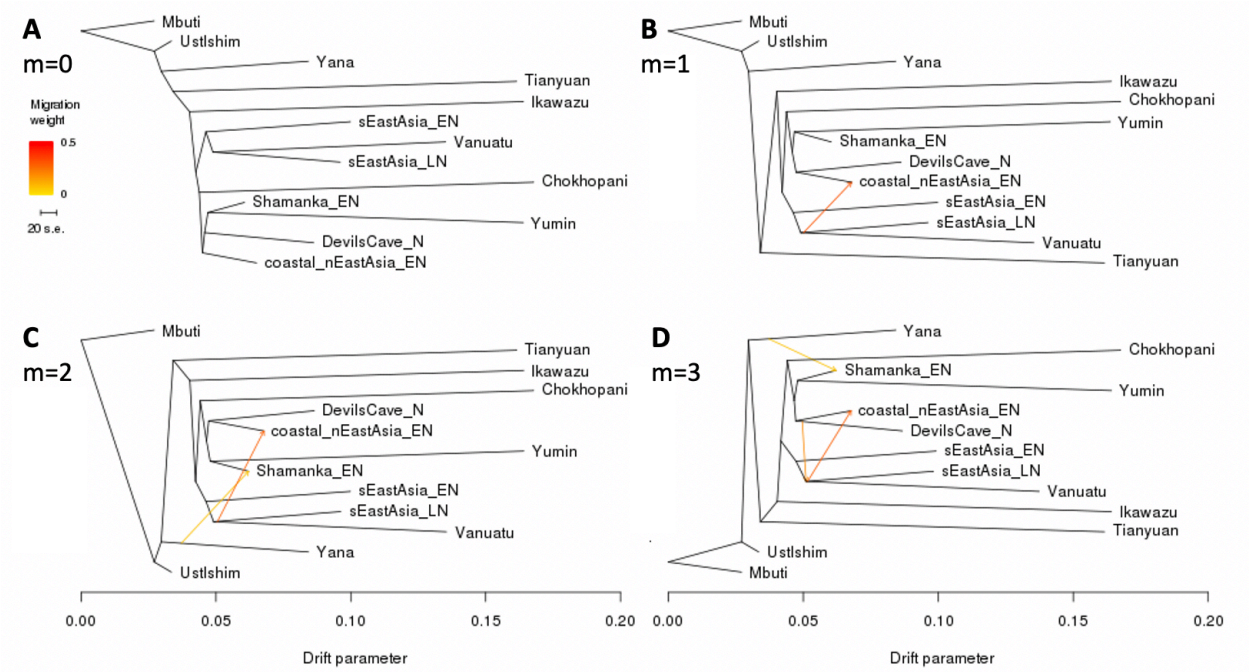

Fig. S5. Maximum likelihood phylogenies with zero through three migration events. The scale bar on the x-axis shows twenty times the average standard error of the entries in the sample covariance matrix. The number of overlapping SNPs is 225,297. We observe that northern East Asians, Siberians, and Tibetans from the Neolithic group together (North), while southern East Asians and Vanuatu from the southwest Pacific group together (South). The 'early Asians' (Tianyuan and Ikawazu) are an outgroup to both the North and the South, and Ust'-Ishim and Yana are an outgroup to 'early Asians', the North, and the South. Migration events are included in the following order: admixture into coastal nEastAsia_EN, admixture from Yana into Shamanka_EN, and admixture from northern East Asians into younger southern East Asians.

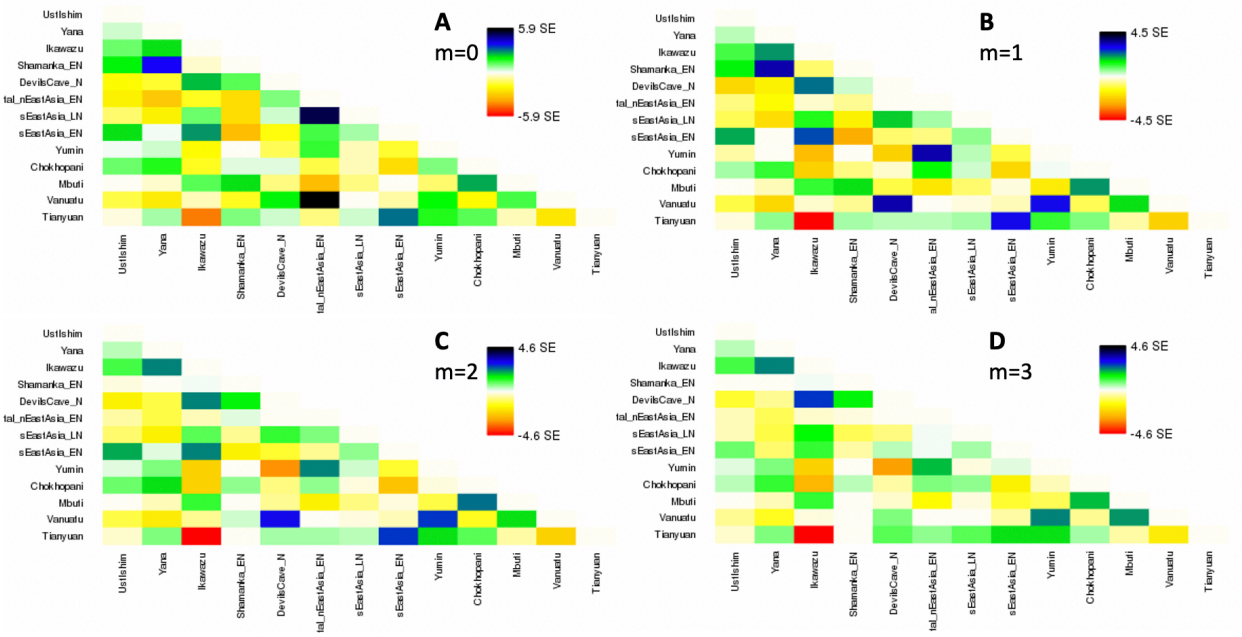

Fig. S6. Pairwise residuals for the phylogenies in Fig. S5. In A, for m=0, the residual is high comparing coastal_nEastAsia_EN to sEastAsia_LN and the Vanuatu from the Southwest Pacific Islands, as well as between Yana and Shamanka_EN from Siberia.

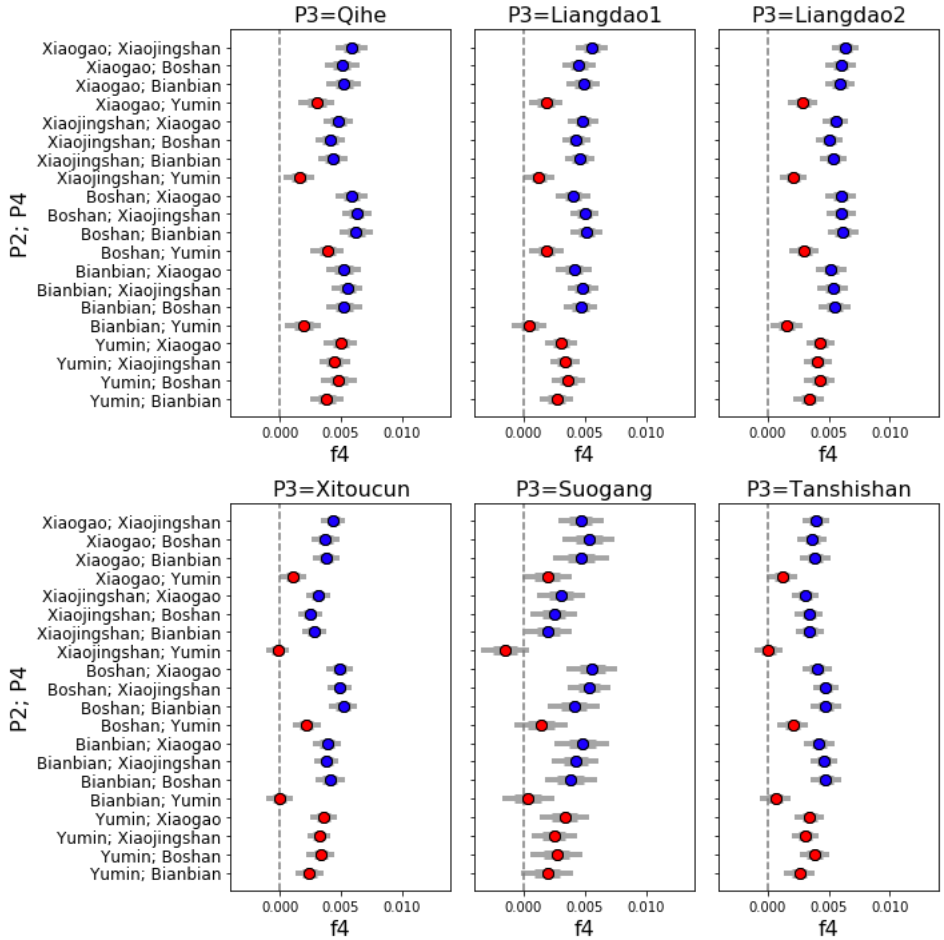

Fig. S7. Results for *f_4(Mbuti, inland or coastal nEastAsia_EN; South, inland or coastal nEastAsia_EN).* We carried out analyses of the form *f_4(Mbuti, P2; P3, P4)* where the Y-axis for each panel gives the samples in the P2 and P4 positions and the label at the top of the panel gives the sample in the P3 position. Different pairs of inland and coastal nEastAsia_EN samples are in the P2 and P4 positions, while in the P3 position are sEastAsia_EN (top row of panels) and sEastAsia_LN (bottom row of panels) samples (Table S1). Red indicates comparisons including the inland nEastAsia_EN sample (Yumin), while blue are comparisons exclusively among coastal nEastAsia_EN samples. The dashed line indicates where $f_4=0$; positive values indicate that the two nEastAsia samples share ancestry, while negative values indicate that the nEastAsia sample in the P2 position shares ancestry with the sEastAsia sample. The thick gray bar indicates one standard error, while the thin gray bar indicates two standard errors. The coastal nEastAsia_EN share a close genetic relationship with each other. This pattern is also observed when the inland nEastAsia_EN (Yumin, red) sample is included, although the results are less significant. An exception is that coastal nEastAsia_EN tend to share a similar number of alleles to both the inland nEastAsia_EN and coastal sEastAsia_LN (second row), suggesting more shared ancestry with Late Neolithic southern East Asians than Early Neolithic southern East Asians.

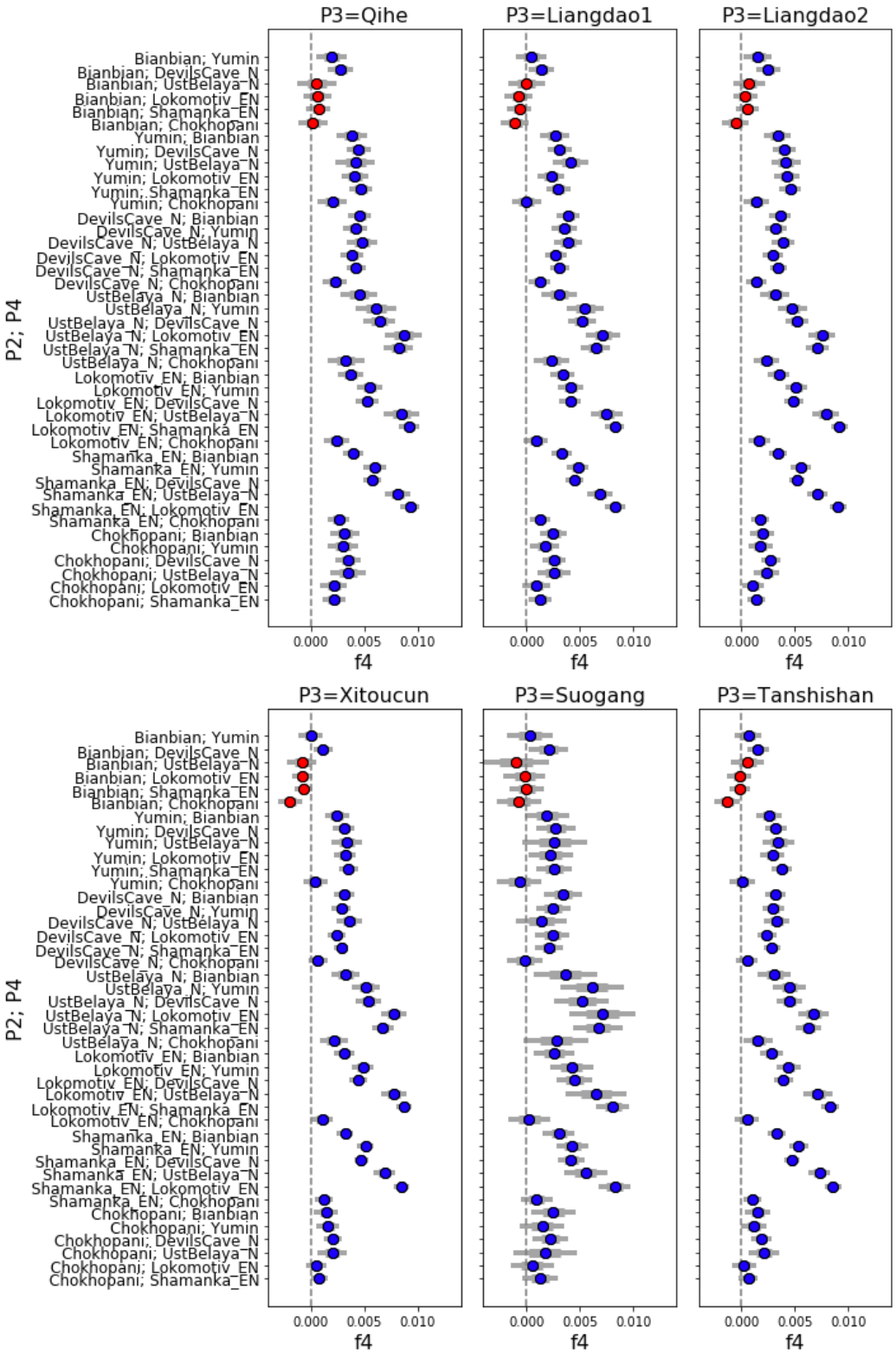

Fig. S8A. F_4-statistics assessing the genetic relationship of Neolithic northern East Asians, Tibetans, and Siberians (North=nEastAsia_EN, Tibet_LN, Siberia_EN) relative to Neolithic southern East Asians (South=sEastAsia_EN/LN). Results for *f_4(Mbuti, North; South, North)*. See legend after Fig. S8B.

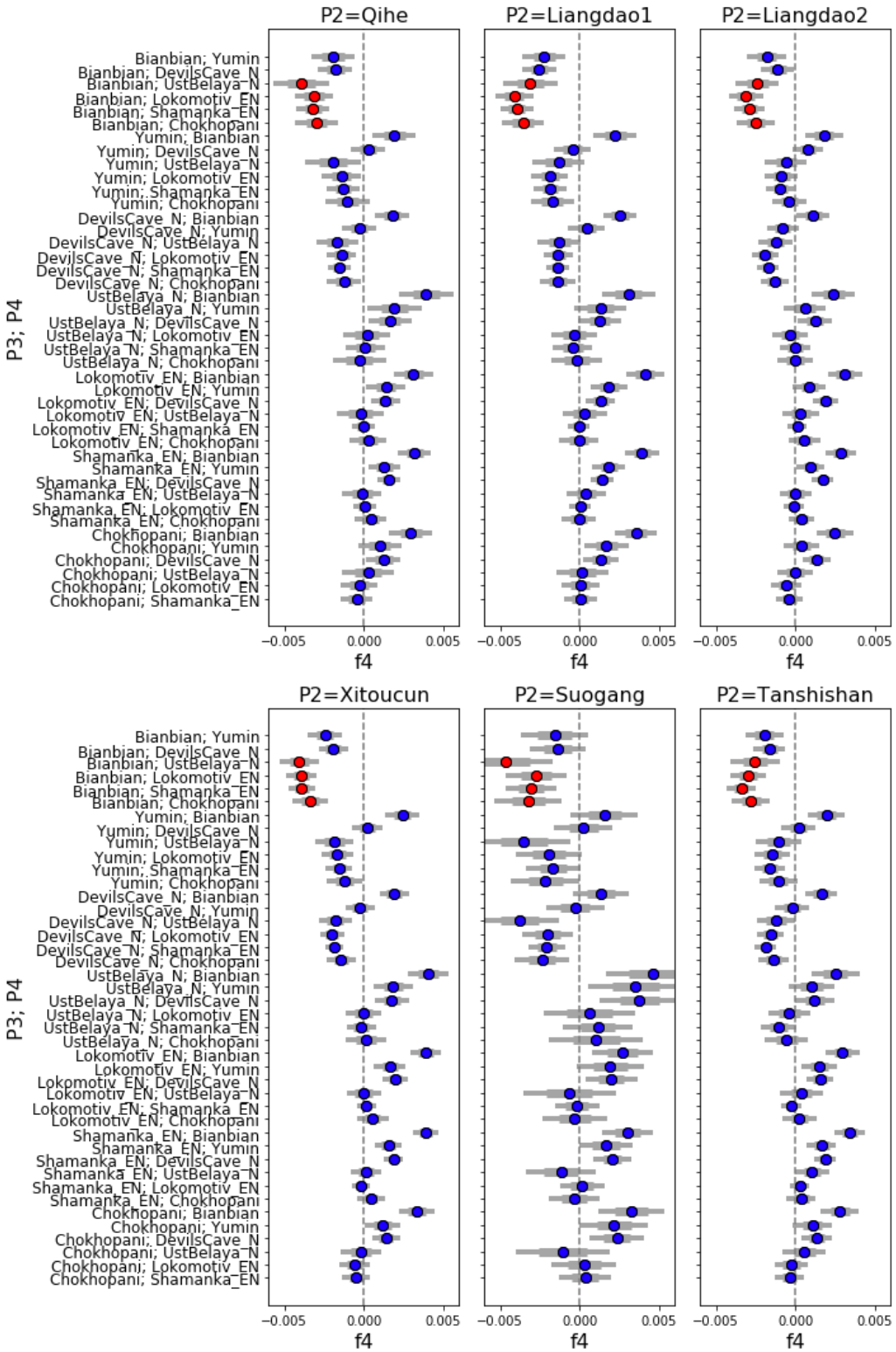

Fig. S8B. F_4-statistics assessing the genetic relationship of Neolithic northern East Asians, Tibetans, and Siberians (North=nEastAsia_EN, Tibet_LN, Siberia_EN) relative to Neolithic southern East Asians (South=sEastAsia_EN/LN). Results for *f_4(Mbuti, South, North, North)*. See legend on next page.

Fig. S8. F_4-statistics assessing the genetic relationship of Neolithic northern East Asians, Tibetans, and Siberians (North=nEastAsia_EN, Tibet_LN, Siberia_EN) relative to Neolithic southern East Asians (South=sEastAsia_EN/LN). We carried out analyses of the form $f_4(Mbuti, P2; P3, P4)$ where the Y-axis for each panel gives the samples in the P2 and P4 positions and the label at the top of the panel gives the sample in the P3 position. Significant positive values of this statistic indicate shared ancestry between the samples in the P2 and P4 positions. Significant negative values indicate shared ancestry between the samples in the P2 and P3 positions. For more details on samples included, see Table S1. Red points indicate comparisons with the coastal Neolithic northern East Asian Bianbian and steppe Siberians and Tibetans. The dashed line indicates where $f_4=0$. The thick gray bar indicates one standard error, while the thin gray bar indicates two standard errors. In (A), which compares $f_4(Mbuti, North; South, North)$, significant positive values indicate shared ancestry between two samples from the North, while significant negative values indicate shared ancestry between a North sample and a South sample. The inland nEastAsia_EN, the coastal and steppe Siberia_EN, and the Tibet_LN generally share a closer genetic relationship to each other than to coastal sEastAsia_EN/LN. The coastal nEastAsia_EN (Bianbian) share a closer genetic relationship to coastal Siberia_EN (DevilsCave_N) and the inland nEastAsia_EN (Yumin) relative to the coastal sEastAsia_EN/LN. The steppe Siberia_EN and Tibet_LN share more alleles with the coastal nEastAsia_EN than with the coastal sEastAsia_EN/LN, but the reverse is not true – coastal nEastAsia_EN (Bianbian) are similarly related to the steppe Siberia_EN and Tibet_LN and coastal sEastAsia_EN/LN (red). In (B), which compares $f_4(Mbuti, South; North, North)$, significant positive or negative values indicate excess connection of a North sample with the South sample, while non-significant values indicate the North samples are similarly related to the South sample. Here, we find that the steppe Siberia_EN and Tibet_LN do not show excess connections with a South sample, but others do. The coastal nEastAsia_EN Bianbian shares excess connection to all South samples relative to other North samples, and the inland nEastAsia_EN Yumin and coastal Siberia_EN DevilsCave_N share excess connection to most South samples relative to the steppe Siberia_EN and Tibet_LN.

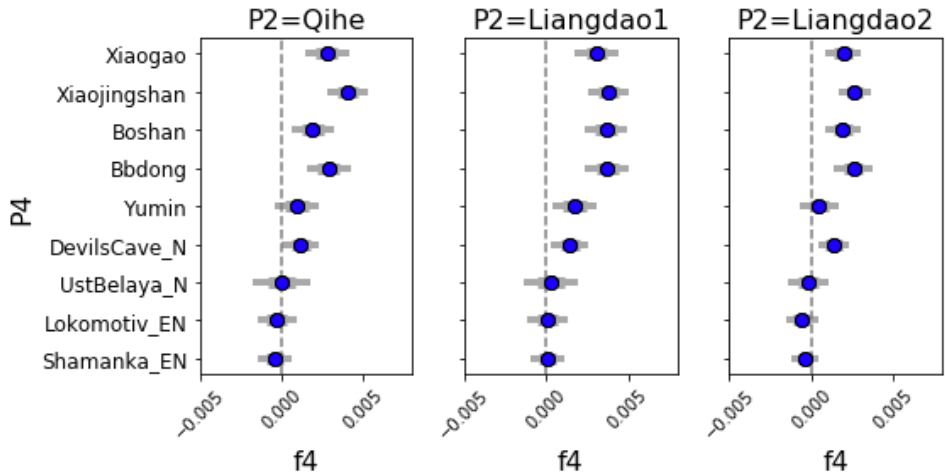

Fig. S9. Results for *f_4(Mbuti, South; Tibet_LN, North)*. We carried out analyses of the form *f_4(Mbuti, P2; Chokhopani, P4)* where the Y-axis for each panel gives the samples in the P4 position and the label at the top of the panel gives the sample in the P2 position. Significant positive values of this statistic indicate that there is excess shared ancestry between the samples in the P2 and P4 positions (i.e., between the Early Neolithic southern East Asians and the North group (, or nEastAsia_EN and Siberia_EN, Table S1). The dashed line indicates where $f_4=0$. The thick gray bar indicates one standard error, while the thin gray bar indicates two standard errors. These results show that Early Neolithic southern East Asians share a connection to coastal Early Neolithic northern East Asians relative to the inland Late Neolithic Tibetan (Chokhopani), while Neolithic inland Siberians do not.

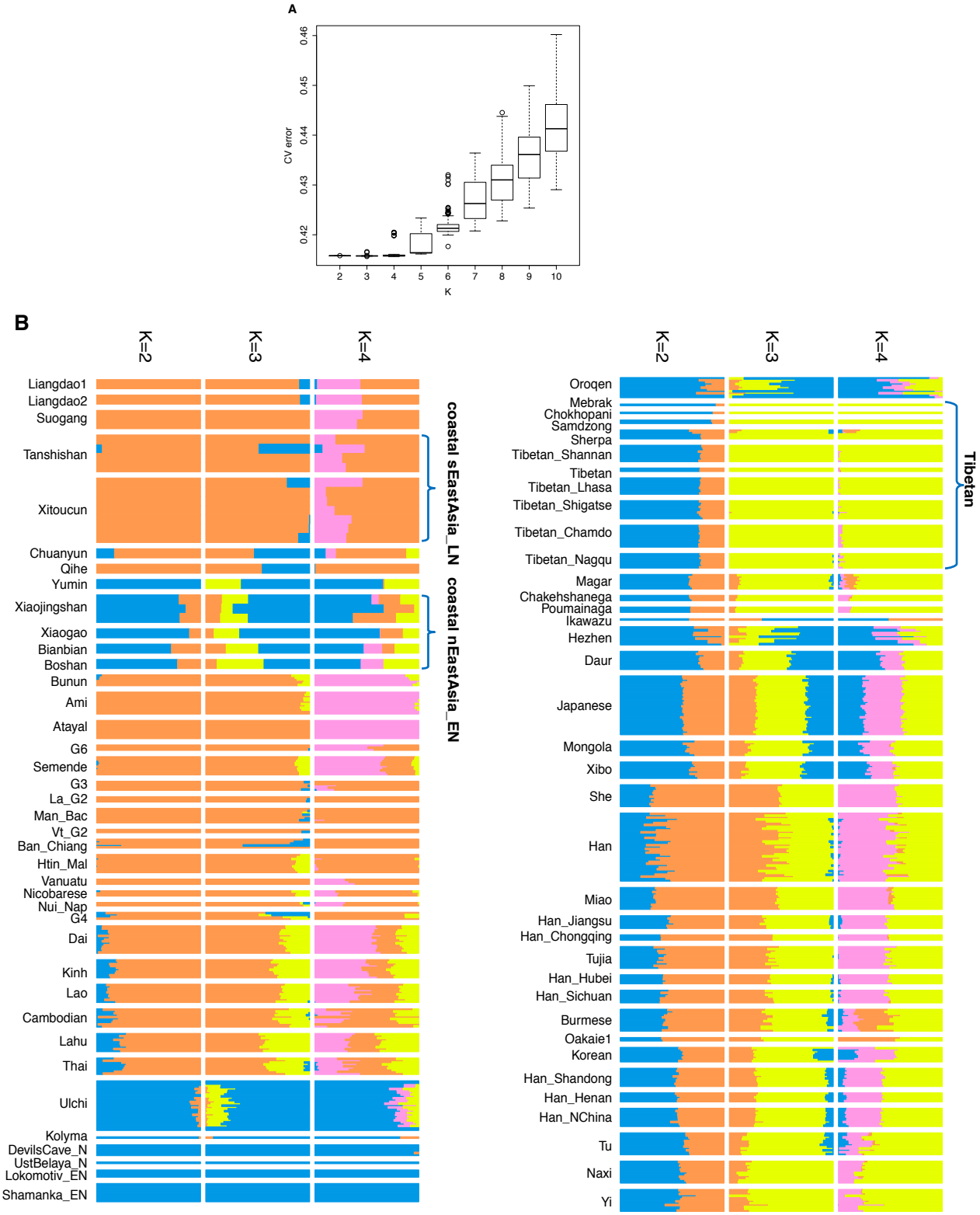

Figure S10. Admixture results for select East and Southeast Asians for K=2 to K=4. (A) Cross-validation (CV) results for different K values ranging from 2 to 10. The lowest CV is when K=3, so in (B), we show Admixture results for K=2 to K=4. After pruning for linkage disequilibrium, the number of SNPs included in this analysis was 200,282. The

newly sampled individuals are at the top. The group information for the labels can found in Table S1. The blue component is predominantly found in northern East Asians; the yellow component is predominantly found in Tibetans, and the orange component is predominantly found in southern East Asians. The southern East Asian-related component can be found across all southern East Asians, past and present, as well as in the coastal nEastAsia_EN, but not in the inland nEastAsian_EN (Yumin) or Siberians from further north, which suggests that the coastal nEastAsia_EN share some ancestry with southern East Asians.

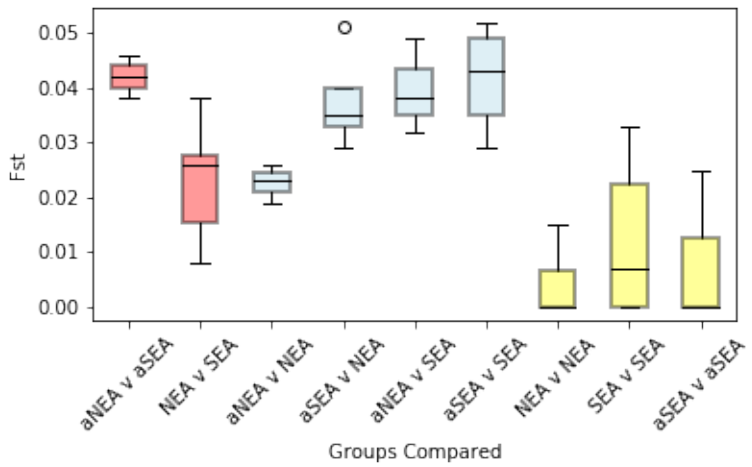

Fig. S11. Fst distributions for different groups of ancient and present-day East Asians. aNEA refers to a group merging the coastal nEastAsia_EN (Table S1); aSEA consists of two groups: a set including Liangdao1 and Liangdao2 (subset of sEastAsia_EN), and the combined set of Xitouchun and Tanshishan (sEastAsia_LN); NEA includes Hezhen, Korean, and Han; SEA includes She, Lahu, and Dai. The Fst comparing any two sets within and between these groups (one aNEA, two aSEA, three NEA, three SEA) was determined. The obtained Fst values are visualized using a boxplot, where the average Fst is indicated by the solid black line, and the first and third quartiles are given by the top and bottom or the rectangular boxes. Red boxplots refer to comparisons between ancient northern and southern East Asians and between present-day northern and southern East Asians. Blue boxplots refer to comparisons of an ancient population to a present-day population, and yellow boxplots refer to comparisons within a grouping (e.g. between the two ancient southern East Asians). The main observation is that present-day northern and southern East Asians (Fst = 0.023, sd=0.01) show a lower Fst than ancient northern and southern East Asians (Fst = 0.042, sd=0.004), and ancient northern East Asians and present-day northern East Asians also have a low Fst (Fst = 0.023, sd=0.003).

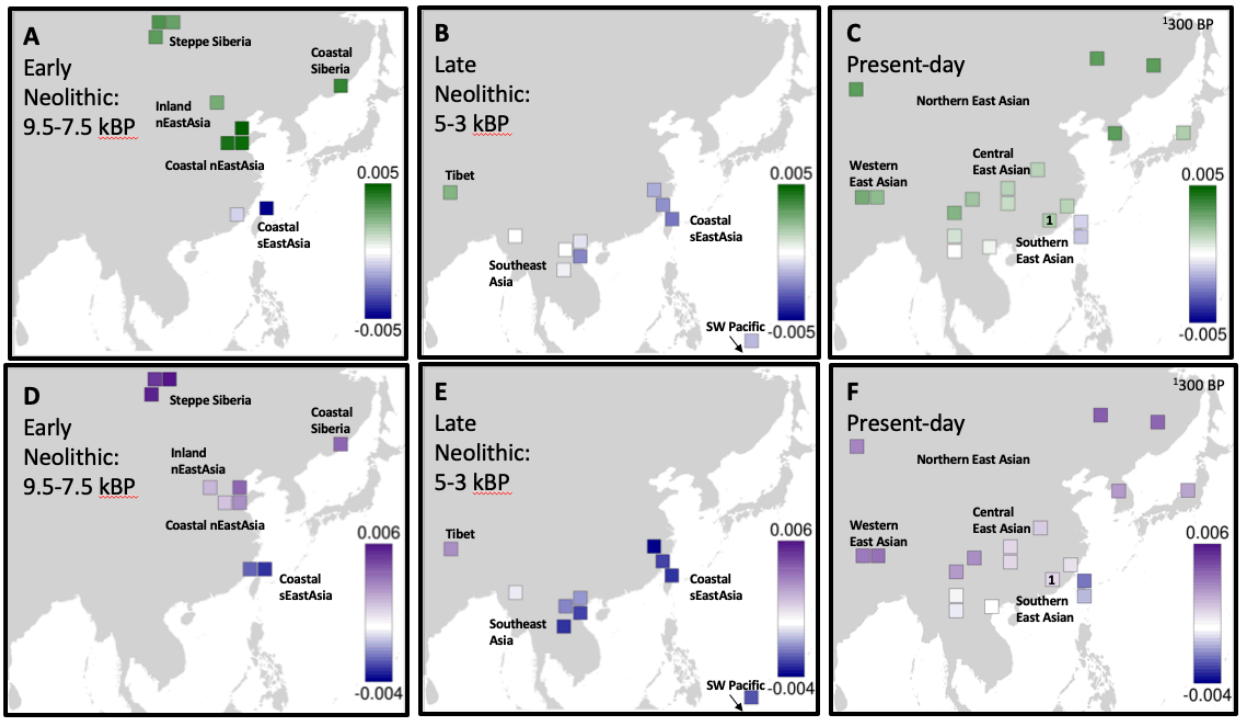

Fig. S12. Heatplot of *f_4(Mbuti, X; South, North)* values mapped onto East Eurasia. Similar to Fig. 3A-3C where we tested *f_4(Mbuti, X; Qihe, Bianbian)*, in A-C we substituted the 8,400 year-old Qihe with another coastal sEastAsia_EN (Liangdao1, 8,300 years old), i.e. *f_4(Mbuti, X; Liangdao1, Bianbian)*. More positive f_4 values (green) indicate a closer affinity to northern East Asian ancestry, while more negative f_4 values (blue) indicate a closer affinity to southern East Asian ancestry. In D-F, we substituted the 9,500-year-old Bianbian with the inland nEastAsia_EN (Yumin, 8,400 years old), i.e. *f_4(Mbuti, X; Qihe, Yumin)*. More positive f_4 values (purple) indicate a closer affinity to northern East Asian ancestry, while more negative f_4 values (blue) indicate a closer affinity to southern East Asian ancestry. In both examples, there is a clear association by geography until the present-day, when southern and central East Asians show greater connections to the inland and coastal nEastAsia_EN. Only present-day Austronesians from Taiwan show connections to coastal sEastAsia_EN, a pattern not observed in Fig. 3C. Numerical values can be found in Table S5B-S5C.

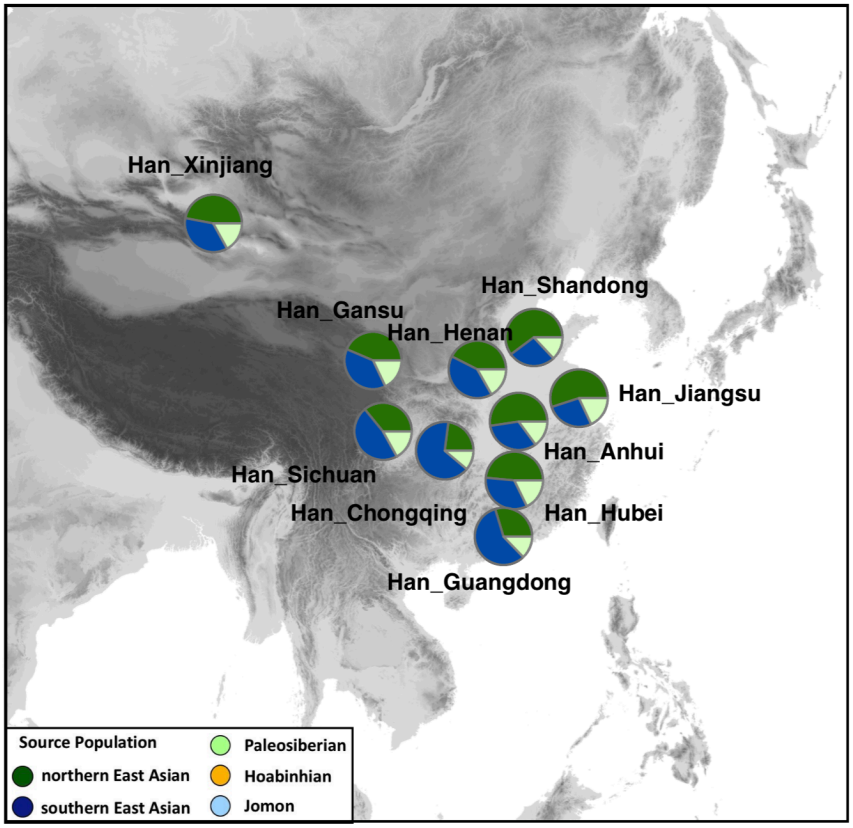

Fig. S13. Ancestry proportions estimated for present-day Han using qpAdm. Possible ancestries are northern East Asian (green), southern East Asian (blue), Paleosiberian (light green), Hoabinhian (orange), and Jōmon (light blue). Proportions were determined using qpAdm, with representative sources and outgroups described in (*14*). The Han in all provinces, north and south, show mixture proportions related to northern East Asians, southern East Asians, and Paleosiberians. The highest northern East Asian-related ancestry is in Shandong province, which is also where the representative source was sampled during the Early Neolithic. This suggests partial continuity into the present in Shandong. Results for other present-day East Asians are in Fig. 3F and point values are in Table S6B.

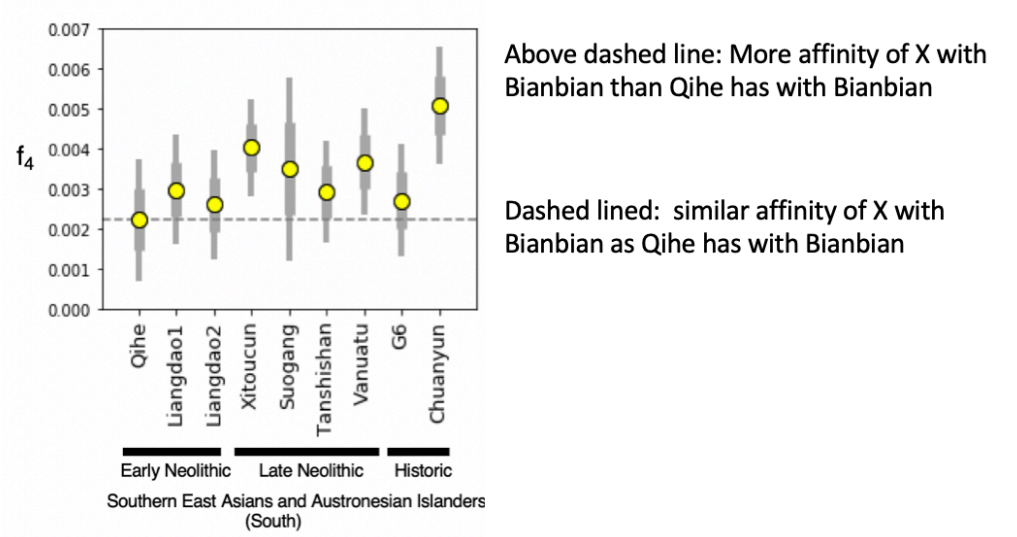

Fig. S14. ***f_4(Mbuti, Bianbian; Kolyma, South)*** **where South includes all Early and Late Neolithic southern East Asians and Austronesians, as well as historical samples.** The thick gray bar indicates one standard error, while the thin gray bar indicates two standard errors. The gray dashed line indicates the f_4 value for *f_4(Mbuti, Bianbian; Kolyma, Qihe)*, such that those combinations with an f_4 value above the dashed line share more affinity with Bianbian than Qihe shares with Bianbian. Without admixture with Early Neolithic coastal northern East Asians (represented by Bianbian), we would expect that every f_4 value would be uniform for all South individuals. However, we find higher f_4 values for several Late Neolithic South individuals, which suggests they show more northern affinities than the Early Neolithic coastal southern East Asians.

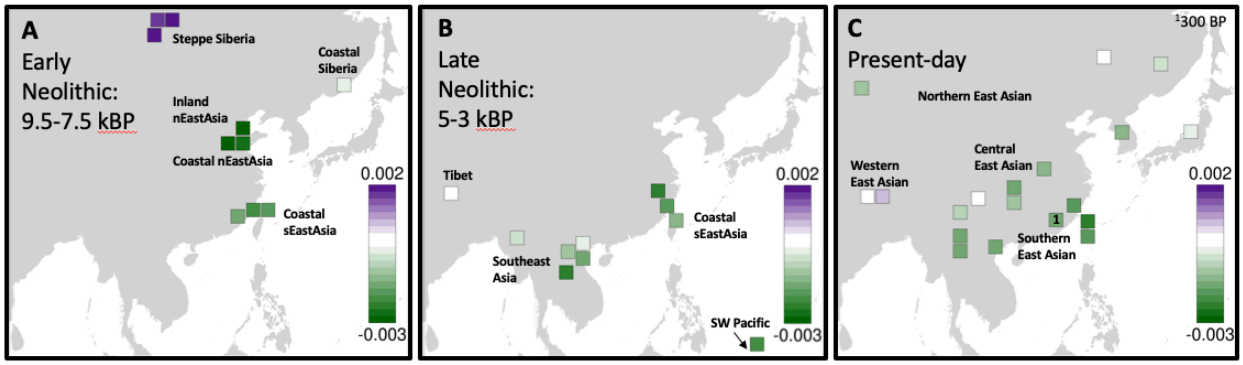

Fig. S15. Heatplot of *f_4(Mbuti, X; coastal nEastAsia_EN, inland nEastAsia_EN)* values for different time periods mapped onto East Eurasia. We computed *f_4(Mbuti, X; Bianbian, Yumin)*, where a more positive value (purple) indicates connections to inland nEastAsia_EN and a more negative value (green) indicates connections to coastal nEastAsia_EN. Numerical values can be found in Data Table 1. Except in Early Neolithic steppe Siberia and Neolithic and present-day Tibet, all North groups (Table S1) in East Asia and Siberia are more related to coastal nEastAsia_EN than inland nEastAsia_EN (Yumin, Table S1). Numerical values can be found in Table S5D.

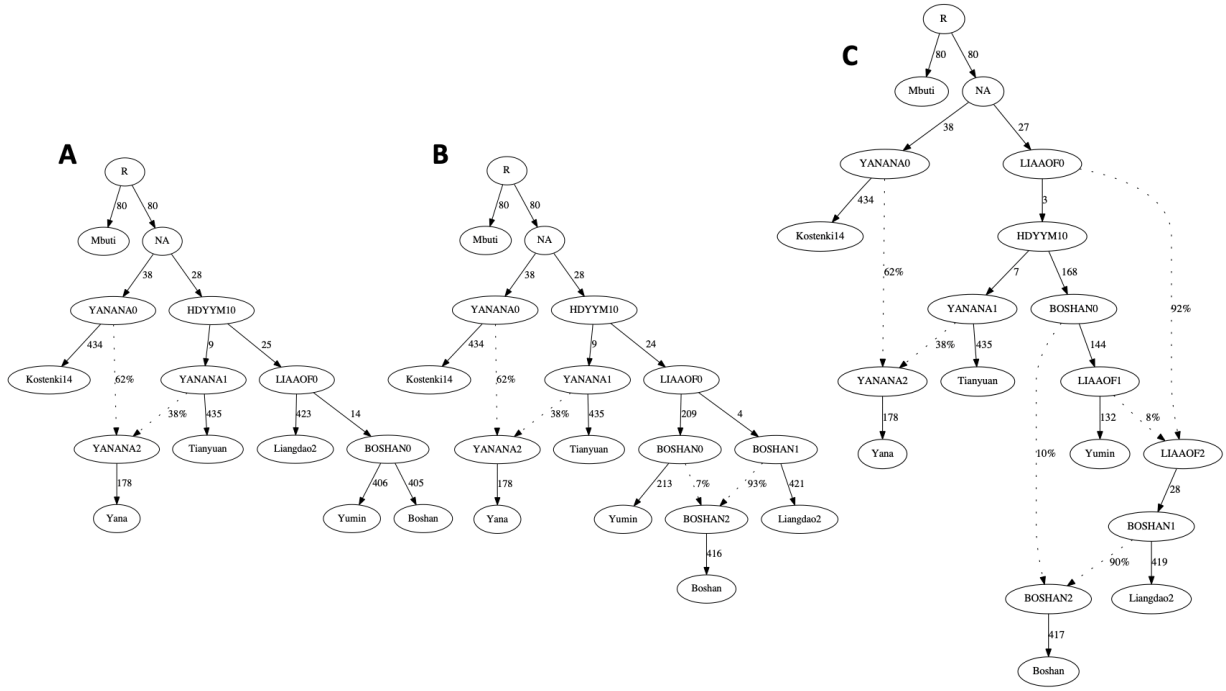

Fig. S16. Selected Admixture Graphs after adding Yumin, Liangdao2, and Boshan to a base graph including the Central African Mbuti and the Upper Paleolithic Eurasians Kostenki14, Tianyuan, and Yana. |maxZ| is (A) -2.467, (B) -2.467, and (C) -2.060. The number of SNPs analyzed is 419,777. Branches are denoted by solid lines with branch lengths given in units of 1000 times the f_2 drift distance, and admixture events are denoted by dotted lines with mixture proportions as shown (all numbers rounded to the nearest integer). All internal node labels are placeholders and do not have a specific meaning. Boshan either groups with Yumin or is a mixture of the Liangdao2 and Yumin branches.

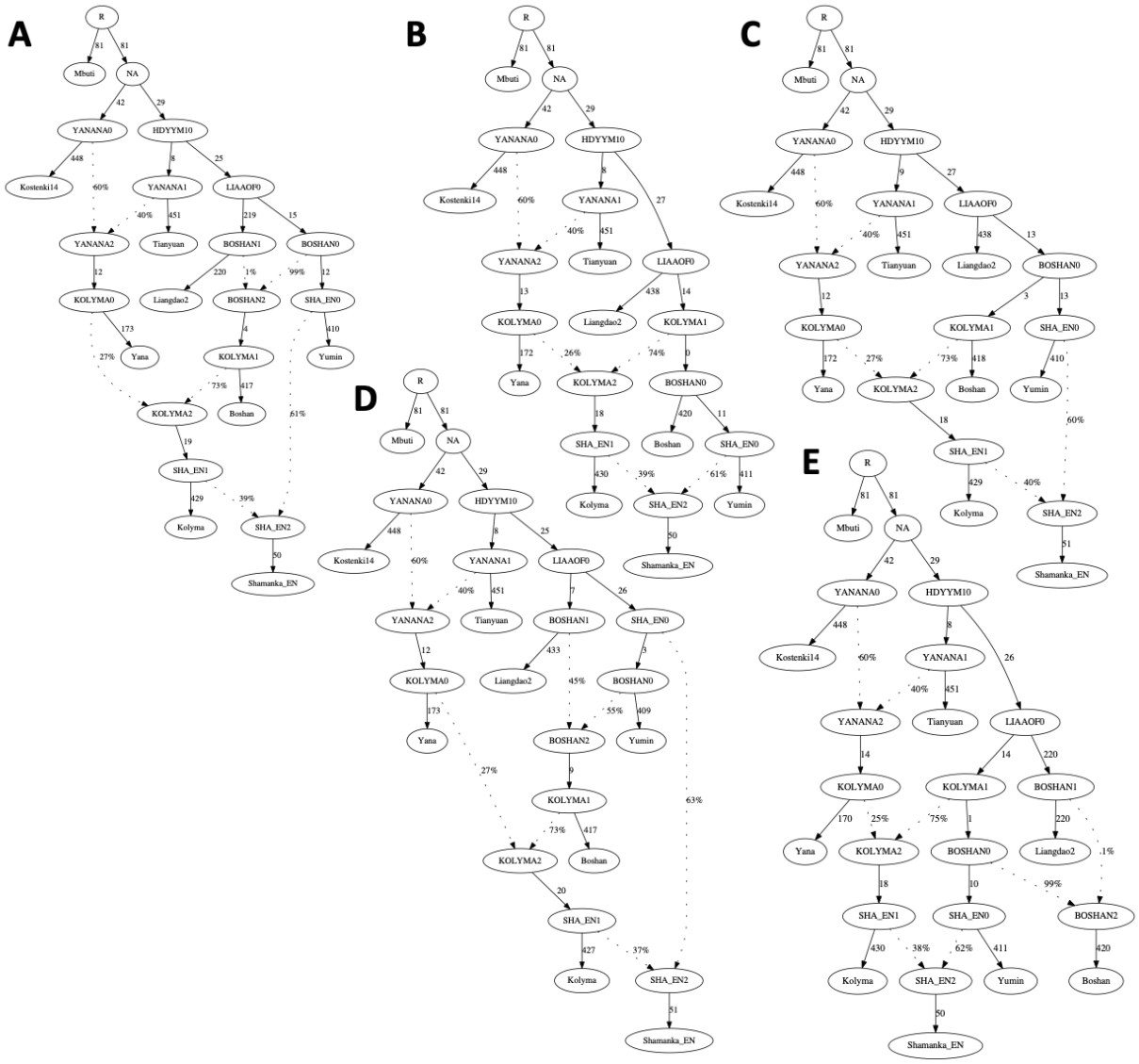

Fig. S17. Selected Admixture Graphs after adding Kolyma and Shamanka_EN to the graphs in Fig. S16. |maxZ| for all graphs is -2.245. The number of SNPs analyzed is 379,902. Branches are denoted by solid lines with branch lengths given in units of 1000 times the f_2 drift distance, and admixture events are denoted by dotted lines with mixture proportions as shown (all numbers rounded to the nearest integer). All internal node labels are placeholders and do not have a specific meaning. Adding Kolyma, we find that in every case, Kolyma is a mixture of the Yana branch and either the Boshan branch or the branch leading to both Yumin and Boshan. Adding Shamanka_EN, we find that in every feasible graph, Shamanka_EN is a mixture of branches leading to Kolyma and Yumin.

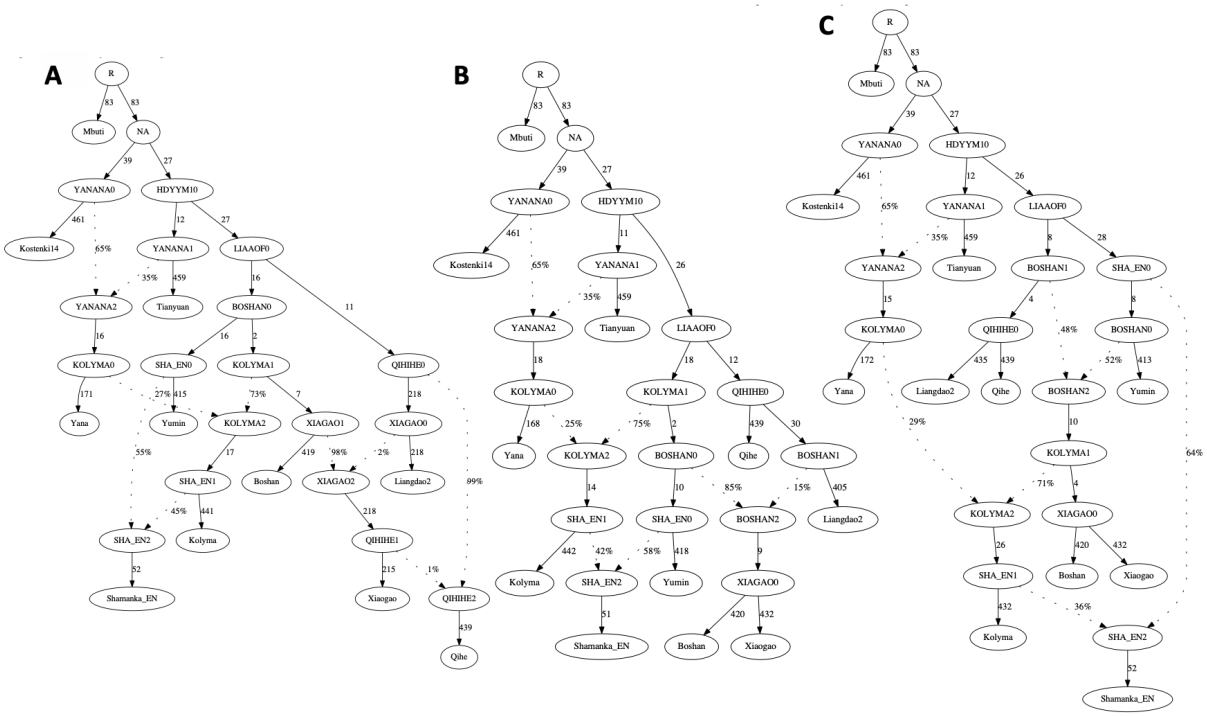

Fig. S18. Selected Admixture Graphs after adding Xiaogao and Qihe to the graphs in Fig. S17. |maxZ| for all graphs is -2.245. The number of SNPs analyzed is 153,247. Qihe shares the most ancestry with Liangdao2 and Xiaogao shares the most ancestry with Boshan. |maxZ| is (A) 2.912, (B) 2.987, and (C) 2.946. A fourth graph equivalent to these is in Fig. 3B. Branches are denoted by solid lines with branch lengths given in units of 1000 times the f_2 drift distance, and admixture events are denoted by dotted lines with mixture proportions as shown (all numbers rounded to the nearest integer). All internal node labels are placeholders and do not have a specific meaning. There are many feasible trees where Boshan is admixed; the most parsimonious are where Qihe is unadmixed and most closely related to Liangdao2. For those feasible trees where Boshan is unadmixed, Qihe is predominantly related to Liangdao2, but can show small amounts of gene flow from the ancestral non-African branch, the Kostenki14 branch, or the Shandong branch. Because we do not find a strong signal of admixture between Qihe and these three groups, we do not consider them in further analysis.

Table S1. Information on all ancient individuals projected onto the principal component analysis.

Newly sampled ancients							
Name	**Region Found[&]**	**Max Date**	**Time[#]**	**Population**	**Ancestry Group "**	**# Samples**	**# SNPs**
Yumin	Inner Mongolia	8,400	EN	inland nEastAsia_EN	North	1	892078
Bianbian	Shandong	9,500	EN	coastal nEastAsia_EN	North	1	722488
Boshan	Shandong	8,300	EN	coastal nEastAsia_EN	North	1	1016121
Xiaojingshan	Shandong	7,900	EN	coastal nEastAsia_EN	North	3	581858
Xiaogao	Shandong	8,800	EN	coastal nEastAsia_EN	North	1	947397
Qihe	Fujian	8,400	EN	coastal nEastAsia_EN	South	1	337994
Liangdao1	Taiwan Strait island	8,300	EN	island sEastAsia_EN	South	1	394474
Liangdao2	Taiwan Strait island	7,600	EN	island sEastAsia_EN	South	1	911854
Suogang	Taiwan Strait island	4,800	LN	island sEastAsia_LN	South	2	75553
Xitoucun	Fujian	4,600	LN	coastal sEastAsia_LN	South	7	579727
Tanshishan	Fujian	4,500	LN	coastal sEastAsia_LN	South	4	424988
Chuanyun	Fujian	300	H	coastal sEastAsia_H	-	1	322561
Select previously published ancients							
Name	**Region**	**Max Date**	**Time[#]**	**Population**	**Ancestry Group^**	**# Samples**	**# SNPs**
Tianyuan	Beijing	40,000	UP	*	-	1	958361
G1	Southeast Asia	7,900	Hòabìnhian	*	-	2	534536
Ikawazu	Japanese Archipelago (island)	2,700	Jōmon	*	-	1	928906
Kolyma	northern Siberia	9,900	Paleosiberian	Paleosiberian	-	1	1231156
Shamanka_EN	steppe Siberia	7,200	EN	steppe Siberia_EN	North	10	1230495
Lokomotiv_EN	steppe Siberia	6,700	EN	steppe Siberia_EN	North	4	1063593
UstBelaya_N	steppe Siberia	5,800	EN	steppe Siberia_EN	North	1	508972
DevilsCave_N	coastal Siberia	7,700	EN	coastal Siberia_EN	North	6	1201365
Chokhopani	Tibetan Plateau	3,100	LN	Tibet_LN	North	1	1226443
Mebrak	Tibetan Plateau	2,400	H	Tibet_H	-	1	768444
Samdzong	Tibetan Plateau	1,700	H	Tibet_H	-	2	1225761
Vanuatu	Southwest Pacific island	3,100	LN/BA	Austronesian_LN/BA	South	3	377379
G6	Southeast Asian island	1,900	H	Austronesian_H	-	3	599658
Man_Bac	Southeast Asia	4,100	LN	coastal SoutheastAsia_LN	-	8	330539
Nui_Nap	Southeast Asia	2,100	BA	coastal SoutheastAsia_B	-	2	353311
Ban_Chiang	Southeast Asia	3,500	LN/BA	inland SoutheastAsia_LN/B	-	5	89398
Oakaie1	Southeast Asia	3,200	LN/BA	inland SoutheastAsia_LN/B	-	2	199739
G3	Southeast Asia	2,300	BA	coastal SoutheastAsia_B	-	5	476875
G4	Southeast Asia	1,800	BA	inland SoutheastAsia_B	-	4	675968
Ma912_G2	Southeast Asia	2,700	BA	inland SoutheastAsia_B	-	1	955193
La_G2	Southeast Asia	3,100	LN/BA	inland SoutheastAsia_LN/B	-	3	986469
Vt_G2	Southeast Asia	4,300	LN	coastal SoutheastAsia_LN	-	2	219388

Present-day East Asians (1240K), ordered by latitude, groupings based on clines in PCA (Fig. S1)						
Northern East Asian	**Tibetan**		**Central East Asian**		**Southern East Asian**	
Ulchi	Tibetan_Chamdo^	Tu	Han_Shandong^	Han_Jiangsu^	Atayal	Dai
Oroqen	Tibetan_Lhasa^	Tibetan	Han	Han_Sichuan^	Lahu	Burmese
Daur	Tibetan_Nagqu^	Sherpa	Tujia	Han_Chongqing^	Ami	Thai
Hezhen	Tibetan_Shannan^	Yi	Miao	Han_Henan^	Kinh	Cambodian
Xibo	Tibetan_Shigate^	Naxi	She	Han_Hubei^		
Japanese	Sherpa_Shigatse^		Han_NChina^			
Korean						

* We refer to these individuals as 'early Asians', because they all are distantly related to present-day East Asians. They are not geographically, temporally, or genetically closely related to each other.

" These are the populations carrying northern East Asian (North) or southern East Asian (South) ancestry during the Neolithic. Historic individuals, 'early Asians', Paleosiberians, and Southeast Asians were considered separately.

[&] Either mainland East Asian province or Taiwan Strait island. Note that all Regions without 'island' attached are on the mainland of Asia.

[#] Time period corresponds to one of the following: Upper Paleolithic (UP: >9,500 years ago), Early Neolithic (EN: 9,500-7,500 years ago), Middle Neolithic (MN: 7,500-5,000 years ago), Late Neolithic (LN: 5,000-3,000 years ago), Bronze Age (BA: 3,000-2,000 years ago), and Historic (H: <2,000 years ago).

^Data obtained from (*44*), whereas other present-day data are from the Simons Genome Diversity Panel (*68*)

Table S2. F_4-statistics comparing the newly sampled individuals with present-day East Asians and early Asians. In (A), we show all results for the present-day Han for *f_4(Mbuti, nEastAsia/sEastAsia; present-day Han, early Asians)* and *f_4(Mbuti, early Asians; Han, nEastAsia/sEastAsia)*, and in (B), we expand to patterns for other present-day East Asians. Early Asians include Tianyuan, G1, and Ikawazu, and more details can be found on them in Table S1. For more detail, see descriptions associated with (A) and (B) below.

Table S2A. We find that (i) our newly sampled individuals are always more closely related to the Han than any early Asian, i.e. *f_4(Mbuti, X; Han, early Asian)<0* (-22.1<Z<-4.4) and that (ii) no newly sampled individual or the Han shares excess connections to an early Asian, *f_4(Mbuti, early Asian; X, Han)~0 (-2.4<Z<2.6)*. Thus, our newly sampled individuals are more closely related to the Han than early Asians such as Tianyuan, G1, and the Ikawazu Jōmon and are primarily of East Asian ancestry.

i. f_4(Mbuti, newly sampled individuals; Han, early Asians)												
P1	**P2**	**P3**	**P4**	**f_4**	**Z**	**N**	**P1**	**P2**	**P3**	**P4**	**f_4**	**Z**	**N**
Mbuti	Yumin	Han	Ikawazu	-0.0049	-9.4	670500	Mbuti	Liangdao1	Han	Ikawazu	-0.0034	-6.4	303324
Mbuti	Yumin	Han	G1	-0.011	-19.8	371246	Mbuti	Liangdao1	Han	G1	-0.0098	-14.9	171165
Mbuti	Yumin	Han	Tianyuan	-0.0089	-15.9	763652	Mbuti	Liangdao1	Han	Tianyuan	-0.0089	-14.1	363420
Mbuti	Bianbian	Han	Ikawazu	-0.0053	-10.3	539236	Mbuti	Liangdao2	Han	Ikawazu	-0.0038	-7.4	686986
Mbuti	Bianbian	Han	G1	-0.0127	-22	291176	Mbuti	Liangdao2	Han	G1	-0.0112	-20.9	386669
Mbuti	Bianbian	Han	Tianyuan	-0.0102	-18	640381	Mbuti	Liangdao2	Han	Tianyuan	-0.01	-18	773809
Mbuti	Boshan	Han	Ikawazu	-0.006	-11.8	751724	Mbuti	Xitoucun	Han	Ikawazu	-0.0048	-10.8	442989
Mbuti	Boshan	Han	G1	-0.012	-21.5	422688	Mbuti	Xitoucun	Han	G1	-0.0112	-21.1	249233
Mbuti	Boshan	Han	Tianyuan	-0.0116	-20.9	832017	Mbuti	Xitoucun	Han	Tianyuan	-0.0102	-21	518941
Mbuti	Xiaojingshan	Han	Ikawazu	-0.0051	-11.7	441786	Mbuti	Tanshishan	Han	Ikawazu	-0.0051	-9.9	322615
Mbuti	Xiaojingshan	Han	G1	-0.0115	-21.1	243124	Mbuti	Tanshishan	Han	G1	-0.011	-19	177796
Mbuti	Xiaojingshan	Han	Tianyuan	-0.0106	-20.6	528635	Mbuti	Tanshishan	Han	Tianyuan	-0.0105	-19.6	385343
Mbuti	Xiaogao	Han	Ikawazu	-0.0051	-10.1	712089	Mbuti	Suogang	Han	Ikawazu	-0.0056	-6.1	58966
Mbuti	Xiaogao	Han	G1	-0.012	-22.1	399409	Mbuti	Suogang	Han	G1	-0.0106	-9.3	32270
Mbuti	Xiaogao	Han	Tianyuan	-0.0104	-18.9	798358	Mbuti	Suogang	Han	Tianyuan	-0.0097	-10.7	71778
Mbuti	Qihe	Han	Ikawazu	-0.0027	-4.4	259942	Mbuti	Chuanyun	Han	Ikawazu	-0.0059	-10.2	243547
Mbuti	Qihe	Han	G1	-0.0081	-11.5	143947	Mbuti	Chuanyun	Han	G1	-0.0136	-20	131538
Mbuti	Qihe	Han	Tianyuan	-0.0082	-13.3	312838	Mbuti	Chuanyun	Han	Tianyuan	-0.0122	-19.6	297071
ii. f_4(Mbuti, early Asians; Han, newly sampled individuals)												
P1	**P2**	**P3**	**P4**	**f_4**	**Z**	**N**	**P1**	**P2**	**P3**	**P4**	**f_4**	**Z**	**N**
Mbuti	Ikawazu	Han	Yumin	-0.0012	-2.4	670500	Mbuti	Ikawazu	Han	Liangdao1	0.0005	1.1	303324
Mbuti	G1	Han	Yumin	-0.0001	-0.3	371246	Mbuti	G1	Han	Liangdao1	0.0009	1.6	171165
Mbuti	Tianyuan	Han	Yumin	0.0006	1.4	763652	Mbuti	Tianyuan	Han	Liangdao1	0.0009	1.8	363420
Mbuti	Ikawazu	Han	Bianbian	0.0002	0.4	539236	Mbuti	Ikawazu	Han	Liangdao2	0.0003	0.6	686986
Mbuti	G1	Han	Bianbian	-0.0004	-1	291176	Mbuti	G1	Han	Liangdao2	-0.0001	-0.2	386669
Mbuti	Tianyuan	Han	Bianbian	0.0011	2.6	640381	Mbuti	Tianyuan	Han	Liangdao2	0.0001	0.3	773809
Mbuti	Ikawazu	Han	Boshan	-0.0002	-0.4	751724	Mbuti	Ikawazu	Han	Xitoucun	-0.0002	-0.6	442989
Mbuti	G1	Han	Boshan	0.0004	1	422688	Mbuti	G1	Han	Xitoucun	0.0001	0.2	249233
Mbuti	Tianyuan	Han	Boshan	0.0001	0.1	832017	Mbuti	Tianyuan	Han	Xitoucun	0.0003	0.8	518941
Mbuti	Ikawazu	Han	Xiaojingshan	0.0001	0.2	441786	Mbuti	Ikawazu	Han	Tanshishan	-0.0003	-0.7	322615
Mbuti	G1	Han	Xiaojingshan	0.001	2.4	243124	Mbuti	G1	Han	Tanshishan	0	-0.1	177796
Mbuti	Tianyuan	Han	Xiaojingshan	0.0006	1.5	528635	Mbuti	Tianyuan	Han	Tanshishan	0.0001	0.3	385343
Mbuti	Ikawazu	Han	Xiaogao	-0.0002	-0.4	712089	Mbuti	Ikawazu	Han	Suogang	-0.0013	-1.5	58966
Mbuti	G1	Han	Xiaogao	0	0	399409	Mbuti	G1	Han	Suogang	0.0001	0.1	32270
Mbuti	Tianyuan	Han	Xiaogao	0.0005	1.2	798358	Mbuti	Tianyuan	Han	Suogang	0.0001	0.1	71778
Mbuti	Ikawazu	Han	Qihe	-0.0003	-0.7	425450	Mbuti	Ikawazu	Han	Chuanyun	0.0004	0.8	243547
Mbuti	G1	Han	Qihe	0.001	1.8	237891	Mbuti	G1	Han	Chuanyun	-0.0003	-0.5	131538
Mbuti	Tianyuan	Han	Qihe	-0.0001	-0.2	501630	Mbuti	Tianyuan	Han	Chuanyun	0.0004	0.7	297071

Table S2B. When we substitute the Han with other present-day East Asians, we observe a similar relationship for most comparisons, where most *f_4(Mbuti, X; present-day East Asian, early Asian)<0* and most *f_4(Mbuti, early Asian; X, present-day East Asian)~0* (not shown). However, there are exceptions. In (i), we show all cases where *f_4(Mbuti, X; present-day East Asian, early Asian)~0* (|Z|<3; note there are no combinations where Z>3. These results show that several southern Neolithic East Asians share a similar relationship to the Ikawazu individual as to primarily northern and Tibetan present-day East Asians, but no other early Asians shows a similar pattern. In (ii), we show all cases where *f_4(Mbuti, early Asian; X, present-day East Asian)* is significantly different from zero (|Z|>3). These results show that Tianyuan, G1, and Ikawazu all show connections to newly sampled individuals relative to some peripheral present-day East Asians, which may be due to more diverged ancestry in the peripheral present-day East Asians. The Ikawazu individual also shares connections to the present-day Ami, Atayal, and Japanese relative to newly sampled individuals, confirming their tie to present-day inhabitants of the Japanese archipelago and highlighting an Austronesian connection. Overall, however, most results were similar to those observed for the Han in Table S2A.

i.*f_4(Mbuti, newly sampled individuals; other present-day East Asians, early Asians)* where Z>-3													
P1	**P2**	**P3**	**P4**	**f_4**	**Z**	**N**	**P1**	**P2**	**P3**	**P4**	**f_4**	**Z**	**N**
Mbuti	Qihe	Hezhen	Ikawazu	-0.0007	-1.1	259937	Mbuti	Liangdao1	Hezhen	Ikawazu	-0.0014	-2.5	303319
Mbuti	Qihe	Daur	Ikawazu	-0.0007	-1	259923	Mbuti	Liangdao1	Daur	Ikawazu	-0.0013	-2	303299
Mbuti	Qihe	Xibo	Ikawazu	-0.0008	-1.2	259937	Mbuti	Liangdao1	Xibo	Ikawazu	-0.0011	-1.8	303320
Mbuti	Qihe	Tibetan	Ikawazu	0	0	259935	Mbuti	Liangdao1	Tibetan	Ikawazu	0.0002	0.4	303318
Mbuti	Qihe	Sherpa	Ikawazu	-0.0003	-0.5	259940	Mbuti	Liangdao1	Sherpa	Ikawazu	-0.0003	-0.6	303315
Mbuti	Qihe	Naxi	Ikawazu	-0.0017	-2.7	259940	Mbuti	Liangdao2	Hezhen	Ikawazu	-0.0013	-2.3	686975
Mbuti	Xitoucun	Tibetan	Ikawazu	-0.0007	-1.6	442979	Mbuti	Liangdao2	Daur	Ikawazu	-0.0009	-1.5	686926
Mbuti	Tanshishan	Sherpa	Ikawazu	-0.0015	-2.8	322609	Mbuti	Liangdao2	Xibo	Ikawazu	-0.0011	-2	686979
Mbuti	Suogang	Tibetan	Ikawazu	-0.0023	-2.4	58965	Mbuti	Liangdao2	Tibetan	Ikawazu	0.0002	0.3	686971
							Mbuti	Liangdao2	Sherpa	Ikawazu	-0.0002	-0.4	686972
ii.*f_4(Mbuti, early Asians; other present-day East Asians, newly sampled individuals)* where |Z|>3													
P1	**P2**	**P3**	**P4**	**f_4**	**Z**	**N**	**P1**	**P2**	**P3**	**P4**	**f_4**	**Z**	**N**
Mbuti	Tianyuan	Hezhen	Bianbian	0.0015	3.1	640368	Mbuti	Ikawazu	Sherpa	Chuanyun	0.0023	3.8	243544
Mbuti	Tianyuan	Kinh	Bianbian	0.0017	3.4	640366	Mbuti	Ikawazu	Sherpa	Liangdao1	0.0022	3.8	303315
Mbuti	Tianyuan	Daur	Xitoucun	0.0015	3.1	518884	Mbuti	Ikawazu	Sherpa	Liangdao2	0.002	3.8	686972
Mbuti	Tianyuan	Daur	Liangdao1	0.0021	3.5	363381	Mbuti	Ikawazu	Sherpa	Xiaogao	0.0015	3	712077
Mbuti	Tianyuan	Daur	Xiaogao	0.0017	3.1	798262	Mbuti	Ikawazu	Sherpa	Bianbian	0.0019	3.6	539227
Mbuti	Tianyuan	Daur	Bianbian	0.0025	4.6	640311	Mbuti	Ikawazu	Sherpa	Boshan	0.0015	3.2	751709
Mbuti	Tianyuan	Daur	Xiaojingshan	0.0018	3.8	528567	Mbuti	Ikawazu	Sherpa	Xiaojingshan	0.0019	4.4	441777
Mbuti	Tianyuan	Daur	Yumin	0.0019	3.4	763559	Mbuti	Ikawazu	Ami	Tanshishan	-0.0018	-3.6	322606
Mbuti	Tianyuan	Xibo	Bianbian	0.0019	4	640374	Mbuti	Ikawazu	Ami	Xitoucun	-0.0015	-3.5	442976
Mbuti	Tianyuan	Xibo	Xiaojingshan	0.0014	3.5	528628	Mbuti	Ikawazu	Ami	Suogang	-0.0027	-3.1	58965
Mbuti	Tianyuan	Tibetan	Xiaogao	0.0015	3	798335	Mbuti	Ikawazu	Ami	Yumin	-0.0025	-4.5	670480
Mbuti	Tianyuan	Tibetan	Bianbian	0.0019	3.8	640366	Mbuti	Ikawazu	Atayal	Yumin	-0.002	-3.1	670389
Mbuti	Tianyuan	Tibetan	Xiaojingshan	0.0014	3.4	528624	Mbuti	Ikawazu	Japanese	Tanshishan	-0.0042	-8.5	322613
Mbuti	Tianyuan	Sherpa	Bianbian	0.0016	3.3	640365	Mbuti	Ikawazu	Japanese	Chuanyun	-0.0032	-5.6	243545
Mbuti	G1	Daur	Xiaojingshan	0.0019	3.5	243095	Mbuti	Ikawazu	Japanese	Xitouchun	-0.0042	-9.5	442987
Mbuti	G1	Xibo	Liangdao1	0.0025	4.1	171165	Mbuti	Ikawazu	Japanese	Liangdao1	-0.0032	-5.9	303322
Mbuti	G1	Xibo	Boshan	0.0015	3.2	422685	Mbuti	Ikawazu	Japanese	Liangdao2	-0.0036	-7.2	686984
Mbuti	G1	Xibo	Xiaojingshan	0.0022	4.7	243123	Mbuti	Ikawazu	Japanese	Xiaogao	-0.0041	-8.2	712086
Mbuti	G1	Tibetan	Liangdao1	0.0019	3.1	171163	Mbuti	Ikawazu	Japanese	Qihe	-0.0044	-7.2	259940
Mbuti	G1	Tibetan	Xiaojingshan	0.0014	3.2	243123	Mbuti	Ikawazu	Japanese	Suogang	-0.0052	-5.9	58965
Mbuti	G1	Sherpa	Xiaojingshan	0.0015	3	243122	Mbuti	Ikawazu	Japanese	Bianbian	-0.0036	-6.9	539234
Mbuti	Ikawazu	Tibetan	Chuanyun	0.002	3.4	243542	Mbuti	Ikawazu	Japanese	Boshan	-0.0041	-8.2	751721
Mbuti	Ikawazu	Tibetan	Liangdao1	0.002	3.3	303318	Mbuti	Ikawazu	Japanese	Xiaojingshan	-0.0038	-8.6	441784
Mbuti	Ikawazu	Tibetan	Liangdao2	0.0017	3.1	686971	Mbuti	Ikawazu	Japanese	Yumin	-0.0051	-10	670498
Mbuti	Ikawazu	Tibetan	Xiaojingshan	0.0015	3.3	441778							

Table S3. Admixture proportion of Denisovan-related ancestry using f_4-ratios. Those rows shaded gray are where D is significantly greater than zero, indicating an archaic admixture proportion (α) significantly greater than zero,(relative to the Han or the French, where the estimated archaic admixture proportion is zero). In the first block are all newly sampled individuals, in the second block are previously published ancient East and Southeast Asians, and in the third block are present-day East Asians. Though we find a significant archaic admixture proportion for Yumin, Liangdao1, and DevilsCave_N, in no case is the result significant for transversions only. This suggests that we do not detect Denisovan-related archaic admixture in these ancient and present-day Asians and any significant result likely reflects shared characteristic ancient DNA damage.

A. f_4(Denisovan, Mbuti; X, Han) / f_4(Denisovan, Mbuti; Papuan, Han)							**B. f_4(Denisovan, Mbuti; X, French) / f_4(Denisovan, Mbuti; Papuan, French)**						
X	**All Sites**			**Transversions Only**			**X**	**All Sites**			**Transversions Only**		
	α	**SE**	**Z**	**alpha**	**SE**	**Z**		**α**	**SE**	**Z**	**alpha**	**SE**	**Z**
Yumin	0.22	0.07	3.04	0.10	0.10	0.94	Yumin	0.27	0.07	3.67	0.01	0.13	0.06
Bianbian	0.14	0.08	1.77	0.29	0.12	2.40	Bianbian	0.19	0.08	2.26	0.24	0.15	1.64
Boshan	0.03	0.07	0.39	0.09	0.11	0.87	Boshan	0.10	0.07	1.42	0.06	0.13	0.43
Xiaojingshan	0.02	0.07	0.29	0.07	0.12	0.59	Xiaojingshan	0.10	0.07	1.33	0.00	0.15	-0.03
Xiaogao	0.08	0.06	1.25	0.08	0.11	0.71	Xiaogao	0.15	0.07	2.05	0.05	0.13	0.38
Qihe	0.11	0.10	1.17	0.06	0.17	0.35	Qihe	0.12	0.10	1.19	-0.15	0.25	-0.59
Liangdao1	0.35	0.09	3.88	0.33	0.16	2.12	Liangdao1	0.40	0.09	4.42	0.27	0.19	1.46
Liangdao2	-0.03	0.07	-0.35	0.01	0.11	0.06	Liangdao2	0.07	0.08	0.88	0.01	0.13	0.06
Xitoucun	0.09	0.06	1.48	0.09	0.11	0.87	Xitoucun	0.14	0.07	1.87	-0.03	0.15	-0.20
Suogang	0.03	0.15	0.21	0.13	0.29	0.44	Suogang	0.03	0.17	0.15	0.23	0.28	0.85
Tanshishan	0.11	0.07	1.67	0.05	0.12	0.39	Tanshishan	0.16	0.08	2.12	-0.05	0.16	-0.28
Chuanyun	0.01	0.10	0.07	0.16	0.18	0.90	Chuanyun	0.11	0.11	1.06	0.14	0.20	0.73
Chokhopani	0.03	0.07	0.51	-0.03	0.10	-0.30	Chokhopani	0.11	0.07	1.58	-0.03	0.12	-0.25
Mebrak	0.00	0.07	-0.07	0.04	0.12	0.38	Mebrak	0.07	0.08	0.94	0.01	0.14	0.04
Samdzong	0.02	0.06	0.42	0.01	0.08	0.17	Samdzong	0.11	0.06	1.64	0.02	0.10	0.15
Shamanka_EN	0.02	0.04	0.49	0.06	0.06	1.00	Shamanka_EN	0.10	0.05	1.97	0.06	0.08	0.78
Lokomotiv_EN	0.02	0.06	0.29	0.00	0.08	0.02	Lokomotiv_EN	0.10	0.06	1.67	-0.01	0.10	-0.07
UstBelaya_N	0.03	0.08	0.42	-0.04	0.14	-0.31	UstBelaya_N	0.11	0.08	1.39	0.03	0.14	0.22
DevilsCave_N	0.13	0.05	2.56	0.11	0.07	1.45	DevilsCave_N	0.20	0.06	3.30	0.11	0.09	1.16
Vanuatu	0.04	0.08	0.56	-0.02	0.13	-0.15	Vanuatu	0.07	0.09	0.74	-0.29	0.20	-1.41
Ma912_G2	-0.05	0.07	-0.72	-0.06	0.10	-0.60	Ma912_G2	0.03	0.07	0.48	-0.06	0.12	-0.48
Vt_G2	-0.02	0.11	-0.18	0.27	0.21	1.27	Vt_G2	-0.01	0.12	-0.08	0.11	0.30	0.36
La_G2	-0.03	0.07	-0.39	-0.04	0.11	-0.35	La_G2	0.07	0.07	1.03	-0.01	0.12	-0.12
G3	-0.18	0.07	-2.50	-0.06	0.14	-0.43	G3	-0.04	0.08	-0.49	-0.03	0.16	-0.20
G6	0.11	0.07	1.59	0.18	0.12	1.58	G6	0.17	0.07	2.44	0.22	0.13	1.72
Man_Bac	0.17	0.07	2.31	0.21	0.15	1.42	Man_Bac	0.20	0.08	2.45	0.11	0.20	0.58
Nui_Nap	0.14	0.09	1.62	0.10	0.16	0.59	Nui_Nap	0.23	0.09	2.53	0.06	0.20	0.28
Oakaie1	0.05	0.10	0.52	0.28	0.19	1.48	Oakaie1	0.16	0.10	1.56	0.24	0.23	1.05
Ban_Chiang	0.14	0.14	0.99	0.40	0.30	1.34	Ban_Chiang	0.21	0.14	1.48	0.45	0.29	1.53
Oroqen	-0.01	0.05	-0.19	0.07	0.07	0.94	Oroqen	0.07	0.06	1.22	0.07	0.09	0.79
Ulchi	0.02	0.05	0.44	0.02	0.07	0.28	Ulchi	0.10	0.06	1.73	0.02	0.09	0.24
Daur	-0.08	0.07	-1.24	-0.03	0.09	-0.30	Daur	0.01	0.07	0.11	-0.02	0.11	-0.21
Hezhen	-0.08	0.05	-1.53	-0.06	0.07	-0.81	Hezhen	0.01	0.06	0.22	-0.05	0.09	-0.59
Xibo	-0.08	0.05	-1.71	-0.12	0.07	-1.71	Xibo	0.01	0.06	0.10	-0.12	0.09	-1.25
Japanese	-0.02	0.04	-0.37	0.00	0.06	0.01	Japanese	0.07	0.06	1.20	0.00	0.08	0.05
Korean	-0.08	0.05	-1.71	-0.08	0.06	-1.28	Korean	0.01	0.06	0.13	-0.08	0.09	-0.84
She	-0.05	0.05	-1.02	-0.02	0.06	-0.29	She	0.04	0.06	0.62	-0.01	0.09	-0.16
Miao	-0.06	0.05	-1.25	-0.03	0.06	-0.42	Miao	0.03	0.06	0.47	-0.02	0.09	-0.27
Tujia	-0.04	0.05	-0.82	0.01	0.06	0.19	Tujia	0.05	0.06	0.76	0.01	0.09	0.16
Dai	-0.04	0.04	-0.99	0.00	0.05	-0.02	Dai	0.05	0.05	0.90	0.00	0.08	0.03
Lahu	0.00	0.05	-0.07	0.02	0.07	0.35	Lahu	0.08	0.06	1.38	0.03	0.09	0.31
Kinh	-0.01	0.05	-0.17	-0.03	0.07	-0.50	Kinh	0.08	0.06	1.21	-0.03	0.09	-0.33
Ami	0.01	0.05	0.15	0.02	0.07	0.31	Ami	0.09	0.06	1.51	0.02	0.09	0.27
Atayal	-0.06	0.06	-1.01	0.01	0.09	0.12	Atayal	0.02	0.07	0.33	0.01	0.11	0.13
Naxi	-0.01	0.04	-0.23	-0.02	0.06	-0.42	Naxi	0.07	0.06	1.30	-0.02	0.09	-0.23
Yi	0.03	0.05	0.66	0.03	0.06	0.48	Yi	0.11	0.05	2.01	0.03	0.08	0.39

Table S4. ***f_4(Mbuti, Paleosiberian; P3, P4)*** **where P3 and P4 are Neolithic East Asians, Siberians and Tibetans where f_4>0 (Z>2.5).** Those shaded gray are where P3 belongs to the South group and P4 belongs to the North group. The Paleosiberian (Kolyma) shares a connection to all northern East Asians relative to southern East Asians. This is particularly true for the Siberians and some of the coastal northern Chinese (Boshan, Xiaogao).

P1	P2	P3	P4	f_4	Z	N	P1	P2	P3	P4	f_4	Z	N
Mbuti	Kolyma	Vanuatu	Shamanka_EN	0.005	10.4	364961	Mbuti	Kolyma	Chuanyun	Shamanka_EN	0.00255		313216
Mbuti	Kolyma	Vanuatu	DevilsCave_N	0.00531	0.2	364949	Mbuti	Kolyma	Xitoucun	Xiaojingshan	0.00244.9		404164
Mbuti	Kolyma	G6	Shamanka_EN	0.00439.7		572408	Mbuti	Kolyma	Vanuatu	UstBelaya_N	0.00414.9		159472
Mbuti	Kolyma	Vanuatu	Lokomotiv_EN	0.00519.4		322507	Mbuti	Kolyma	G6	Xiaojingshan	0.00284.9		270682
Mbuti	Kolyma	G6	DevilsCave_N	0.00489.4		572389	Mbuti	Kolyma	Liangdao2	Xiaojingshan	0.00274.8		525303
Mbuti	Kolyma	Xitoucun	DevilsCave_N	0.00419.2		560456	Mbuti	Kolyma	Suogang	Shamanka_EN	0.00384.7		73750
Mbuti	Kolyma	Xitoucun	Shamanka_EN	0.00369.1		560509	Mbuti	Kolyma	Xitoucun	Yumin	0.00264.6		511674
Mbuti	Kolyma	Qihe	DevilsCave_N	0.00528.5		328694	Mbuti	Kolyma	Liangdao1	Xiaojingshan	0.00294.6		282015
Mbuti	Kolyma	Qihe	Shamanka_EN	0.00478.4		328720	Mbuti	Kolyma	Liangdao2	UstBelaya_N	0.00324.6		376164
Mbuti	Kolyma	Liangdao2	DevilsCave_N	0.00448.2		879033	Mbuti	Kolyma	Liangdao2	Yumin	0.00294.5		751642
Mbuti	Kolyma	Xitoucun	Lokomotiv_EN	0.00387.8		494054	Mbuti	Kolyma	Suogang	DevilsCave_N	0.004	4.5	73743
Mbuti	Kolyma	Liangdao2	Shamanka_EN	0.00397.8		879143	Mbuti	Kolyma	Suogang	Lokomotiv_EN	0.00454.4		65002
Mbuti	Kolyma	Vanuatu	Boshan	0.00497.7		353677	Mbuti	Kolyma	Bianbian	DevilsCave_N	0.00234.3		693343
Mbuti	Kolyma	G6	Lokomotiv_EN	0.00417.6		506012	Mbuti	Kolyma	Vanuatu	Bianbian	0.00264.2		312148
Mbuti	Kolyma	Qihe	Lokomotiv_EN	0.00497.5		289465	Mbuti	Kolyma	Qihe	UstBelaya_N	0.00394.2		142539
Mbuti	Kolyma	Liangdao2	Lokomotiv_EN	0.004	7.3	773427	Mbuti	Kolyma	Tanshishan	Boshan	0.00254.1		398002
Mbuti	Kolyma	Vanuatu	Xiaojingshan	0.00366.6		275415	Mbuti	Kolyma	Bianbian	Shamanka_EN	0.00194.1		693443
Mbuti	Kolyma	G6	Boshan	0.004	6.6	474372	Mbuti	Kolyma	Liangdao1	UstBelaya_N	0.00314		166080
Mbuti	Kolyma	Liangdao1	DevilsCave_N	0.00376.5		383896	Mbuti	Kolyma	Liangdao1	Bianbian	0.00264		311738
Mbuti	Kolyma	Liangdao1	Shamanka_EN	0.00326.4		383942	Mbuti	Kolyma	Tanshishan	UstBelaya_N	0.003	3.9	177792
Mbuti	Kolyma	Vanuatu	Yumin	0.00396.2		344075	Mbuti	Kolyma	Qihe	Bianbian	0.00283.9		283304
Mbuti	Kolyma	Qihe	Boshan	0.00446.2		321513	Mbuti	Kolyma	Vanuatu	Chuanyun	0.00293.8		148114
Mbuti	Kolyma	Vanuatu	Xiaogao	0.00386.1		349556	Mbuti	Kolyma	Suogang	Xiaogao	0.004	3.8	72105
Mbuti	Kolyma	Tanshishan	DevilsCave_N	0.00316		410778	Mbuti	Kolyma	Liangdao1	Xiaogao	0.00253.7		365563
Mbuti	Kolyma	Tanshishan	Shamanka_EN	0.00286		410809	Mbuti	Kolyma	Tanshishan	Xiaogao	0.00213.6		394087
Mbuti	Kolyma	G6	Xiaogao	0.00356		447506	Mbuti	Kolyma	Chuanyun	UstBelaya_N	0.00333.6		134431
Mbuti	Kolyma	Qihe	Xiaogao	0.00426		317758	Mbuti	Kolyma	Chuanyun	Boshan	0.00243.6		305887
Mbuti	Kolyma	Xitoucun	Xiaogao	0.00315.7		532132	Mbuti	Kolyma	Liangdao1	Yumin	0.00243.6		352079
Mbuti	Kolyma	Liangdao1	Lokomotiv_EN	0.00355.6		338568	Mbuti	Kolyma	Suogang	Xiaojingshan	0.00343.6		64393
Mbuti	Kolyma	G6	Yumin	0.00355.5		417778	Mbuti	Kolyma	Bianbian	Lokomotiv_EN	0.00193.5		608283
Mbuti	Kolyma	Liangdao1	Boshan	0.00355.5		375467	Mbuti	Kolyma	Liangdao2	Bianbian	0.002	3.3	628090
Mbuti	Kolyma	Chuanyun	DevilsCave_N	0.00315.4		313171	Mbuti	Kolyma	Xitoucun	Bianbian	0.00173.2		453564
Mbuti	Kolyma	Xitoucun	UstBelaya_N	0.00375.4		242302	Mbuti	Kolyma	G6	Bianbian	0.00213.2		332145
Mbuti	Kolyma	Xitoucun	Boshan	0.00295.4		539930	Mbuti	Kolyma	Suogang	Yumin	0.00343.2		70696
Mbuti	Kolyma	G6	UstBelaya_N	0.00415.4		245064	Mbuti	Kolyma	Vanuatu	Tanshishan	0.00183.1		206455
Mbuti	Kolyma	Tanshishan	Lokomotiv_EN	0.003	5.3	361418	Mbuti	Kolyma	Tanshishan	Yumin	0.00193		379921
Mbuti	Kolyma	Liangdao2	Boshan	0.00335.3		825218	Mbuti	Kolyma	Suogang	Boshan	0.00323		72920
Mbuti	Kolyma	Chuanyun	Lokomotiv_EN	0.00335.2		274889	Mbuti	Kolyma	Tanshishan	Xiaojingshan	0.00152.8		306767
Mbuti	Kolyma	Liangdao2	Xiaogao	0.00315.1		790496	Mbuti	Kolyma	Chuanyun	Xiaogao	0.00192.7		301010
Mbuti	Kolyma	Qihe	Xiaojingshan	0.00335.1		259858	Mbuti	Kolyma	Qihe	Chokhopani	0.00182.6		328013
Mbuti	Kolyma	Qihe	Yumin	0.00365.1		309436	Mbuti	Kolyma	Qihe	Chuanyun	0.00212.5		153355

Table S5. Numerical values for the heatplots shown in Fig. 3A-3C and Fig. S12, S15. Below are the f_4 values for (A) *f_4(Mbuti, X; Qihe, Bianbian)* which corresponds to Fig. 3A-3C, (B) *f_4(Mbuti, X; Liangdao1, Bianbian)* and (C) *f_4(Mbuti, X; Qihe, Yumin)*, which correspond to Fig. S12, and (D) *f_4(Mbuti, X; Bianbian, Yumin)* which corresponds to Fig. S15.

Time	X	Lat	Lon	A. f_4(M, X; Q, B)			B. f_4(M, X; L, B)			C. f_4(M, X; Q, Y)			D. f_4(M, X; B, Y)		
				f4	Z	N	f4	Z	N	f4	Z	N	f4	Z	N
Early Neolithic	Lokomotiv_EN	53.9	104.2	0.0037	6.0	249094	0.0034	6.2	274454	0.0055	8.8	272268	0.0017	3.3	559456
	UstBelaya_N	53.9	106.7	0.0046	5.1	122969	0.0029	3.6	135248	0.0064	6.7	134225	0.0019	2.6	273543
	Shamanka_EN	51.7	103.7	0.0039	8.1	283325	0.0033	7.2	311773	0.0059	11.8	309474	0.0021	4.6	638209
	DevilsCave_N	44.5	135.4	0.0046	8.2	283300	0.0040	7.4	311727	0.0042	7.2	309437	-0.0005	-1.0	638115
	Yumin (Y)	42.0	114.2	0.0039	5.5	275213	0.0027	4.0	300173	-	-	-	-	-	-
	Bianbian (B)	38.2	113.5	-	-	-	-	-	-	0.0020	2.8	275213	-	-	-
	Boshan	38.2	118.5	0.0065	9.1	280839	0.0052	7.9	309171	0.0040	5.9	305498	-0.0031	-4.8	621186
	Xiaojingshan	36.0	116.0	0.0044	7.3	239701	0.0046	7.7	253382	0.0017	2.6	252747	-0.0033	-5.9	455134
	Xiaogao	36.0	118.5	0.0053	7.5	279197	0.0048	7.1	305987	0.0030	4.0	303168	-0.0029	-4.6	613420
	Liangdao1 (L)	26.4	120.2	-0.0007	-0.9	169144	-	-	-	-0.0027	-3.3	178442	-0.0023	-3.4	300173
	Liangdao2	26.4	122.7	-0.0009	-1.3	274926	-0.0054	-7.9	301721	-0.0035	-4.8	297908	-0.0020	-3.2	591044
	Qihe (Q)	25.4	117.6	-	-	-	-0.0009	-1.2	169144	-	-	-	-0.0019	-2.7	275213
Late Neolithic	Chokhopani	28.8	84.0	0.0031	4.5	282656	0.0025	4.1	311108	0.0030	4.2	308784	0.0000	0.0	636593
	Xitouchun	29.2	118.5	-0.0019	-3.0	232457	-0.0018	-2.9	245874	-0.0044	-6.7	246012	-0.0025	-4.5	436300
	Tanshishan	27.0	120.0	-0.0016	-2.2	181544	-0.0024	-3.4	188181	-0.0031	-4.4	189525	-0.0019	-3.2	332992
	Suogang	24.9	121.5	-0.0017	-1.4	45946	-0.0029	-2.2	45849	-0.0033	-2.5	46215	-0.0015	-1.4	65884
	Oakaie1	22.4	95.0	-0.0003	-0.3	72516	0.0000	0.0	74911	-0.0004	-0.4	77755	-0.0007	-0.8	136406
	Vt_G2	21.6	106.0	-0.0002	-0.2	50621	-0.0007	-0.6	55969	-0.0018	-1.5	56013	-0.0004	-0.5	109798
	La_G2	20.4	103.5	-0.0009	-1.4	229681	-0.0003	-0.4	253551	-0.0020	-2.9	251653	-0.0014	-2.5	514196
	Man_Bac	19.4	106.0	-0.0017	-2.3	137297	-0.0026	-3.5	137110	-0.0032	-4.1	144259	-0.0016	-2.6	250050
	Ban_Chiang	17.4	103.2	-0.0019	-1.3	35895	-0.0005	-0.4	36218	-0.0033	-2.5	38053	-0.0025	-2.2	64456
	Vanuatu	7.0	135.0	-0.0005	-0.7	162864	-0.0015	-2.1	161510	-0.0029	-3.8	169509	-0.0024	-3.8	303165
Present-day	Daur	48.5	124.0	0.0044	7.2	283332	0.0031	5.3	311782	0.0044	6.8	309463	-0.0002	-0.4	638198
	Hezhen	47.5	133.5	0.0046	8.8	283351	0.0033	6.6	311806	0.0041	7.4	309486	-0.0006	-1.1	638259
	Xibo	44.0	83.5	0.0043	8.3	283353	0.0033	6.7	311810	0.0033	6.0	309487	-0.0011	-2.4	638264
	Japanese	37.7	138.5	0.0029	5.7	283351	0.0017	3.6	311805	0.0026	4.9	309487	-0.0005	-1.1	638263
	Korean	37.6	127.0	0.0039	7.3	283353	0.0032	6.2	311805	0.0027	4.8	309489	-0.0015	-3.0	638250
	Han	32.3	114.0	0.0028	5.9	283358	0.0014	3.1	311815	0.0015	3.0	309492	-0.0016	-3.6	638271
	Tujia	29.6	109.0	0.0028	5.2	283353	0.0015	2.8	311805	0.0012	2.1	309489	-0.0017	-3.4	638256
	Sherpa	28.3	87.0	0.0032	6.1	283353	0.0023	4.5	311804	0.0038	6.9	309489	0.0007	1.3	638256
	Tibetan	28.3	84.5	0.0036	6.8	283349	0.0026	5.4	311805	0.0036	6.3	309485	0.0001	0.2	638258
	Yi	28.0	103.0	0.0032	5.9	283352	0.0020	3.9	311809	0.0031	5.2	309486	-0.0002	-0.3	638258
	Miao	27.4	109.0	0.0025	4.6	283352	0.0011	2.1	311806	0.0012	2.1	309490	-0.0013	-2.7	638263
	She	27.0	119.0	0.0030	5.5	283353	0.0015	2.8	311809	0.0010	1.8	309488	-0.0019	-3.9	638263
	Naxi	26.0	100.0	0.0037	7.5	283356	0.0025	5.3	311813	0.0027	5.2	309490	-0.0010	-2.2	638268
	Atayal	24.7	121.3	0.0001	0.2	283316	-0.0011	-1.6	311752	-0.0022	-3.4	309451	-0.0025	-4.3	638155
	Lahu	22.6	100.0	0.0022	4.0	283349	0.0008	1.5	311803	0.0005	0.8	309485	-0.0018	-3.6	638254
	Ami	22.5	121.3	0.0007	1.3	283346	-0.0012	-2.3	311804	-0.0011	-1.9	309481	-0.0021	-4.3	638243
	Kinh	21.0	105.9	0.0016	3.0	283352	0.0003	0.7	311804	-0.0001	-0.1	309488	-0.0018	-3.7	638258
	Dai	20.4	100.0	0.0014	3.0	283358	0.0001	0.2	311815	-0.0003	-0.6	309493	-0.0018	-4.2	638272
300 BP	Chuanyun	24.9	116.0	0.0020	2.5	143073	0.0017	2.1	152853	0.0013	1.5	149016	-0.0018	-2.4	255674

Table S6A. Three-, two-, and single-source mixture models for ancient Tibetans, Siberians, East Asians, and Southeast Asians. Targets were modeled as one or more of five ancestries - northern East Asian (Boshan), southern East Asian (Liangdao2), Hòabìnhian (G1), Paleosiberian (Kolyma), and Jōmon (Ikawazu), and estimates were determined by comparing against a set of other populations in the **Right** group described in section 6 (*14*). Ancient Siberians are a mixture of northern East Asian and Paleosiberian ancestry. Ancient Southern East Asians and the Vanuatu are best modeled as single-source ancestry related to Liangdao2. Almost all ancient Southeast Asians are modeled with Hòabìnhian-related ancestry. Ancient Tibetans, like present-day Tibetans, are modeled as northern East Asian ancestry and Jōmon ancestry. However, due to the lack of a connection to the Jōmon in f_4-statistics, this result is likely due to not having an appropriate source to represent more distantly related ancestry also found in Tibetans. S1, S2, and S3 indicate the ancient individual used to represent a source population, with the mixture proportion corresponding to f_1, f_2, and f_3, respectively. *rank0* indicates the p-value for the mixture model including all sources indicated (S1, S2, and/or S3), *pnest2* indicates the p-value comparing a three-source mixture model to a nested two-source model, and *pnest1* indicates the p-value comparing a two-source mixture model to a nested single source model.

Model^	Target	S1	S2	S3	rank0	f_1	f_2	f_3	se"	pnest1	pnest2	N
Tibetans												
2	Chokhopani	Boshan	Ikawazu	*	0.21	0.48	0.53	*	0.10	1.E-05	*	499426
2	Mebrak	Boshan	Ikawazu	*	0.56	0.47	0.53	*	0.16	1.E-03	*	337703
2	Samdzong	Boshan	Ikawazu	*	0.45	0.36	0.64	*	0.09	2.E-04	*	455775
Siberians and northern East Asians												
2	Shamanka_EN	Boshan	Kolyma	*	0.05	0.55	0.45	*	0.05	9.E-17	*	440977
2	Lokomotiv_EN	Boshan	Kolyma	*	0.09	0.59	0.41	*	0.07	1.E-09	*	521430
2	UstBelaya_N	Boshan	Kolyma	*	0.05	0.64	0.37	*	0.14	1.E-03	*	281459
2	DevilsCave_N	Boshan	Kolyma	*	0.04	0.81	0.19	*	0.05	1.E-03	*	545165
2	Yumin	Boshan	Kolyma	*	0.06	0.72	0.28	*	0.08	2.E-04	*	536156
1	Xiaojingshan	*	Liangdao2	*	0.30	1.00	*	*	*	*	*	405400
1	Xiaogao	*	Liangdao2	*	0.90	1.00	*	*	*	*	*	665751
southern East Asians and Southwest Pacific												
1	Liangdao1	*	Liangdao2	*	0.40	*	1.00	*	*	*	*	296335
1	Xitoucun	*	Liangdao2	*	0.30	*	1.00	*	*	*	*	384411
1	Suogang#	*	Liangdao2	*	0.50	*	1.00	*	*	*	*	69463
1	Tanshishan	*	Liangdao2	*	0.10	*	1.00	*	*	*	*	298287
1	Vanuatu	*	Liangdao2	*	0.50	*	1.00	*	*	*	*	262496
300-year-old southern East Asians and Austronesians												
2	Chuanyun	Boshan	Liangdao2	*	0.72	0.33	0.67	*	0.21	6.E-02	*	205859
1	G6	*	Liangdao2	*	0.10	*	1.00	*	*	*	*	338045
Southeast Asians												
2	Man_Bac	Liangdao2	G1	*	0.39	0.89	0.11	*	0.07	9.E-02	*	120796
2	Vt_G2	Boshan	G1	*	0.80	0.72	0.28	*	0.08	1.E-03	*	87939
2	La_G2	Liangdao2	G1	*	0.78	0.81	0.19	*	0.06	3.E-03	*	235300
2	Oakaie1	Boshan	G1	*	0.10	0.76	0.24	*	0.08	2.E-03	*	88456
2	Ban_Chiang	Boshan	G1	*	0.14	0.54	0.47	*	0.12	3.E-05	*	57887
2	Nui_Nap	Boshan	Liangdao2	*	0.28	0.47	0.53	*	0.18	2.E-03	*	212794
2	G3	Boshan	G1	*	0.16	0.86	0.14	*	0.07	4.E-02	*	154983
3	G4	Boshan	G1	Liangdao2	0.07	0.45	0.14	0.41	0.07	2.E-02	2.E-03	159597
2	Ma912_G2	Liangdao2	G1	*	0.58	0.75	0.25	*	0.06	1.E-04	*	240111
Ancient East Eurasians from above with alternative models that fit												
2	Vt_G2	Liangdao2	G1	*	0.21	0.76	0.24	*	0.09	8.E-03	*	84088
2	Ma912_G2	Liangdao2	Ikawazu	*	0.50	0.39	0.62	*	0.19	1.E-02	*	377836
2	Mebrak	Boshan	G1	*	0.15	0.80	0.20	*	0.06	1.E-03	*	213065
2	Chuanyun	Boshan	Ikawazu	*	0.40	0.73	0.27	*	0.15	2.E-05	*	373483

^A three-source mixture model (S1, S2, S3) was estimated if mixture proportions (f_1, f_2, and f_3) were between 0 and 1, the mixture model was not rejected (rank0>0.05), and the three-source model was better than a one-source or two-source model (pnest1<0.05, pnest2<0.05). If conditions were not satisfied, than a two-source model was estimated (S3, f_3, pnest2 not applicable, indicated by a *). If not applicable, then a one-source model was estimated (fields not used indicated by a *).
"The standard error shown for the triple-source model is the lowest of the standard errors estimated.

Table S6B. Three-, two-, and single-source mixture models for present-day East Asians. Description of table found in Table S6A. The Han and many other central (e.g. Korean, Miao) and southern (e.g. Lahu, Kinh) East Asians can be described by three ancestries.

Model^	Target	S1	S2	S3	rank0	f_1	f_2	f_3	se"	pnest1	pnest2	N
Present-day East and Southeast Asians from the Simons Genome Diversity Panel												
2	Daur	Boshan	Kolyma	*	0.72	0.7	0.3	*	0.06	2.E-06	*	571334
2	Hezhen	Boshan	Kolyma	*	0.05	0.77	0.24	*	0.05	1.E-05	*	501117
1	Ulchi+	Boshan	*	*	1.00E-13	1	*	*	*	*	*	545007
1	Oroqen+	Boshan	*	*	3.00E-13	1	*	*	*	*	*	543687
3	Korean	Boshan	Kolyma	Liangdao2	0.46	0.5	0.14	0.36	0.05	2.E-03	2.E-02	411109
3	Xibo	Boshan	Kolyma	Liangdao2	0.67	0.39	0.27	0.35	0.04	5.E-04	3.E-05	407472
2	Japanese	Boshan	Ikawazu	*	0.11	0.62	0.38	*	0.08	2.E-05	*	373483
3	Han	Boshan	Kolyma	Liangdao2	0.64	0.38	0.15	0.47	0.04	2.E-04	8.E-04	360369
3	She	Boshan	Kolyma	Liangdao2	0.67	0.35	0.15	0.5	0.05	2.E-03	3.E-04	413323
3	Miao	Boshan	Kolyma	Liangdao2	0.36	0.33	0.15	0.52	0.04	2.E-03	7.E-05	412258
3	Tujia	Boshan	Kolyma	Liangdao2	0.33	0.33	0.14	0.53	0.05	4.E-03	6.E-05	410981
3	Naxi	Boshan	Kolyma	Liangdao2	0.4	0.41	0.14	0.45	0.05	1.E-03	4.E-03	380758
3	Yi	Boshan	Kolyma	Liangdao2	0.17	0.34	0.15	0.52	0.05	4.E-03	4.E-04	408582
3	Dai	Boshan	Ikawazu	Liangdao2	0.83	0.28	0.23	0.5	0.08	3.E-02	3.E-02	289643
3	Lahu	Boshan	Kolyma	Liangdao2	0.63	0.21	0.12	0.66	0.05	6.E-02	2.E-03	412231
3	Kinh	Boshan	Kolyma	Liangdao2	0.89	0.28	0.12	0.6	0.04	1.E-02	5.E-04	409256
2	Atayal	Boshan	Liangdao2	*	0.9	0.28	0.72	*	0.12	2.E-02	*	505551
1	Ami	*	Liangdao2	*	0.3	*	1	*	*	*	*	507665
3	Tu	Boshan	Kolyma	Liangdao2	0.07	0.33	0.27	0.401	0.13	5.E-03	5.E-05	403556
3	Cambodian	Boshan	G1	Liangdao2	0.59	0.20	0.28	0.516	0.12	3.E-02	6.E-06	217038
2	Burmese	Boshan	Ikawazu	*	0.34	0.20	0.80	*	0.09	2.E-02	*	390415
2	Thai	Boshan	Ikawazu	*	0.21	0.35	0.66	*	0.08	9.E-05	*	392644
Present-day Han from different provinces of China from Lu et al. (2016)												
3	Han_Jiangsu	Boshan	Kolyma	Liangdao2	0.79	0.55	0.18	0.27	0.04	7.E-03	3.E-03	364088
3	Han_Anhui	Boshan	Kolyma	Liangdao2	0.22	0.53	0.15	0.33	0.06	1.E-02	8.E-02	456361
3	Han_Sichuan	Boshan	Kolyma	Liangdao2	0.75	0.36	0.17	0.47	0.04	1.E-04	3.E-04	338716
3	Han_Hubei	Boshan	Kolyma	Liangdao2	0.18	0.49	0.18	0.34	0.06	8.E-03	2.E-02	455243
3	Han_Guangdong	Boshan	Kolyma	Liangdao2	0.41	0.3	0.13	0.58	0.06	3.E-02	3.E-03	456524
3	Han_Chongqing	Boshan	Kolyma	Liangdao2	0.44	0.23	0.11	0.66	0.05	5.E-02	2.E-03	410524
3	Han_Henan	Boshan	Kolyma	Liangdao2	0.53	0.43	0.17	0.41	0.04	2.E-05	3.E-02	311631
3	Han_Gansu	Boshan	Kolyma	Liangdao2	0.53	0.44	0.18	0.39	0.04	1.E-04	6.E-03	348090
3	Han_Xinjiang	Boshan	Kolyma	Liangdao2	0.56	0.47	0.17	0.36	0.04	4.E-04	1.E-02	348173
3	Han_Shandong	Boshan	Kolyma	Liangdao2	0.44	0.6	0.13	0.27	0.04	8.E-03	3.E-02	364357
Present-day Tibetans and Sherpa from the Simons Genome Diversity Panel and Lu et al. (2016)												
2	Sherpa	Boshan	Ikawazu	*	0.48	0.47	0.53	*	0.09	2.E-07	*	402471
2	Tibetan	Boshan	Ikawazu	*	0.16	0.45	0.55	*	0.08	1.E-07	*	396680
1	Sherpa_Shigatse+	Boshan	*	*	5.00E-14	1	*	*	*	*	*	411447
2	Tibetan_Shannan	Boshan	Ikawazu	*	0.31	0.47	0.53	*	0.07	4.E-09	*	310320
2	Tibetan_Chamdo	Boshan	Ikawazu	*	0.15	0.54	0.46	*	0.07	1.E-08	*	321134
2	Tibetan_Shigatse	Boshan	Ikawazu	*	0.19	0.47	0.53	*	0.07	1.E-08	*	284584
2	Tibetan_Lhasa	Boshan	Ikawazu	*	0.06	0.5	0.51	*	0.08	4.E-08	*	364237
2	Tibetan_Nagqu	Boshan	Ikawazu	*	0.28	0.48	0.52	*	0.08	2.E-08	*	364936
Present-day East and Southeast Asians from above with alternative models that fit												
3	Lahu	Boshan	Ikawazu	Liangdao2	0.67	0.33	0.25	0.43	0.09	4.E-02	2.E-02	335739
3	Kinh	Boshan	Ikawazu	Liangdao2	0.89	0.39	0.23	0.38	0.09	4.E-02	1.E-03	333753
3	Lahu	Boshan	G1	Liangdao2	0.6	0.41	0.11	0.49	0.04	1.E-02	3.E-03	219992
3	Kinh	Boshan	G1	Liangdao2	0.83	0.5	0.11	0.39	0.04	1.E-02	2.E-04	219099
3	Naxi	Boshan	G1	Liangdao2	0.07	0.63	0.09	0.28	0.05	4.E-02	3.E-04	208323
3	Yi	Boshan	G1	Liangdao2	0.14	0.61	0.13	0.25	0.05	6.E-02	7.E-06	218507
2	Thai	*	Kolyma	Liangdao2	0.28	*	0.18	0.82	0.05	5.E-04	*	447021

^See description in Table S6A.

+Largest p-value is shown.

"The standard error shown for the triple-source model is the lowest of the standard errors estimated.

Table S7A. ***f_4(Mbuti, coastal sEastAsia_EN/LN; Dai, Ami).***

P1	P2	P3	P4	f_4	Z	N
Mbuti	Qihe	Dai	Ami	0.0017	5.2	540361
Mbuti	Liangdao1	Dai	Ami	0.0025	7.4	384072
Mbuti	Liangdao2	Dai	Ami	0.0025	7.6	879457
Mbuti	Xitoucun	Dai	Ami	0.0022	7.8	560694
Mbuti	Tanshishan	Dai	Ami	0.0027	8.5	410919
Mbuti	Suogang	Dai	Ami	0.0030	6.0	73771
Mbuti	Vanuatu	Dai	Ami	0.0041	12.7	365098

Table S7B. ***f_4(Mbuti, SoutheastAsia; Ami or Dai, X)*** **where X are select coastal northern and southern East Asians.** Results shaded gray are where the ancient Southeast Asian set shares a closer relationship to the ancient East Asian than the present-day southern East Asian. The 4,000-year-old Man Bac individuals from northern Vietnam share a close relationship to the coastal sEastAsia_LN (Xitoucun, Tanshishan) relative to both the Ami and Dai, but particularly the Dai. Results are also significant for transversions only (2.6<Z<5.0, not shown here), indicating the result is robust to ancient DNA damage patterns.

P1	P2	P3	P4	f_4	Z	N	P1	P2	P3	P4	f_4	Z	N
Mbuti	La_G2	Ami	Xitoucun	-0.0013	-3.3	456918	Mbuti	La_G2	Dai	Xitoucun	-0.0014	-4.2	456940
Mbuti	Ma912_G2	Ami	Xitoucun	-0.0008	-2.2	454824	Mbuti	Ma912_G2	Dai	Xitoucun	-0.0008	-2.1	454842
Mbuti	G3	Ami	Xitoucun	-0.001	-2.4	231556	Mbuti	G3	Dai	Xitoucun	-0.0002	-0.5	231562
Mbuti	G6	Ami	Xitoucun	-0.0028	-6.1	272758	Mbuti	G6	Dai	Xitoucun	0.0002	0.6	272767
Mbuti	G4	Ami	Xitoucun	-0.001	-2.5	324399	Mbuti	G4	Dai	Xitoucun	-0.0006	-1.7	324412
Mbuti	Vt_G2	Ami	Xitoucun	0.0001	0.1	103406	Mbuti	Vt_G2	Dai	Xitoucun	-0.0005	-0.8	103407
Mbuti	Ban_Chiang	Ami	Xitoucun	0.0014	1.9	61320	Mbuti	Ban_Chiang	Dai	Xitoucun	0.0017	2.6	61326
Mbuti	Man_Bac	Ami	Xitoucun	0.0024	5.4	229512	Mbuti	Man_Bac	Dai	Xitoucun	0.0029	7.2	229524
Mbuti	Nui_Nap	Ami	Xitoucun	0.0003	0.6	239491	Mbuti	Nui_Nap	Dai	Xitoucun	0.002	4.7	239504
Mbuti	Oakaie1	Ami	Xitoucun	0.0013	2	127993	Mbuti	Oakaie1	Dai	Xitoucun	0.0018	3.2	127998
Mbuti	La_G2	Ami	Tanshishan	-0.0012	-2.7	333197	Mbuti	La_G2	Dai	Tanshishan	-0.001	-2.5	333207
Mbuti	Ma912_G2	Ami	Tanshishan	-0.0007	-1.5	331494	Mbuti	Ma912_G2	Dai	Tanshishan	-0.0004	-1	331502
Mbuti	G3	Ami	Tanshishan	-0.0005	-1	166143	Mbuti	G3	Dai	Tanshishan	0.0004	0.9	166144
Mbuti	G6	Ami	Tanshishan	-0.0023	-4.1	197522	Mbuti	G6	Dai	Tanshishan	0.0011	2.3	197528
Mbuti	G4	Ami	Tanshishan	-0.0014	-3.1	236074	Mbuti	G4	Dai	Tanshishan	-0.0009	-2.1	236082
Mbuti	Vt_G2	Ami	Tanshishan	-0.001	-1.3	73623	Mbuti	Vt_G2	Dai	Tanshishan	-0.001	-1.3	73624
Mbuti	Ban_Chiang	Ami	Tanshishan	0.0013	1.3	46452	Mbuti	Ban_Chiang	Dai	Tanshishan	0.0024	2.7	46457
Mbuti	Man_Bac	Ami	Tanshishan	0.0015	2.9	174819	Mbuti	Man_Bac	Dai	Tanshishan	0.0017	3.8	174826
Mbuti	Nui_Nap	Ami	Tanshishan	-0.0009	-1.7	181760	Mbuti	Nui_Nap	Dai	Tanshishan	0.0009	1.8	181768
Mbuti	Oakaie1	Ami	Tanshishan	0.0002	0.3	95206	Mbuti	Oakaie1	Dai	Tanshishan	0.0008	1.2	95208
Mbuti	La_G2	Ami	Qihe	-0.002	-3.6	267748	Mbuti	La_G2	Dai	Qihe	-0.0021	-4.1	267757
Mbuti	Ma912_G2	Ami	Qihe	-0.0026	-4.7	266872	Mbuti	Ma912_G2	Dai	Qihe	-0.0028	-5.2	266878
Mbuti	G3	Ami	Qihe	-0.0012	-2	135228	Mbuti	G3	Dai	Qihe	-0.0006	-1	135232
Mbuti	G6	Ami	Qihe	-0.0063	-9.8	158567	Mbuti	G6	Dai	Qihe	-0.0031	-5.1	158573
Mbuti	G4	Ami	Qihe	-0.0027	-4.8	190676	Mbuti	G4	Dai	Qihe	-0.002	-3.9	190682
Mbuti	Vt_G2	Ami	Qihe	-0.0013	-1.5	59982	Mbuti	Vt_G2	Dai	Qihe	-0.001	-1.3	59982
Mbuti	Ban_Chiang	Ami	Qihe	-0.0001	-0.1	39518	Mbuti	Ban_Chiang	Dai	Qihe	0.0004	0.4	39522
Mbuti	Man_Bac	Ami	Qihe	0.0003	0.5	149020	Mbuti	Man_Bac	Dai	Qihe	0.0003	0.5	149028
Mbuti	Nui_Nap	Ami	Qihe	-0.002	-2.9	154158	Mbuti	Nui_Nap	Dai	Qihe	-0.0005	-0.9	154168
Mbuti	Oakaie1	Ami	Qihe	0.0001	0.1	81049	Mbuti	Oakaie1	Dai	Qihe	0.0005	0.6	81052
Mbuti	La_G2	Ami	Bianbian	-0.0031	-6.8	559756	Mbuti	La_G2	Dai	Bianbian	-0.0031	-7.5	559780
Mbuti	Ma912_G2	Ami	Bianbian	-0.0028	-5.6	553899	Mbuti	Ma912_G2	Dai	Bianbian	-0.0027	-6	553916
Mbuti	G3	Ami	Bianbian	-0.0033	-6.8	269769	Mbuti	G3	Dai	Bianbian	-0.0023	-5.4	269776
Mbuti	G6	Ami	Bianbian	-0.0049	-8.7	332185	Mbuti	G6	Dai	Bianbian	-0.0016	-3.3	332197
Mbuti	G4	Ami	Bianbian	-0.0018	-3.7	392442	Mbuti	G4	Dai	Bianbian	-0.0013	-3.1	392458
Mbuti	Vt_G2	Ami	Bianbian	-0.0018	-2.7	120248	Mbuti	Vt_G2	Dai	Bianbian	-0.0023	-3.5	120250
Mbuti	Ban_Chiang	Ami	Bianbian	-0.0014	-1.6	67370	Mbuti	Ban_Chiang	Dai	Bianbian	-0.0003	-0.3	67375
Mbuti	Man_Bac	Ami	Bianbian	-0.002	-4.1	259424	Mbuti	Man_Bac	Dai	Bianbian	-0.0015	-3.2	259435
Mbuti	Nui_Nap	Ami	Bianbian	-0.0024	-4.3	271951	Mbuti	Nui_Nap	Dai	Bianbian	-0.0006	-1.2	271964
Mbuti	Oakaie1	Ami	Bianbian	0.0001	0.1	143480	Mbuti	Oakaie1	Dai	Bianbian	0.0003	0.5	143486

Table S8A. Top thirty *f_3(Mbuti; Hòabìnhian, X)* where X are all present-day and ancient East Eurasians, ordered from largest to smallest. We used the G1 set to represent Hòabìnhians. Two sets are shaded gray, for the Neolithic Southeast Asian Man Bac and for the Ikawazu Jōmon. The Man Bac result is lower than that observed for most other Southeast Asians, and the Ikawazu result is lower or similar to that observed for several present-day East Asians, and ancient individuals from the Tibetan Plateau and coastal northern East Asia.

X	f3	SE	Z	N	X	f3	SE	Z	N
Vt_G2	0.2648	0.004	59.5	73244	Han_Chongqing	0.2548	0.003	81.0	382752
Ban_Chiang	0.2628	0.006	43.4	28921	Mebrak	0.2546	0.004	72.4	228240
G3	0.2617	0.004	74.3	156958	Chokhopani	0.2545	0.003	77.6	353824
Nui_Nap	0.2592	0.004	65.4	107253	She	0.2545	0.003	81.1	381929
Oakaie1	0.2585	0.005	55.3	63426	Japanese	0.2544	0.003	82.7	391602
G4	0.2580	0.003	75.2	208661	Korean	0.2544	0.003	81.8	382789
G6	0.2580	0.004	70.7	182423	Han_Anhui	0.2541	0.003	76.2	366739
Ma912_G2	0.2580	0.003	76.1	286653	Dai	0.2541	0.003	82.6	402021
UstBelaya_N	0.2575	0.004	68.4	152176	Kinh	0.2539	0.003	81.8	382630
La_G2	0.2573	0.003	76.5	297744	Ikawazu	0.2538	0.004	71.7	280931
Ami	0.2558	0.003	81.5	380309	Boshan	0.2538	0.003	73.2	289377
Han_Guangdong	0.2556	0.003	78.0	367121	Tujia	0.2536	0.003	80.1	382445
Yi	0.2553	0.003	81.5	383139	Naxi	0.2536	0.003	80.5	392391
Xiaojingshan	0.2552	0.003	73.2	169631	Han_Sichuan	0.2535	0.003	83.9	406806
Man_Bac	0.2551	0.004	67.5	101955	Han_Shandong	0.2534	0.003	82.4	398708

Table S8B. *f_4(Mbuti; Hòabìnhian, Jōmon, X)* where X are the ancient coastal sEastAsians, ordered from oldest to youngest (8,400-300 BP). We used the G1 set to represent Hòabìnhians and Ikawazu to represent Jōmon. We found that *f_4(Mbuti, G1; Ikawazu, North/South)~0* (-1.3<Z<1.7), which suggests that the Jōmon individual does not show genetic affinities to Hòabìnhians.

P1	P2	P3	P4	f_4	Z	N
Mbuti	G1	Ikawazu	Qihe	0.0009	1.2	192171
Mbuti	G1	Ikawazu	Liangdao1	0.0014	1.7	138738
Mbuti	G1	Ikawazu	Liangdao2	-0.0001	-0.1	310243
Mbuti	G1	Ikawazu	Suogang	-0.0014	-0.9	26509
Mbuti	G1	Ikawazu	Xitoucun	0.0004	0.5	201763
Mbuti	G1	Ikawazu	Tanshishan	-0.0001	-0.2	143175
Mbuti	G1	Ikawazu	Chuanyun	0.0006	0.7	105005

Table S9. Values for *f_4(Mbuti, Jōmon; X, Y)* where f_4 is significantly greater than zero (Z>2.5). X and Y are ancient East Asians, Tibetans, and Siberians, as well as ancient Austronesians. Results shaded in gray are where X is an inland population (steppe Siberia_EN, inland nEastAsia_EN, Tibet_LN) and Y is a coastal population (coastal Siberia_EN, coastal nEastAsia_EN, coastal sEastAsia_EN/LN/H), or where the Jōmon shares a closer relationship to the coastal population than an inland population. Results indicate that most significant results follow a coastal connection pattern.

P1	P2	P3	P4	f_4	Z	N
Mbuti	Ikawazu	Shamanka_EN	DevilsCave_N	0.002	5.7	890360
Mbuti	Ikawazu	Chokhopani	DevilsCave_N	0.0022	4.5	888826
Mbuti	Ikawazu	G6	DevilsCave_N	0.0021	3.8	447728
Mbuti	Ikawazu	Shamanka_EN	Xiaojingshan	0.0014	3.7	441768
Mbuti	Ikawazu	Yumin	DevilsCave_N	0.0019	3.5	670390
Mbuti	Ikawazu	Lokomotiv_EN	DevilsCave_N	0.0015	3.4	786730
Mbuti	Ikawazu	Shamanka_EN	Chuanyun	0.0018	3.2	243537
Mbuti	Ikawazu	Shamanka_EN	Liangdao1	0.0017	3.2	303307
Mbuti	Ikawazu	Shamanka_EN	Liangdao2	0.0015	3	686946
Mbuti	Ikawazu	Vanuatu	DevilsCave_N	0.0016	2.9	290767
Mbuti	Ikawazu	Shamanka_EN	Bianbian	0.0014	2.9	539208
Mbuti	Ikawazu	Yumin	Chuanyun	0.0022	2.9	227007
Mbuti	Ikawazu	Vanuatu	Liangdao2	0.0018	2.8	271699
Mbuti	Ikawazu	Chokhopani	Liangdao2	0.0017	2.8	685706
Mbuti	Ikawazu	Vanuatu	Xiaojingshan	0.0015	2.5	220222
Mbuti	Ikawazu	Shamanka_EN	UstBelaya_N	0.0012	2.5	381330
Mbuti	Ikawazu	Chokhopani	Chuanyun	0.0018	2.5	243040

References and Notes

1. F. Zhang, B. Su, Y.-P. Zhang, L. Jin, Genetic studies of human diversity in East Asia. *Phil. Trans. R. Soc. B* **362**, 987–996 (2007). doi:10.1098/rstb.2007.2028 Medline

2. The HUGO Pan-Asian SNP Consortium, Mapping Human Genetic Diversity in Asia. *Science* **326**, 1541–1545 (2009). doi:10.1126/science.1177074 Medline

3. C. Tian, R. Kosoy, A. Lee, M. Ransom, J. W. Belmont, P. K. Gregersen, M. F. Seldin, Analysis of East Asia genetic substructure using genome-wide SNP arrays. *PLOS ONE* **3**, e3862 (2008). doi:10.1371/journal.pone.0003862 Medline

4. J. Chen, H. Zheng, J.-X. Bei, L. Sun, W. H. Jia, T. Li, F. Zhang, M. Seielstad, Y.-X. Zeng, X. Zhang, J. Liu, Genetic structure of the Han Chinese population revealed by genome-wide SNP variation. *Am. J. Hum. Genet.* **85**, 775–785 (2009). doi:10.1016/j.ajhg.2009.10.016 Medline

5. A. Keinan, J. C. Mullikin, N. Patterson, D. Reich, Measurement of the human allele frequency spectrum demonstrates greater genetic drift in East Asians than in Europeans. *Nat. Genet.* **39**, 1251–1255 (2007). doi:10.1038/ng2116 Medline

6. M. Lipson, O. Cheronet, S. Mallick, N. Rohland, M. Oxenham, M. Pietrusewsky, T. O. Pryce, A. Willis, H. Matsumura, H. Buckley, K. Domett, G. H. Nguyen, H. H. Trinh, A. A. Kyaw, T. T. Win, B. Pradier, N. Broomandkhoshbacht, F. Candilio, P. Changmai, D. Fernandes, M. Ferry, B. Gamarra, E. Harney, J. Kampuansai, W. Kutanan, M. Michel, M. Novak, J. Oppenheimer, K. Sirak, K. Stewardson, Z. Zhang, P. Flegontov, R. Pinhasi, D. Reich, Ancient genomes document multiple waves of migration in Southeast Asian prehistory. *Science* **361**, 92–95 (2018). doi:10.1126/science.aat3188 Medline

7. H. McColl, F. Racimo, L. Vinner, F. Demeter, T. Gakuhari, J. V. Moreno-Mayar, G. van Driem, U. Gram Wilken, A. Seguin-Orlando, C. de la Fuente Castro, S. Wasef, R. Shoocongdej, V. Souksavatdy, T. Sayavongkhamdy, M. M. Saidin, M. E. Allentoft, T. Sato, A.-S. Malaspinas, F. A. Aghakhanian, T. Korneliussen, A. Prohaska, A. Margaryan, P. de Barros Damgaard, S. Kaewsutthi, P. Lertrit, T. M. H. Nguyen, H. C. Hung, T. Minh Tran, H. Nghia Truong, G. H. Nguyen, S. Shahidan, K. Wiradnyana, H. Matsumae, N. Shigehara, M. Yoneda, H. Ishida, T. Masuyama, Y. Yamada, A. Tajima, H. Shibata, A. Toyoda, T. Hanihara, S. Nakagome, T. Deviese, A.-M. Bacon, P. Duringer, J.-L. Ponche, L. Shackelford, E. Patole-Edoumba, A. T. Nguyen, B. Bellina-Pryce, J.-C. Galipaud, R. Kinaston, H. Buckley, C. Pottier, S. Rasmussen, T. Higham, R. A. Foley, M. M. Lahr, L. Orlando, M. Sikora, M. E. Phipps, H. Oota, C. Higham, D. M. Lambert, E. Willerslev, The prehistoric peopling of Southeast Asia. *Science* **361**, 88–92 (2018). doi:10.1126/science.aat3628 Medline

8. P. de Barros Damgaard, R. Martiniano, J. Kamm, J. V. Moreno-Mayar, G. Kroonen, M. Peyrot, G. Barjamovic, S. Rasmussen, C. Zacho, N. Baimukhanov, V. Zaibert, V. Merz, A. Biddanda, I. Merz, V. Loman, V. Evdokimov, E. Usmanova, B. Hemphill, A. Seguin-Orlando, F. E. Yediay, I. Ullah, K.-G. Sjögren, K. H. Iversen, J. Choin, C. de la Fuente, M. Ilardo, H. Schroeder, V. Moiseyev, A. Gromov, A. Polyakov, S. Omura, S. Y. Senyurt, H. Ahmad, C. McKenzie, A.

Margaryan, A. Hameed, A. Samad, N. Gul, M. H. Khokhar, O. I. Goriunova, V. I. Bazaliiskii, J. Novembre, A. W. Weber, L. Orlando, M. E. Allentoft, R. Nielsen, K. Kristiansen, M. Sikora, A. K. Outram, R. Durbin, E. Willerslev, The first horse herders and the impact of early Bronze Age steppe expansions into Asia. *Science* **360**, eaar7711 (2018). doi:10.1126/science.aar7711 Medline

9. M. Sikora, V. V. Pitulko, V. C. Sousa, M. E. Allentoft, L. Vinner, S. Rasmussen, A. Margaryan, P. de Barros Damgaard, C. de la Fuente, G. Renaud, M. A. Yang, Q. Fu, I. Dupanloup, K. Giampoudakis, D. Nogués-Bravo, C. Rahbek, G. Kroonen, M. Peyrot, H. McColl, S. V. Vasilyev, E. Veselovskaya, M. Gerasimova, E. Y. Pavlova, V. G. Chasnyk, P. A. Nikolskiy, A. V. Gromov, V. I. Khartanovich, V. Moiseyev, P. S. Grebenyuk, A. Y. Fedorchenko, A. I. Lebedintsev, S. B. Slobodin, B. A. Malyarchuk, R. Martiniano, M. Meldgaard, L. Arppe, J. U. Palo, T. Sundell, K. Mannermaa, M. Putkonen, V. Alexandersen, C. Primeau, N. Baimukhanov, R. S. Malhi, K.-G. Sjögren, K. Kristiansen, A. Wessman, A. Sajantila, M. M. Lahr, R. Durbin, R. Nielsen, D. J. Meltzer, L. Excoffier, E. Willerslev, The population history of northeastern Siberia since the Pleistocene. *Nature* **570**, 182–188 (2019). doi:10.1038/s41586-019-1279-z Medline

10. P. Skoglund, C. Posth, K. Sirak, M. Spriggs, F. Valentin, S. Bedford, G. R. Clark, C. Reepmeyer, F. Petchey, D. Fernandes, Q. Fu, E. Harney, M. Lipson, S. Mallick, M. Novak, N. Rohland, K. Stewardson, S. Abdullah, M. P. Cox, F. R. Friedlaender, J. S. Friedlaender, T. Kivisild, G. Koki, P. Kusuma, D. A. Merriwether, F.-X. Ricaut, J. T. S. Wee, N. Patterson, J. Krause, R. Pinhasi, D. Reich, Genomic insights into the peopling of the Southwest Pacific. *Nature* **538**, 510–513 (2016). doi:10.1038/nature19844 Medline

11. L. Liu, X. Chen, *The Archaeology of China: From the Late Paleolithic to the Early Bronze Age* (Cambridge Univ. Press, 2012).

12. B. Sun, S. Cui, A Study of the Early Neolithic Relics in Shandong Province [in Chinese]. *Cultural Relics of Central China* **3**, 23–28 (2008).

13. H. Matsumura, H. C. Hung, C. Higham, C. Zhang, M. Yamagata, L. C. Nguyen, Z. Li, X. C. Fan, T. Simanjuntak, A. A. Oktaviana, J. N. He, C. Y. Chen, C. K. Pan, G. He, G. P. Sun, W. J. Huang, X. W. Li, X. T. Wei, K. Domett, S. Halcrow, K. D. Nguyen, H. H. Trinh, C. H. Bui, K. T. K. Nguyen, A. Reinecke, Craniometrics Reveal "Two Layers" of Prehistoric Human Dispersal in Eastern Eurasia. *Sci. Rep.* **9**, 1451 (2019). doi:10.1038/s41598-018-35426-z Medline

14. See the supplementary materials for more details.

15. W. Haak, I. Lazaridis, N. Patterson, N. Rohland, S. Mallick, B. Llamas, G. Brandt, S. Nordenfelt, E. Harney, K. Stewardson, Q. Fu, A. Mittnik, E. Bánffy, C. Economou, M. Francken, S. Friederich, R. G. Pena, F. Hallgren, V. Khartanovich, A. Khokhlov, M. Kunst, P. Kuznetsov, H. Meller, O. Mochalov, V. Moiseyev, N. Nicklisch, S. L. Pichler, R. Risch, M. A. Rojo Guerra, C. Roth, A. Szécsényi-Nagy, J. Wahl, M. Meyer, J. Krause, D. Brown, D. Anthony, A. Cooper, K. W. Alt, D. Reich, Massive migration from the steppe was a source for Indo-European

languages in Europe. *Nature* **522**, 207–211 (2015). doi:10.1038/nature14317 Medline

16. Q. Fu, M. Hajdinjak, O. T. Moldovan, S. Constantin, S. Mallick, P. Skoglund, N. Patterson, N. Rohland, I. Lazaridis, B. Nickel, B. Viola, K. Prüfer, M. Meyer, J. Kelso, D. Reich, S. Pääbo, An early modern human from Romania with a recent Neanderthal ancestor. *Nature* **524**, 216–219 (2015). doi:10.1038/nature14558 Medline

17. A. W. Briggs, U. Stenzel, P. L. F. Johnson, R. E. Green, J. Kelso, K. Prüfer, M. Meyer, J. Krause, M. T. Ronan, M. Lachmann, S. Pääbo, Patterns of damage in genomic DNA sequences from a Neandertal. *Proc. Natl. Acad. Sci. U.S.A.* **104**, 14616–14621 (2007). doi:10.1073/pnas.0704665104 Medline

18. T. S. Korneliussen, A. Albrechtsen, R. Nielsen, ANGSD: Analysis of Next Generation Sequencing Data. *BMC Bioinformatics* **15**, 356 (2014). doi:10.1186/s12859-014-0356-4 Medline

19. Q. Fu, M. Meyer, X. Gao, U. Stenzel, H. A. Burbano, J. Kelso, S. Pääbo, DNA analysis of an early modern human from Tianyuan Cave, China. *Proc. Natl. Acad. Sci. U.S.A.* **110**, 2223–2227 (2013). doi:10.1073/pnas.1221359110 Medline

20. M. A. Yang, X. Gao, C. Theunert, H. Tong, A. Aximu-Petri, B. Nickel, M. Slatkin, M. Meyer, S. Pääbo, J. Kelso, Q. Fu, 40,000-year-old individual from Asia provides insight into early population structure in Eurasia. *Curr. Biol.* **27**, 3202–3208.e9 (2017). doi:10.1016/j.cub.2017.09.030 Medline

21. C. Jeong, A. T. Ozga, D. B. Witonsky, H. Malmström, H. Edlund, C. A. Hofman, R. W. Hagan, M. Jakobsson, C. M. Lewis, M. S. Aldenderfer, A. Di Rienzo, C. Warinner, Long-term genetic stability and a high-altitude East Asian origin for the peoples of the high valleys of the Himalayan arc. *Proc. Natl. Acad. Sci. U.S.A.* **113**, 7485–7490 (2016). doi:10.1073/pnas.1520844113 Medline

22. M. Raghavan, P. Skoglund, K. E. Graf, M. Metspalu, A. Albrechtsen, I. Moltke, S. Rasmussen, T. W. Stafford Jr., L. Orlando, E. Metspalu, M. Karmin, K. Tambets, S. Rootsi, R. Mägi, P. F. Campos, E. Balanovska, O. Balanovsky, E. Khusnutdinova, S. Litvinov, L. P. Osipova, S. A. Fedorova, M. I. Voevoda, M. DeGiorgio, T. Sicheritz-Ponten, S. Brunak, S. Demeshchenko, T. Kivisild, R. Villems, R. Nielsen, M. Jakobsson, E. Willerslev, Upper Palaeolithic Siberian genome reveals dual ancestry of Native Americans. *Nature* **505**, 87–91 (2014). doi:10.1038/nature12736 Medline

23. J. K. Pickrell, J. K. Pritchard, Inference of population splits and mixtures from genome-wide allele frequency data. *PLOS Genet.* **8**, e1002967 (2012). doi:10.1371/journal.pgen.1002967 Medline

24. W. Yan, Unity and Diversity in Chinese Neolithic Culture [in Chinese]. *Wen Wu* **3**, 38–50 (1987).

25. T. Jiao, in *A Companion to Chinese Archaeology*, A. P. Underhill, Ed. (Wiley, 2013), pp. 599–611.

26. Fujian Museum, Longyan Municipal Bureau of Culture and Publishing, The excavation of the Qihe Cave prehistoric remains in Zhangping City,Fujian [in Chinese]. *Kaogu.* **5**, 7–19 (2013).

27. W. Kutanan, J. Kampuansai, A. Brunelli, S. Ghirotto, P. Pittayaporn, S. Ruangchai, R. Schröder, E. Macholdt, M. Srikummool, D. Kangwanpong, A. Hübner, L. Arias, M. Stoneking, New insights from Thailand into the maternal genetic history of Mainland Southeast Asia. *Eur. J. Hum. Genet.* **26**, 898–911 (2018). doi:10.1038/s41431-018-0113-7 Medline

28. A. M.-S. Ko, C.-Y. Chen, Q. Fu, F. Delfin, M. Li, H.-L. Chiu, M. Stoneking, Y.-C. Ko, Early Austronesians: Into and out of Taiwan. *Am. J. Hum. Genet.* **94**, 426–436 (2014). doi:10.1016/j.ajhg.2014.02.003 Medline

29. P. Bellwood, A Hypothesis for Austronesian Origins. *Asian Perspect.* **26**, 107–117 (1984).

30. H. Matsumura, K. I. Shinoda, T. Shimanjuntak, A. A. Oktaviana, S. Noerwidi, H. Octavianus Sofian, D. Prastiningtyas, L. C. Nguyen, T. Kakuda, H. Kanzawa-Kiriyama, N. Adachi, H. C. Hung, X. Fan, X. Wu, A. Willis, M. F. Oxenham, Cranio-morphometric and aDNA corroboration of the Austronesian dispersal model in ancient Island Southeast Asia: Support from Gua Harimau, Indonesia. *PLOS ONE* **13**, e0198689 (2018). doi:10.1371/journal.pone.0198689 Medline

31. Y. Wang, F. Song, J. Zhu, S. Zhang, Y. Yang, T. Chen, B. Tang, L. Dong, N. Ding, Q. Zhang, Z. Bai, X. Dong, H. Chen, M. Sun, S. Zhai, Y. Sun, L. Yu, L. Lan, J. Xiao, X. Fang, H. Lei, Z. Zhang, W. Zhao, GSA: Genome Sequence Archive. *Genomics Proteomics Bioinformatics* **15**, 14–18 (2017). doi:10.1016/j.gpb.2017.01.001 Medline

32. BIG Data Center Members, Database Resources of the BIG Data Center in 2018, *Nucleic Acids Res.* **46**, D14–D20 (2018). doi:10.1093/nar/gkx897 Medline

33. J. Dabney, M. Knapp, I. Glocke, M.-T. Gansauge, A. Weihmann, B. Nickel, C. Valdiosera, N. García, S. Pääbo, J.-L. Arsuaga, M. Meyer, Complete mitochondrial genome sequence of a Middle Pleistocene cave bear reconstructed from ultrashort DNA fragments. *Proc. Natl. Acad. Sci. U.S.A.* **110**, 15758–15763 (2013). doi:10.1073/pnas.1314445110 Medline

34. R. Pinhasi, D. Fernandes, K. Sirak, M. Novak, S. Connell, S. Alpaslan-Roodenberg, F. Gerritsen, V. Moiseyev, A. Gromov, P. Raczky, A. Anders, M. Pietrusewsky, G. Rollefson, M. Jovanovic, H. Trinhhoang, G. Bar-Oz, M. Oxenham, H. Matsumura, M. Hofreiter, Optimal Ancient DNA Yields from the Inner Ear Part of the Human Petrous Bone. *PLOS ONE* **10**, e0129102 (2015). doi:10.1371/journal.pone.0129102 Medline

35. R. Pinhasi, D. M. Fernandes, K. Sirak, O. Cheronet, Isolating the human cochlea to generate bone powder for ancient DNA analysis. *Nat. Protoc.* **14**, 1194–1205 (2019). doi:10.1038/s41596-019-0137-7 Medline

36. M. Meyer, M. Kircher, M.-T. Gansauge, H. Li, F. Racimo, S. Mallick, J. G. Schraiber, F. Jay, K. Prüfer, C. de Filippo, P. H. Sudmant, C. Alkan, Q. Fu, R.

Do, N. Rohland, A. Tandon, M. Siebauer, R. E. Green, K. Bryc, A. W. Briggs, U. Stenzel, J. Dabney, J. Shendure, J. Kitzman, M. F. Hammer, M. V. Shunkov, A. P. Derevianko, N. Patterson, A. M. Andrés, E. E. Eichler, M. Slatkin, D. Reich, J. Kelso, S. Pääbo, A high-coverage genome sequence from an archaic Denisovan individual. *Science* **338**, 222–226 (2012). doi:10.1126/science.1224344 Medline

37. M. T. Gansauge, M. Meyer, Single-stranded DNA library preparation for the sequencing of ancient or damaged DNA. *Nat. Protoc.* **8**, 737–748 (2013). doi:10.1038/nprot.2013.038 Medline

38. G. Renaud, U. Stenzel, J. Kelso, leeHom: Adaptor trimming and merging for Illumina sequencing reads. *Nucleic Acids Res.* **42**, e141 (2014). doi:10.1093/nar/gku699 Medline

39. R. M. Andrews, I. Kubacka, P. F. Chinnery, R. N. Lightowlers, D. M. Turnbull, N. Howell, Reanalysis and revision of the Cambridge reference sequence for human mitochondrial DNA. *Nat. Genet.* **23**, 147 (1999). doi:10.1038/13779 Medline

40. H. Li, R. Durbin, Fast and accurate short read alignment with Burrows-Wheeler transform. *Bioinformatics* **25**, 1754–1760 (2009). doi:10.1093/bioinformatics/btp324 Medline

41. S. Sawyer, J. Krause, K. Guschanski, V. Savolainen, S. Pääbo, Temporal patterns of nucleotide misincorporations and DNA fragmentation in ancient DNA. *PLOS ONE* **7**, e34131 (2012). doi:10.1371/journal.pone.0034131 Medline

42. P. Skoglund, B. H. Northoff, M. V. Shunkov, A. P. Derevianko, S. Pääbo, J. Krause, M. Jakobsson, Separating endogenous ancient DNA from modern day contamination in a Siberian Neandertal. *Proc. Natl. Acad. Sci. U.S.A.* **111**, 2229–2234 (2014). doi:10.1073/pnas.1318934111 Medline

43. N. Patterson, P. Moorjani, Y. Luo, S. Mallick, N. Rohland, Y. Zhan, T. Genschoreck, T. Webster, D. Reich, Ancient admixture in human history. *Genetics* **192**, 1065–1093 (2012). doi:10.1534/genetics.112.145037 Medline

44. D. Lu, H. Lou, K. Yuan, X. Wang, Y. Wang, C. Zhang, Y. Lu, X. Yang, L. Deng, Y. Zhou, Q. Feng, Y. Hu, Q. Ding, Y. Yang, S. Li, L. Jin, Y. Guan, B. Su, L. Kang, S. Xu, Ancestral Origins and Genetic History of Tibetan Highlanders. *Am. J. Hum. Genet.* **99**, 580–594 (2016). doi:10.1016/j.ajhg.2016.07.002 Medline

45. N. Patterson, A. L. Price, D. Reich, Population structure and eigenanalysis. *PLOS Genet.* **2**, e190 (2006). doi:10.1371/journal.pgen.0020190 Medline

46. E. Y. Durand, N. Patterson, D. Reich, M. Slatkin, Testing for ancient admixture between closely related populations. *Mol. Biol. Evol.* **28**, 2239–2252 (2011). doi:10.1093/molbev/msr048 Medline

47. D. Reich, N. Patterson, M. Kircher, F. Delfin, M. R. Nandineni, I. Pugach, A. M.-S. Ko, Y.-C. Ko, T. A. Jinam, M. E. Phipps, N. Saitou, A. Wollstein, M. Kayser, S. Pääbo, M. Stoneking, Denisova admixture and the first modern human dispersals into Southeast Asia and Oceania. *Am. J. Hum. Genet.* **89**, 516–528 (2011). doi:10.1016/j.ajhg.2011.09.005 Medline

48. S. Purcell, B. Neale, K. Todd-Brown, L. Thomas, M. A. R. Ferreira, D. Bender, J. Maller, P. Sklar, P. I. W. de Bakker, M. J. Daly, P. C. Sham, PLINK: A tool set for whole-genome association and population-based linkage analyses. *Am. J. Hum. Genet.* **81**, 559–575 (2007). doi:10.1086/519795 Medline

49. D. H. Alexander, J. Novembre, K. Lange, Fast model-based estimation of ancestry in unrelated individuals. *Genome Res.* **19**, 1655–1664 (2009). doi:10.1101/gr.094052.109 Medline

50. M. Ding, T. Wang, A. M.-S. Ko, H. Chen, H. Wang, G. Dong, H. Lu, W. He, S. Wangdue, H. Yuan, Y. He, L. Cai, Z. Chen, G. Hou, D. Zhang, Z. Zhang, P. Cao, Q. Dai, X. Feng, M. Zhang, H. Wang, M. A. Yang, Q. Fu, Ancient mitogenomes show plateau populations from last 5200 years partially contributed to present-day Tibetans. *Proc. Biol. Sci.* **287**, 20192968 (2020). doi:10.1098/rspb.2019.2968 Medline

51. Z. Du, *Chinese Ecological Geographic Area System Research* (The Commercial Press, 2008).

52. M. Han, *Historical Agricultural Geography of China* (Peking Univ. Press, 2012).

53. Q. Fu, A. Mittnik, P. L. F. Johnson, K. Bos, M. Lari, R. Bollongino, C. Sun, L. Giemsch, R. Schmitz, J. Burger, A. M. Ronchitelli, F. Martini, R. G. Cremonesi, J. Svoboda, P. Bauer, D. Caramelli, S. Castellano, D. Reich, S. Pääbo, J. Krause, A revised timescale for human evolution based on ancient mitochondrial genomes. *Curr. Biol.* **23**, 553–559 (2013). doi:10.1016/j.cub.2013.02.044 Medline

54. C.-Y. Chen, H.-L. Chiu, *Excavation of Liangdao-Daowei Sites Group, Liangdao, Matsu Archipalego and the Treatments of "Liangdao Man" of the Liangdao-Daowei-I Site* (Culture Bureau Liangjian County, 2013).

55. C.-H. Tsang, *Archaeology of the P'eng-hu Islands* (Institute of History and Philology Academia Sinica, 1992).

56. C. B. Ramsey, S. Lee, Recent and Planned Developments of the Program OxCal. *Radiocarbon* **55**, 720–730 (2013). doi:10.1017/S0033822200057878

57. P. J. Reimer, E. Bard, A. Bayliss, J. W. Beck, P. G. Blackwell, C. B. Ramsey, C. E. Buck, H. Cheng, R. L. Edwards, M. Friedrich, P. M. Grootes, T. P. Guilderson, H. Haflidason, I. Hajdas, C. Hatté, T. J. Heaton, D. L. Hoffmann, A. G. Hogg, K. A. Hughen, K. F. Kaiser, B. Kromer, S. W. Manning, M. Niu, R. W. Reimer, D. A. Richards, E. M. Scott, J. R. Southon, R. A. Staff, C. S. M. Turney, J. van der Plicht, IntCal13 and Marine13 Radiocarbon Age Calibration Curves 0–50,000 Years cal BP. *Radiocarbon* **55**, 1869–1887 (2013). doi:10.2458/azu_js_rc.55.16947

58. B. Sun, M. Wagner, Z. Zhao, G. Li, X. Wu, P. E. Tarasov, Archaeological discovery and research at Bianbiandong early Neolithic cave site, Shandong, China. *Quat. Int.* **348**, 169–182 (2014). doi:10.1016/j.quaint.2014.06.013

59. Y. Hu, S. Wang, F. Luan, C. Wang, M. P. Richards, Stable isotope analysis of humans from Xiaojingshan site: Implications for understanding the origin of

millet agriculture in China. *J. Archaeol. Sci.* **35**, 2960–2965 (2008). doi:10.1016/j.jas.2008.06.002

60. Y. Song, B. Sun, Y. Gao, H. Yi, The environment and subsistence in the lower reaches of the Yellow River around 10,000 BP ——faunal evidence from the bianbiandong cave site in Shandong Province, China. *Quat. Int.* **521**, 35–43 (2019). doi:10.1016/j.quaint.2019.06.022

61. F. Wang, in *A Companion to Chinese Archaeology*, A. P. Underhill, Ed. (Wiley, 2013), pp. 389–410.

62. Institute of Cultural Relics and Archaeology of Inner Mongolia, "The discovery of an 8000 years ago village in Huade, Inner Mongolia" [in Chinese], *Zhongguo Wenwubao*, 3 June 2016.

63. J. Lu, X. Fan, C. Shen, The excavation of the Qihe Cave prehistoric remains in Zhangping City, Fujian. *Chinese Archaeology* **14**, 86–91 (2014). doi:10.1515/char-2014-0009

64. L. Zhong, *The Archaeology Research into Neolithic Culture of Tanshishan Fujian* [in Chinese] (Yuelu Publishing House, 2005).

65. Fujian Museum, Investigation on cultural relics around the Qihe cave site [in Chinese]. *Fujian Wenbo* **3**, 15–20 (2016).

66. Y. Liu, *Monograph on Taiwan Prehistory* [in Chinese] (Linking Publishing, 2016).

67. C.-h. Tsang, H.-c. Hung, A Preliminary Study on Three Lithic Workshops found on the Chi-mei Island, Penghu [in Chinese]. *The Bulletin of the Institute of History and Philology* **72**, 889–940 (2001).

68. S. Mallick, H. Li, M. Lipson, I. Mathieson, M. Gymrek, F. Racimo, M. Zhao, N. Chennagiri, S. Nordenfelt, A. Tandon, P. Skoglund, I. Lazaridis, S. Sankararaman, Q. Fu, N. Rohland, G. Renaud, Y. Erlich, T. Willems, C. Gallo, J. P. Spence, Y. S. Song, G. Poletti, F. Balloux, G. van Driem, P. de Knijff, I. G. Romero, A. R. Jha, D. M. Behar, C. M. Bravi, C. Capelli, T. Hervig, A. Moreno-Estrada, O. L. Posukh, E. Balanovska, O. Balanovsky, S. Karachanak-Yankova, H. Sahakyan, D. Toncheva, L. Yepiskoposyan, C. Tyler-Smith, Y. Xue, M. S. Abdullah, A. Ruiz-Linares, C. M. Beall, A. Di Rienzo, C. Jeong, E. B. Starikovskaya, E. Metspalu, J. Parik, R. Villems, B. M. Henn, U. Hodoglugil, R. Mahley, A. Sajantila, G. Stamatoyannopoulos, J. T. S. Wee, R. Khusainova, E. Khusnutdinova, S. Litvinov, G. Ayodo, D. Comas, M. F. Hammer, T. Kivisild, W. Klitz, C. A. Winkler, D. Labuda, M. Bamshad, L. B. Jorde, S. A. Tishkoff, W. S. Watkins, M. Metspalu, S. Dryomov, R. Sukernik, L. Singh, K. Thangaraj, S. Pääbo, J. Kelso, N. Patterson, D. Reich, The Simons Genome Diversity Project: 300 genomes from 142 diverse populations. *Nature* **538**, 201–206 (2016). doi:10.1038/nature18964 Medline

69. P. Skoglund, S. Mallick, M. C. Bortolini, N. Chennagiri, T. Hünemeier, M. L. Petzl-Erler, F. M. Salzano, N. Patterson, D. Reich, Genetic evidence for two founding populations of the Americas. *Nature* **525**, 104–108 (2015). doi:10.1038/nature14895 Medline

70. Q. Fu, C. Posth, M. Hajdinjak, M. Petr, S. Mallick, D. Fernandes, A. Furtwängler, W. Haak, M. Meyer, A. Mittnik, B. Nickel, A. Peltzer, N. Rohland, V. Slon, S. Talamo, I. Lazaridis, M. Lipson, I. Mathieson, S. Schiffels, P. Skoglund, A. P. Derevianko, N. Drozdov, V. Slavinsky, A. Tsybankov, R. G. Cremonesi, F. Mallegni, B. Gély, E. Vacca, M. R. G. Morales, L. G. Straus, C. Neugebauer-Maresch, M. Teschler-Nicola, S. Constantin, O. T. Moldovan, S. Benazzi, M. Peresani, D. Coppola, M. Lari, S. Ricci, A. Ronchitelli, F. Valentin, C. Thevenet, K. Wehrberger, D. Grigorescu, H. Rougier, I. Crevecoeur, D. Flas, P. Semal, M. A. Mannino, C. Cupillard, H. Bocherens, N. J. Conard, K. Harvati, V. Moiseyev, D. G. Drucker, J. Svoboda, M. P. Richards, D. Caramelli, R. Pinhasi, J. Kelso, N. Patterson, J. Krause, S. Pääbo, D. Reich, The genetic history of Ice Age Europe. *Nature* **534**, 200–205 (2016). doi:10.1038/nature17993 Medline

71. Q. Fu, H. Li, P. Moorjani, F. Jay, S. M. Slepchenko, A. A. Bondarev, P. L. F. Johnson, A. Aximu-Petri, K. Prüfer, C. de Filippo, M. Meyer, N. Zwyns, D. C. Salazar-García, Y. V. Kuzmin, S. G. Keates, P. A. Kosintsev, D. I. Razhev, M. P. Richards, N. V. Peristov, M. Lachmann, K. Douka, T. F. G. Higham, M. Slatkin, J.-J. Hublin, D. Reich, J. Kelso, T. B. Viola, S. Pääbo, Genome sequence of a 45,000-year-old modern human from western Siberia. *Nature* **514**, 445–449 (2014). doi:10.1038/nature13810 Medline

72. P. B. Damgaard, N. Marchi, S. Rasmussen, M. Peyrot, G. Renaud, T. Korneliussen, J. V. Moreno-Mayar, M. W. Pedersen, A. Goldberg, E. Usmanova, N. Baimukhanov, V. Loman, L. Hedeager, A. G. Pedersen, K. Nielsen, G. Afanasiev, K. Akmatov, A. Aldashev, A. Alpaslan, G. Baimbetov, V. I. Bazaliiskii, A. Beisenov, B. Boldbaatar, B. Boldgiv, C. Dorzhu, S. Ellingvag, D. Erdenebaatar, R. Dajani, E. Dmitriev, V. Evdokimov, K. M. Frei, A. Gromov, A. Goryachev, H. Hakonarson, T. Hegay, Z. Khachatryan, R. Khaskhanov, E. Kitov, A. Kolbina, T. Kubatbek, A. Kukushkin, I. Kukushkin, N. Lau, A. Margaryan, I. Merkyte, I. V. Mertz, V. K. Mertz, E. Mijiddorj, V. Moiyesev, G. Mukhtarova, B. Nurmukhanbetov, Z. Orozbekova, I. Panyushkina, K. Pieta, V. Smrčka, I. Shevnina, A. Logvin, K. G. Sjögren, T. Štolcová, A. M. Taravella, K. Tashbaeva, A. Tkachev, T. Tulegenov, D. Voyakin, L. Yepiskoposyan, S. Undrakhbold, V. Varfolomeev, A. Weber, M. A. Wilson Sayres, N. Kradin, M. E. Allentoft, L. Orlando, R. Nielsen, M. Sikora, E. Heyer, K. Kristiansen, E. Willerslev, 137 ancient human genomes from across the Eurasian steppes. *Nature* **557**, 369–374 (2018). doi:10.1038/s41586-018-0094-2 Medline

73. P. Skoglund, D. Reich, A genomic view of the peopling of the Americas. *Curr. Opin. Genet. Dev.* **41**, 27–35 (2016). doi:10.1016/j.gde.2016.06.016 Medline

74. M. Gallego Llorente, E. R. Jones, A. Eriksson, V. Siska, K. W. Arthur, J. W. Arthur, M. C. Curtis, J. T. Stock, M. Coltorti, P. Pieruccini, S. Stretton, F. Brock, T. Higham, Y. Park, M. Hofreiter, D. G. Bradley, J. Bhak, R. Pinhasi, A. Manica, Ancient Ethiopian genome reveals extensive Eurasian admixture in Eastern Africa. *Science* **350**, 820–822 (2015). doi:10.1126/science.aad2879 Medline

75. A. Seguin-Orlando, T. S. Korneliussen, M. Sikora, A.-S. Malaspinas, A. Manica, I. Moltke, A. Albrechtsen, A. Ko, A. Margaryan, V. Moiseyev, T. Goebel, M.

Westaway, D. Lambert, V. Khartanovich, J. D. Wall, P. R. Nigst, R. A. Foley, M. M. Lahr, R. Nielsen, L. Orlando, E. Willerslev, Genomic structure in Europeans dating back at least 36,200 years. *Science* **346**, 1113–1118 (2014). doi:10.1126/science.aaa0114 Medline

76. I. Lazaridis, D. Nadel, G. Rollefson, D. C. Merrett, N. Rohland, S. Mallick, D. Fernandes, M. Novak, B. Gamarra, K. Sirak, S. Connell, K. Stewardson, E. Harney, Q. Fu, G. Gonzalez-Fortes, E. R. Jones, S. A. Roodenberg, G. Lengyel, F. Bocquentin, B. Gasparian, J. M. Monge, M. Gregg, V. Eshed, A.-S. Mizrahi, C. Meiklejohn, F. Gerritsen, L. Bejenaru, M. Blüher, A. Campbell, G. Cavalleri, D. Comas, P. Froguel, E. Gilbert, S. M. Kerr, P. Kovacs, J. Krause, D. McGettigan, M. Merrigan, D. A. Merriwether, S. O'Reilly, M. B. Richards, O. Semino, M. Shamoon-Pour, G. Stefanescu, M. Stumvoll, A. Tönjes, A. Torroni, J. F. Wilson, L. Yengo, N. A. Hovhannisyan, N. Patterson, R. Pinhasi, D. Reich, Genomic insights into the origin of farming in the ancient Near East. *Nature* **536**, 419–424 (2016). doi:10.1038/nature19310 Medline

77. V. M. Narasimhan, N. Patterson, P. Moorjani, N. Rohland, R. Bernardos, S. Mallick, I. Lazaridis, N. Nakatsuka, I. Olalde, M. Lipson, A. M. Kim, L. M. Olivieri, A. Coppa, M. Vidale, J. Mallory, V. Moiseyev, E. Kitov, J. Monge, N. Adamski, N. Alex, N. Broomandkhoshbacht, F. Candilio, K. Callan, O. Cheronet, B. J. Culleton, M. Ferry, D. Fernandes, S. Freilich, B. Gamarra, D. Gaudio, M. Hajdinjak, É. Harney, T. K. Harper, D. Keating, A. M. Lawson, M. Mah, K. Mandl, M. Michel, M. Novak, J. Oppenheimer, N. Rai, K. Sirak, V. Slon, K. Stewardson, F. Zalzala, Z. Zhang, G. Akhatov, A. N. Bagashev, A. Bagnera, B. Baitanayev, J. Bendezu-Sarmiento, A. A. Bissembaev, G. L. Bonora, T. T. Chargynov, T. Chikisheva, P. K. Dashkovskiy, A. Derevianko, M. Dobeš, K. Douka, N. Dubova, M. N. Duisengali, D. Enshin, A. Epimakhov, A. V. Fribus, D. Fuller, A. Goryachev, A. Gromov, S. P. Grushin, B. Hanks, M. Judd, E. Kazizov, A. Khokhlov, A. P. Krygin, E. Kupriyanova, P. Kuznetsov, D. Luiselli, F. Maksudov, A. M. Mamedov, T. B. Mamirov, C. Meiklejohn, D. C. Merrett, R. Micheli, O. Mochalov, S. Mustafokulov, A. Nayak, D. Pettener, R. Potts, D. Razhev, M. Rykun, S. Sarno, T. M. Savenkova, K. Sikhymbaeva, S. M. Slepchenko, O. A. Soltobaev, N. Stepanova, S. Svyatko, K. Tabaldiev, M. Teschler-Nicola, A. A. Tishkin, V. V. Tkachev, S. Vasilyev, P. Velemínský, D. Voyakin, A. Yermolayeva, M. Zahir, V. S. Zubkov, A. Zubova, V. S. Shinde, C. Lalueza-Fox, M. Meyer, D. Anthony, N. Boivin, K. Thangaraj, D. J. Kennett, M. Frachetti, R. Pinhasi, D. Reich, The formation of human populations in South and Central Asia. *Science* **365**, eaat7487 (2019). doi:10.1126/science.aat7487 Medline

78. J. V. Moreno-Mayar, B. A. Potter, L. Vinner, M. Steinrücken, S. Rasmussen, J. Terhorst, J. A. Kamm, A. Albrechtsen, A.-S. Malaspinas, M. Sikora, J. D. Reuther, J. D. Irish, R. S. Malhi, L. Orlando, Y. S. Song, R. Nielsen, D. J. Meltzer, E. Willerslev, Terminal Pleistocene Alaskan genome reveals first founding population of Native Americans. *Nature* **553**, 203–207 (2018). doi:10.1038/nature25173 Medline

79. H. Kanzawa-Kiriyama, T. A. Jinam, Y. Kawai, T. Sato, K. Hosomichi, A. Tajima, N. Adachi, H. Matsumura, K. Kryukov, N. Saitou, K.-I. Shinoda, Late Jomon male

and female genome sequences from the Funadomari site in Hokkaido, Japan. *Anthropol. Sci.* **127**, 83–108 (2019). doi:10.1537/ase.190415